

VOLUME 12 NO. 4

AUGUST 1957

JOURNAL of the

*AMERICAN
SOCIETY
OF CIVIL ENGINEERS*

*Journal of
Structural Division*

PROCEEDINGS OF THE

AMERICAN SOCIETY

OF CIVIL ENGINEERS



Journal of the
HYDRAULICS DIVISION
Proceedings of the American Society of Civil Engineers

HYDRAULICS DIVISION
COMMITTEE ON PUBLICATIONS

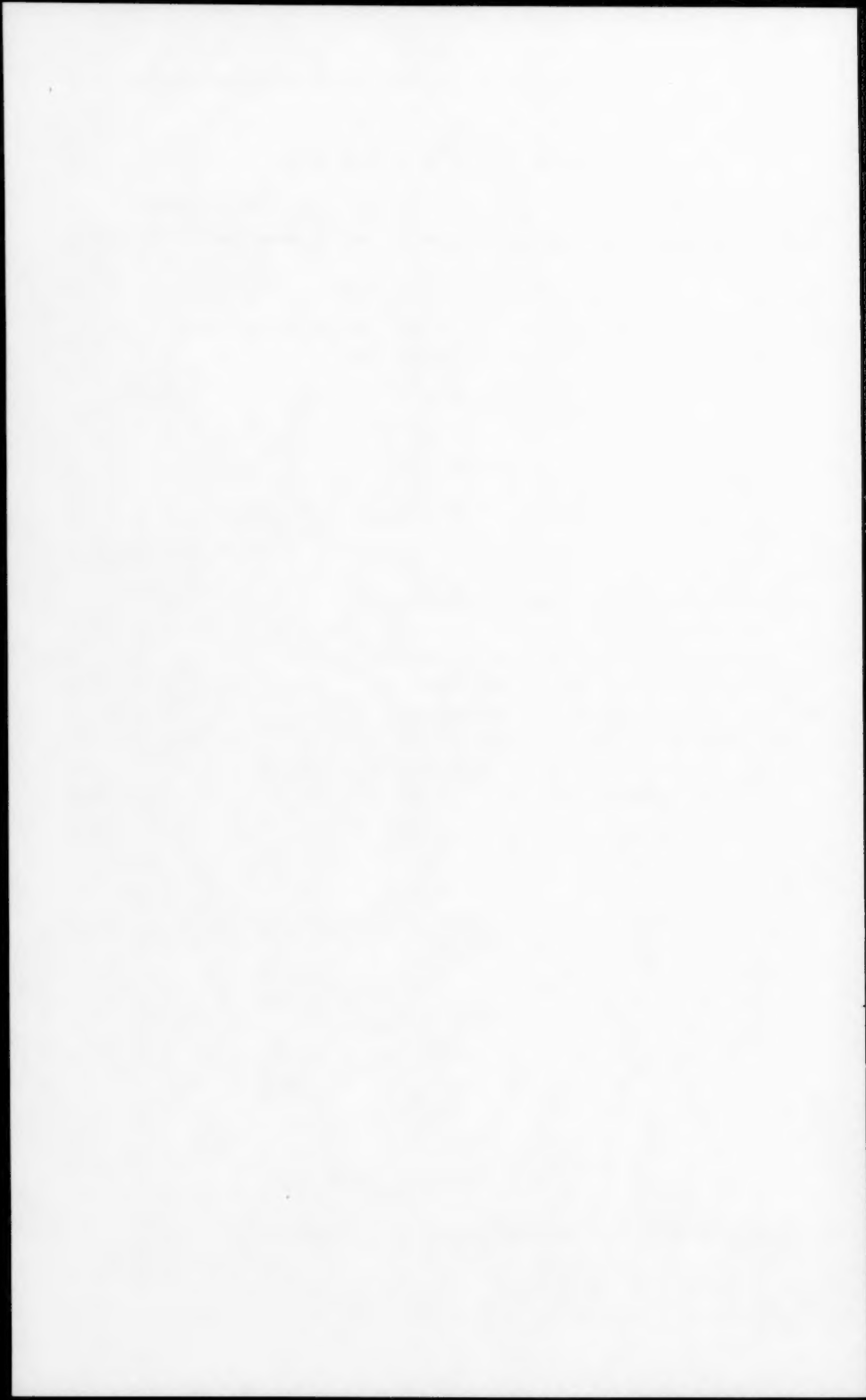
Haywood G. Dewey, Jr., Chairman; Wallace M. Lansford;
Joseph B. Tiffany, Jr.

CONTENTS

August, 1957

Papers

	Number
Hurricane Effect on Sea Level at Charleston by Bernard D. Zetler	1330
Systematic Changes in the Beds of Alluvial Rivers by Walter C. Carey and M. Dean Keller	1331
Synthetic Storm Pattern for Drainage Design by Clint J. Keifer and Henry Hsien Chu	1332
Characteristics of Flow over Terminal Weirs and Sills by P. K. Kandaswamy and Hunter Rouse	1345
Discussion	1348



Journal of the
HYDRAULICS DIVISION
Proceedings of the American Society of Civil Engineers

HURRICANE EFFECT ON SEA LEVEL AT CHARLESTON

Bernard D. Zetler*
(Proc. Paper 1330)

ABSTRACT

Tropical cyclones from 1922 to 1955 have been classified according to the orientation of their tracks with respect to Charleston Harbor. Theoretically, the displacement of sea level depends on this orientation; the tabulated displacements caused by tropical cyclones during 34 years of tide observations bear out the relationships.

When it was decided in the Coast and Geodetic Survey to make a study of the effect of hurricanes on sea level, Charleston was chosen as the area of the pilot study for several reasons. Its position makes it vulnerable to periodic hurricanes, and the low elevation of its downtown section creates the need for accurate forecasting of storm heights. Furthermore the problem appeared to be simpler for a port just off the ocean than, for example, a port on Chesapeake Bay in which interference oscillations may be anticipated. Lastly there was available for Charleston a relatively long series of tide observations dating back to 1922.

The attempt in this study has been to classify hurricanes into categories such that some groups are likely to have a large effect on sea level while others have little or none. Figure 1 shows the basis of one set of criteria which was chosen. Considering the Atlantic coastline near Charleston to lie in a SW to NE direction, the optimum direction of water motion to raise sea level is from the SE. Considering the Coriolis effect in the northern hemisphere of water moving about 45 degrees to the right of the wind, water movement from the SE will be set up by easterly winds. If an observer faces into the wind, the storm center will be on a line about ten points (112°) to the right. Therefore with easterly winds at Charleston, the storm center will have a bearing of approximately SSW. Accordingly, all other things being

Note: Discussion open until January 1, 1958. Paper 1330 is part of the copyrighted Journal of the Hydraulics Division of the American Society of Civil Engineers, Vol. 83, No. HY 1, August, 1957.

*Oceanographer, Coast and Geodetic Survey, U. S. Dept. of Commerce, Washington, D. C.

equal, storms having a bearing from Charleston of about SSW will cause a rise in sea level at Charleston while storms having a bearing of about WNW or ESE will cause currents to move parallel to the coast with little effect on sea level. A tropical cyclone bearing NNE from Charleston should lower sea level by moving water away from the coast. Storms having other bearings from Charleston will have effects proportionate to their departures from the above directions.

Figure 2 shows eight octants radiating out from Charleston, each representing an arc used in classifying the bearing of a cyclone center. Each name represents the direction in the center of the octant. By tabulating the octants through which the center of a cyclone moves in approaching and moving away from Charleston, one really is enumerating the changing bearing of the storm center as observed from Charleston.

Those storms classified as having Charleston on the right side of their tracks ordinarily move inland whereas those with Charleston on the left side remain out at sea. The criteria was first considered important on the assumption that storms moving inland pass a critical depth in shallow water at which resonance contributes to a surge.(1) Using this reasoning in studying the surge effect at Charleston, it would be necessary to distinguish between storms crossing the Atlantic coast and those crossing the Gulf coast. However this study shows large positive displacements with the track crossing the coastline in the Gulf of Mexico as well as the Atlantic coast. Apparently the criteria of Charleston being on the right side of the track is important because of associated strong winds over shallow water outside the harbor rather than because of a surge being set up at a critical depth. A storm with Charleston on the left side of its track contributes to changing sea level in the form of forerunners which are moderate rises in sea level over a period of time due largely to currents set up by wind circulation. In deep water much of this effect is dissipated before reaching the coast.

The question of how close a cyclone had to come to Charleston to affect sea level appreciably was resolved by including all storms shown on the track charts for the first few years considered. It became apparent that it was possible to restrict the study to cyclones coming within 345 miles (300 nautical miles) of Charleston. This is a convenient figure to work with as it is measured on a chart by five degrees of latitude near the latitude of Charleston. In the final tabulations, only the portions of tropical cyclones within a radius of 345 miles of Charleston are considered. This probably includes some cyclones which need not be considered but the effective diameters of tropical cyclones vary considerably in size and the diameters of particular storms are not usually listed in the published statistics.

The cyclones are classified first according to the octants in which they came closest to Charleston but the data on other octants are also important. For example two cyclones may have been closest to Charleston in Octant ESE. If one of them has passed through Octants SSW and SSE in approaching ESE, it presumably is more likely to have raised sea level than the other. The final tabulation also subdivides the storms classified within an octant to those with Charleston on the right side of the cyclone track and those with Charleston on the left. Tropical cyclones with Charleston on the right side are presumed to have a greater effect on sea level. The results bring this out very clearly.

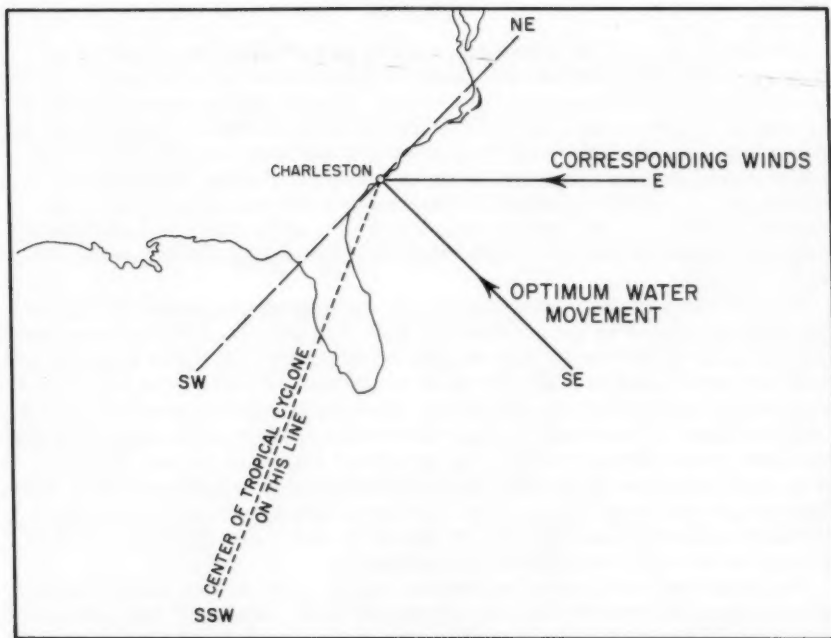


Figure 1. Theoretical bearing of center of tropical cyclone for maximum rise in sea level at Charleston.

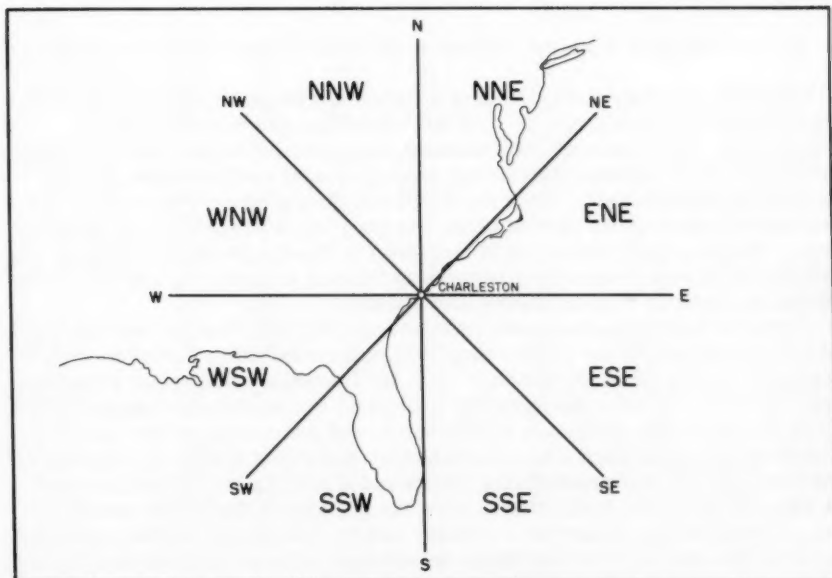


Figure 2. Octants radiating from Charleston used in classifying the bearing of the center of a tropical cyclone.

Tide Records

In determining the displacement of water level caused by a tropical cyclone, it was found desirable and necessary to consider the continuous record as represented by the complete tide curve. In most cases, a comparison of the observed and predicted heights on each hour presented a true picture, but it was found unsatisfactory for final results to compare heights only at the times of high and low tides, for, being so far apart in time, they seldom showed the maximum variation. Furthermore the time of high or low tide may be advanced or retarded several hours by a storm and a comparison of observed and predicted high or low tides would deal with water level at different times.

Despite these limitations comparisons of observed and predicted high and low tides were used as the preliminary step in determining what storms were to be included in the study. Any storms for which the calculated displacements did not include at least one value of one foot or more were eliminated from further consideration. These are shown in the tabular results as having a displacement of less than one foot. Obviously, in using this arbitrary rejection limit, some storms in which the calculated maximum hourly displacement would have been somewhat over a foot were rejected from further study. However, in each case the observed tide curve was examined for unusual fluctuations between the high and low waters in order that no important displacements would be rejected by this method.

Predicted tides at Charleston are referred to a datum of mean low water, based on gage records for the 19-year period 1924 - 1942, and take into account seasonal variations in sea level. Inasmuch as sea level along our east coast has been rising gradually (approximately 0.4 foot in the last few decades), each year's observations were referred to mean low water observed in the same year before being compared with predictions.

Tabulation of Tropical Cyclone Data and Sea Level Displacement

The following tables furnish data on tropical cyclones from 1922 to 1955, describing their paths, speeds, and their bearings and distances from Charleston. They indicate the maximum displacement of sea level and the interval of time between the cyclone coming closest to Charleston and the maximum displacement. When the maximum displacement occurred before the cyclone reached its closest point, the time lag is preceded by a negative sign. The maximum water height (referred to Mean Low Water) attained during the period of the storm is given in the last column. Underlined names of storms indicate that they were hurricanes.

Tropical cyclones are numbered in accordance with Weather Bureau track charts except that those earlier than 1933 are numbered in accordance with the track charts in "HURRICANES" by I. R. Tannehill. Numerous adjectives were found to describe the intensity of tropical cyclones in various sources. Even the clear-cut distinction of whether or not a tropical cyclone attained hurricane status is somewhat unsatisfactory since that degree of intensity may not apply to the storm during the period it may have affected sea level at Charleston. Some track charts show the position of the storm center every twelve hours; others give it every twenty-four hours. It was necessary to infer that the center of the storm moved at a uniform rate between adjacent

TABLE 1

Storm Tides at Charleston, S. C., 1922 to 1955
 Tropical Cyclones in Octant SSE When Closest to Charleston

Storm Data for Octants Traversed

Tropical Cyclone	Octant	Length of Path			Duration	Speed m.p.h.	Minimum Distance to Charleston	Height feet	Maximum Displacement Of Sea Level	Time Lag hours	Maximum Height Above MLW feet
		miles	hours								
<u>Charleston on right side of cyclone track</u>											
<u>1940 II</u>	SSE	110	11	10			140		+2.2	+24	7.4
	SSW	235	18	13			170				
<u>1951 Able (1st Approach)</u>	ESE	215	11	20			235		+1.1	- 2	5.9
	SSE	220	11	20			230				
<u>Charleston on left side of cyclone track</u>											
<u>1938 VII</u>	WSW	205	4	51			200		<1.0	-	6.8
	SSW	150	3	50			25				
	SSE	20	(0.4)	(50)			15				
	ESE	20	(0.4)	(50)			20				
	ENE	340	(7)	(49)			30				
<u>1924 IV</u>	WSW	185	19	10			175		<1.0	-	6.6
	SSW	145	9	16			55				
	SSE	40	3	13			45				
	ESE	55	2	28			50				
	ENE	275	11	25			70				
<u>1932 IV</u>	SSW	285	11	26			105		<1.0	-	6.4
	SSE	65	3	22			70				
	ESE	95	4	24			75				
	ENE	270	12	23			115				
<u>1937 I</u>	SSW	240	14	17			145		<1.0	-	5.5
	SSE	105	6	18			85				
	ESE	105	6	18			90				
	ENE	265	15	15			115				
<u>1953 Hazel</u>	SSW	110	5	22			265		+1.3	-22	6.7
	SSE	195	7	28			205				
	ESE	215	8	27			215				
<u>1938 VI</u>	SSE	140	?	?			230		<1.0	-	6.9
<u>1941 III (1st Approach)</u>	SSE	275	34	8			230		<1.0	-	6.1
	ESE	45	3	15			295				
<u>1931 IV</u>	SSW	60	6	10			275		<1.0	-	6.2
	SSE	195	21	9			250				
	ESE	100	?	?			270				
<u>1948 VIII</u>	SSE	195	11	18			320		<1.0	-	5.8
	ESE	100	4	25			325				

TABLE 2

Storm Tides at Charleston, S. C., 1922 to 1955
 Tropical Cyclones in Octant SSW When Closest to Charleston

Storm Data for Octants Traversed

Tropical Cyclone	Octant	Length of Path		Duration hours	Speed m.p.h.	Minimum Distance to Charleston miles	Maximum Displacement Of Sea Level		Maximum Height Above MLW feet
		miles	Path				Height feet	Time Lag hours	
<u>Charleston on right side of cyclone track</u>									
<u>1940 III</u>	ESE	100	13	8	280	+5.1*	?		10.7
	SSE	250	32	8	35				
	SSW	30	5	6	30				
	WSW	95	15	6	35				
	WNW	250	23	11	125				
<u>1947 IX</u>	SSE	95	6	16	315	+2.6	+1		8.6
	ESE	Course	(46)	-	(300)	+2.6	+1		8.6
	ENE								
	ESE								
	SSE	75	8	9	80				
	SSW	70	6	12	70				
	WSW	95	?	-	100				
<u>1947 VIII</u>	SSE	210	(13)	(16)	160	+1.3	-2		6.7
	SSW	150	7	21	140				
	WSW	200	?	-	160				
<u>1936 IX</u>	SSE	125	6	21	270	<1.0	-		5.7
	SSW	215	12	18	240				
	WSW	125	(9)	(14)	275				
<u>1937 III</u>	SSE	85	8	11	300	<1.0	-		6.6
	SSW	230	22	10	250				
	WSW	145	14	10	275				
<u>1939 II (1st Approach)</u>	SSW	210	16	13	315	<1.0	-		6.7
	WSW	40	5	8	330				
<u>Charleston on left side of cyclone track</u>									
<u>1946 VI</u>	SSW	285	?	?	60	+1.4	?		6.2
<u>1950 XII</u>	SSW	140	?	-	230	+1.7	?		6.7
<u>1937 VI</u>	WSW	90	12	8	265	<1.0	-		6.5
	SSW	85	?	-	240				
<u>1941 VI</u>	SSW	220	?	-	240	<1.0	-		7.0

* According to measured high water mark. At time gage ceased operating, displacement was +3.7 feet.

TABLE 3

Storm Tides at Charleston, S. C., 1922 to 1955
 Tropical Cyclones in Octant WSW When Closest to Charleston

Storm Data for Octants Traversed

Tropical Cyclone	Octant	Length of Path			Duration	Speed m.p.h.	Minimum Distance to Charleston	Maximum Displacement of Sea Level	Maximum Height Above MLW
		miles	hours	feet					
<u>Charleston on right side of cyclone track</u>									
<u>1953 Florence</u>	WSW	285	?	?		40	+1.5	-72	7.7
1934 I	SSW	70	4	18		300	+3.9	-3	9.1
	SSE	145	9	16		130			
	SSW	90	8	11		45			
	WSW	40	3	13		40			
	WNW	45	6	8		50			
	NNW	80	17	5		115			
	WNW	150	?	-		95			
1927 V	SSE	145	8	18		205	(+1.9)	+1	5.3
	SSW	150	10	15		80	(-1.0)	+8	
	WSW	50	3	17		60			
	WNW	65	4	16		65			
	NNW	225	(12)	(19)		85			
	NNE	65	(4)	(16)		270			
<u>1952 Able</u>	SSE	205	18	11		190	+3.0*	+2*	6.6
	SSW	155	12	13		70			
	WSW	55	3	18		60			
	WNW	70	4	18		65			
	NNW	215	16	13		105			
	NNE	80	(6)	(13)		270			
<u>1950 V</u>	SSW	330	60	6		180	+2.7	+5	6.8
	WSW	190	13	15		175			
	WNW	85	6	14		270			
<u>1926 I</u>	SSW	255	13	20		215	+2.8	+2	7.7
	WSW	195	10	20		210			
	WNW	60	3	20		265			
<u>1950 XI</u>	SSW	230	18	13		230	+2.3	+6	6.9
	WSW	230	?	-		225			
<u>1933 VI</u>	SSW	45	6	8		320	<1.0	-	6.6
	WSW	180	?	-		235			
<u>1953 Alice</u>	WSW	85	?	?		300	<1.0	-	5.9
<u>1948 III</u>	WSW	60	11	5		330	<1.0	-	7.3
	WNW	45	7	6		335			

* The maximum displacement may have been exceeded and the time lag changed during the period the gage was inoperative.

TABLE 4a

Storm Tides at Charleston, S. C., 1922 to 1955
 Tropical Cyclones in Octant WNW When Closest to Charleston

Storm Data for Octants Traversed

Tropical Cyclone	Octant	Length of Path		Duration hours	Speed m.p.h.	Minimum Distance to Charleston miles	Maximum Displacement Of Sea Level		Maximum Height Above MLW feet
		miles	hours				Height feet	Lag hours	
<u>Charleston on right side of cyclone track</u>									
1924 V	WSW	320	11	29	30	(+1.9)	+3		6.7
	WNW	25	1	25	25	(-2.2)	+5		
	NNW	25	1	25	25				
	NNE	310	(10)	(31)	35				
<u>1945 IX</u>	SSW	260	26	10	110	+4.0	-3	7.9	
	WSW	75	5	15	60				
	WNW	50	3	17	50				
	NNW	90	6	15	60				
	NNE	205	12	17	135				
<u>1944 X</u>	SSW	255	17	15	105	+3.8	-3	8.5	
	WSW	85	4	21	65				
	WNW	45	2	22	60				
	NNW	100	5	20	65				
	NNE	240	11	22	130				
1947 VII	SSW	195	12	16	180	+2.2	-5	6.5	
	WSW	130	7	19	75				
	WNW	45	2	22	60				
	NNW	60	3	20	65				
	NNE	275	13	21	95				
<u>1946 V</u>	SSW	215	10	22	150	+2.3	-4	7.2	
	WSW	105	5	21	90				
	WNW	75	3	25	85				
	NNW	100	8	12	90				
	NNE	205	15	14	125				
	ENE	100	(6)	17	270				
<u>1935 II</u>	SSW								
	WSW								
	WNW					90	-	-	-
	NNW								
	MNE								
The tide gage at Charleston was inoperative during this storm.									
<u>1933 XII</u>	SSW	200	28	7	270	+1.0*	(-40)*	(6.3)	
	WSW	230	24	10	125				
	WNW	80	?	-	100				
	NNW	40	?	-	105				

* The maximum displacement may have been exceeded and the time lag changed during the period the gage was inoperative.

TABLE 4b

Storm Tides at Charleston, S. C., 1922 to 1955
 Tropical Cyclones in Octant WNW When Closest to Charleston
 Storm Data for Octants Traversed

Tropical Cyclone	Octant	Length of Path		Duration	Speed m.p.h.	Minimum Distance to Charleston	Maximum Displacement Of Sea Level		Maximum Height Above MLW feet
		miles	hours				feet	hours	
<u>Charleston on right side of cyclone track - cont'd</u>									
<u>1949 II</u>	SSW	185	14		13	240	(+1.9	+5	7.5
	WSW	165	11		15	150	(-1.5	+10	
	WNW	110	5		22	135			
	NNW	230	9		26	150			
	NNE	50	1		50	305			
<u>1928 II</u>	WSW	235	20		12	310	< 1.0	-	6.4
	WNW	260	21		12	300			
	NNW	100	7		14	305			
<u>1932 VII</u>	WNW					340	-	-	-
	NNW								

The tide gage at Charleston was inoperative during this storm.

TABLE 5

Storm Tides at Charleston, S. C., 1922 to 1955
 Tropical Cyclones in Octant NNW When Closest to Charleston

Storm Data for Octants Traversed

Tropical Cyclone	Octant	Length of Path miles	Duration hours	Speed m.p.h.	Minimum Distance to Charleston miles	Maximum Displacement Of Sea Level		Maximum Height Above MLW feet
						Height feet	Time Lag hours	
Charleston on right side of cyclone track								
<u>1928 V</u>	SSW	295	19	16	90	(+3.8	-6	(8.1)
	WSW	90	6	15	30	(-1.2	+21	
	WNW	20	2	10	20			
	NNW	20	2	10	15			
	NNE	330	24	14	20			
<u>1941 V</u>	WSW	320	26	12	70	<1.0	-	5.7
	WNW	70	5	14	35			
	NNW	25	2	12	20			
	NNE	30	2	15	25			
	ENE	115	9	13	35			
	ESE	235	18	13	130			
<u>1929 II</u>	WSW	310	24	13	90	(+1.6	+4	7.0
	WNW	70	5	14	65	(-2.2	+10	
	NNW	80	5	16	60			
	NNE	250	12	21	100			
<u>1928 I</u>	SSW	220	32	7	285	+1.4	-6	6.3
	WSW	230	24	10	225			
	WNW	155	12	13	155			
	NNW	140	10	14	145			
	NNE	200	10	20	190			
<u>1936 XVI</u>	WSW	170	11	15	240	<1.0	-	6.3
	WNW	170	14	12	165			
	NNW	160	6	27	160			
	NNE	160	6	27	220			
<u>1939 II</u> (2nd Approach)	WNW	200	18	11	270	<1.0	-	5.7
	NNW	230	12	19	250			
	NNE	35	1 $\frac{1}{2}$	23	310			
<u>1934 II</u>	NNW	120	6	20	340	<1.0	-	5.3

TABLE 6

Storm Tides at Charleston, S. C., 1922 to 1955
Tropical Cyclones in Octant NNE When Closest to Charleston

Storm Data for Octants Traversed

Tropical Cyclone	Octant	Length of Path			Duration	Speed m.p.h.	Minimum Distance to Charleston	Height feet	Displacement Of Sea Level	Time Lag hours	Maximum Height Above MLW feet
		miles	hours	miles							
<u>Charleston on left side of cyclone track</u>											
1942 VI	ENE	50	4	12			310	<1.0	-	-	7.0
	NNE	115	?	-			240				

points to obtain a time lag measured in hours. Occasionally an extrapolation was necessary for this measurement and parentheses are set around these figures to indicate an inference. A number of cyclones dissipated near the points on their tracks closest to Charleston; a time lag estimate would be unreliable for these and a question mark appears in the column. Within each classification, the tropical cyclones are listed in order of increasing minimum distance to Charleston. Several cyclones came within the 345 mile range of Charleston, moved away, and then came back again. These approaches are listed independently in the tables but are distinguished by a notation "1st approach" or "2nd approach."

Tropical Cyclones In Octant SSE

Theoretically a cyclone in Octant SSE will raise sea level but not as much as one in SSW. However a cyclone approaching Charleston from SSW will usually pass over Florida and in doing so, lose some of its energy.

There are 11 storms listed in this classification. There was a rise in sea level for the two cyclones with Charleston on the right side of their cyclone tracks. All nine having Charleston on the left showed little displacement.

Hurricane II, 1940, had a displacement of +2.2 feet 24 hours after coming closest to Charleston. This storm moved from Octant SSE into Octant SSW and the maximum displacement took place while the storm was in SSW, accounting for the large time lag.

Hurricane Able, 1951, had a maximum displacement of +1.1 feet, two hours before coming closest to Charleston in its first approach. It then turned counter-clockwise, out of range of Charleston, without crossing the coast, thus accounting for the small displacement and small lag. Hurricane II, 1940, came almost a hundred miles closer to Charleston than did Hurricane Able, 1951, and moved considerably slower.

Four of the remaining nine came within less than one hundred miles of Charleston and all four passed through Octant SSW. One of them, IV 1924, attained hurricane intensity but had a small diameter. The fact that

TABLE 7

Storm Tides at Charleston, S. C., 1922 to 1955
 Tropical Cyclones in Octant ENE When Closest to Charleston

Storm Data for Octants Traversed

Tropical Cyclone	Octant	Length of Path miles	Duration hours	Speed m.p.h.	Minimum Distance to Charleston miles	Maximum Displacement Of Sea Level		Maximum Height Above MLW feet
						Height feet	Time Lag hours	
<u>Charleston on left side of cyclone track</u>								
<u>1954 Hazel</u>	SSE	220	8	28	145	(+1.7	-4	7.1
	ESE	105	4	26	100	(-1.5	15	
	ENE	105	3	35	90			
	NNE	255	5	51	125			
<u>1944 III</u>	SSE	165	11	15	180	<1.0	-	6.5
	ESE	140	9	16	105			
	ENE	80	5	16	100			
	NNE	230	13	18	120			
<u>1955 Connie</u>	ESE	255	40	6	165	+2.0	-7	6.9
	ENE	200	32	6	160			
	NNE	60	4	15	315			
<u>1955 Diane</u>	ESE	215	14	15	185	+1.7	-5	7.8
	ENE	145	12	12	170			
	NNE	230	17	14	185			
<u>1953 Barbara</u>	SSE	30	4	8	290	<1.0	-	5.8
	ESE	230	25	9	185			
	ENE	195	15	13	180			
	NNE	35	3	12	265			
<u>1955 Ione</u>	ESE	230	13	18	220	+1.3	-10	6.9
	ENE	160	13	12	215			
	NNE	90	10	9	255			
<u>1944 VI</u>	ESE	230	14	16	230	<1.0	-	6.1
	ENE	235	10	24	225			
<u>1933 XIII</u>	ESE	140	15	9	270	<1.0	-	5.9
	ENE	195	18	11	265			
<u>1936 XIII</u>	ENE	185	16	12	310	<1.0	-	6.1
<u>1940 IV</u>	ESE	35	4	9	330	<1.0	-	6.9
	ENE	145	15	10	310			
<u>1933 VIII</u>	ENE	105	8	13	325	+1.7	-2	6.6
	NNE	50	4	12	330			
<u>1941 III</u> (2nd Approach)	ESE	50	6	8	330	+1.8	-2	7.2
	ENE	100	11	9	325			

Charleston was on the left side of their hurricane tracks appears to be the explanation for their failure to raise sea level appreciably.

Tropical Cyclones in Octant SSW

Theoretically, cyclones with centers in Octant SSW will have the maximum ability to raise sea level at Charleston. Of the six cyclones which had Charleston on the right side of their tracks, the three closest caused notable rises in sea level; the three furthest away did not. Furthermore the amount of displacement by the first three appears directly related to their minimum distances to Charleston. This ordered sequence may also be due to the first two cyclones, III 1940 and IX 1947, attaining hurricane intensity while the third, VIII 1947, did not. The time lags for the second and third cyclones are negligible, as is to be expected of most cyclones coming closest to Charleston in Octant SSW. The time lag on the first, with a displacement of +5.1 feet, was not determined because of tide gage difficulties.

The loss of some tide data for Hurricane III 1940 illustrates a basic difficulty in a study such as this. The storms which strike Charleston hard and cause large displacements in sea level frequently cause tide gage failure and on a few occasions have destroyed the tide gage installation. The loss of record of some extreme conditions is a serious handicap to a study such as this. The program now being carried out of modifying the tide gage design, raising the gages and remoting recorders will help in the future.

There were four cyclones which were closest to Charleston in Octant SSW with Charleston to the left of their tracks. Tropical cyclone VI 1946, which came within 60 miles of Charleston caused a displacement of +1.4 feet. Hurricane XII 1950, was 230 miles from Charleston and caused a displacement of +1.7 feet. The other two, both 240 miles from Charleston, had little effect on sea level at Charleston. Since all four dissipated in Octant SSW there is no data on time lag.

Tropical Cyclones in Octant WSW

As is to be expected in view of the usual paths of West Indian tropical cyclones, all the storms which came closest to Charleston in Octant WSW have Charleston on the right side of their cyclone tracks. Since many of these passed through Octant SSW and even SSE prior to reaching WSW, a large positive sea level displacement with little time lag is to be expected from these cyclones. This is found to be the case.

Six of the ten cyclones in this category raised sea level from 2 to 4 feet; the time lag in each case was small. Of the remaining four, one dissipated in the octant and the other three were not hurricanes and their distances from Charleston were large.

Sometimes the elevation of sea level, as caused by a tropical cyclone, is followed by a lowering of sea level appreciably below the predicted value. The maximum negative displacement sometimes occurs just a few hours after the maximum positive displacement; at other times the time difference is a day or more. As noted previously, tropical cyclones in Octant NNE should lower sea level at Charleston most effectively and cyclones in Octants NNW and ENE should have similar effects. None of the tropical cyclones classified as coming closest to Charleston in Octants SSE and SSW passed through

TABLE 8a

 Storm Tides at Charleston, S. C., 1922 to 1955
 Tropical Cyclones in Octant ESE When Closest to Charleston

Storm Data for Octants Traversed

Tropical Cyclone	Octant	Length of Path miles	Duration hours	Speed m.p.h.	Minimum Distance to Charleston miles	Maximum Displacement Of Sea Level		Maximum Height Above MLW feet
						Height feet	Time Lag hours	
<u>Charleston on right side of cyclone track</u>								
1934 III	ENE	120	?	-	60	-1.2	-16½	5.6
	ESE	50	8	6	50			
	SSE	140	16	9	60			
	SSW	255	17	15	155			
<u>1935 V</u>	ENE	100	10	10	265	+1.4	+13	6.4
	ESE	230	23	10	240			
	SSE	70	7	10	300			
<u>Charleston on left side of cyclone track</u>								
<u>1930 II</u>	SSW	230	44	5	160	<1.0	-	5.8
	SSE	115	12	10	110			
	ESE	115	12	10	100			
	ENE	235	18	13	145			
<u>1945 I</u>	SSW	265	21	13	140	+2.6	+1	7.0
	SSE	100	6	17	105			
	ESE	100	6	17	100			
	ENE	265	14	19	125			
<u>1925 III</u>	SSW	160	6	27	230	+2.0	+2	6.9
	SSE	165	11	15	120			
	ESE	110	6	18	110			
	ENE	165	13	13	130			
	NNE	110	9	12	230			
<u>1954 Carol</u>	SSE	80	17	5	310	+2.0	+3	6.8
	ESE	260	72	4	140			
	ENE	255	15	17	160			
<u>1934 VI</u>	SSE	190	17	11	185	<1.0	-	5.9
	ESE	140	6	23	150			
	ENE	230	8	29	170			
<u>1922 III</u>	SSW	60	?	-	290	+1.8	-5	7.2
	SSE	195	(29)	(7)	185			
	ESE	190	39	5	180			
	ENE	100	18	6	260			
<u>1951 How</u>	SSW	50	3	17	320	+1.2	+7	7.2
	SSE	215	12	18	215			
	ESE	180	12	15	195			
	ENE	150	18	8	270			

TABLE 8b

 Storm Tides at Charleston, S. C., 1922 to 1955
 Tropical Cyclones in Octant ESE When Closest to Charleston

Storm Data for Octants Traversed

Tropical Cyclone	Octant	Length of Path			Duration	Speed m.p.h.	Minimum Distance to Charleston	Maximum Displacement Of Sea Level	Time Lag	hours	Maximum Height Above MLW feet
		miles	hours	miles							
<u>Charleston on left side of cyclone track - cont'd</u>											
1933 XVI	SSE	15	0.7	21			330	+1.3	(+14)		6.9
	ESE	205	?	-			200				
1937 II	SSE	110	13	8			240	<1.0	-		6.7
	ESE	190	18	11			200				
	ENE	160	12	13			220				
<u>1924 II</u>	SSE	195	40	5			265	+1.5	-7		6.1
	ESE	195	12	16			210				
	ENE	185	8	23			235				
<u>1950 I</u>	ESE	235	25	9			225	<1.0	-		6.4
	ENE	180	10	18			230				
<u>1948 IV</u>	ESE	180	19	9			240	<1.0	-		7.0
	ENE	125	12	10			245				
<u>1949 I</u>	ESE	230	15	15			240	<1.0	-		6.8
	ENE	200	10	20			245				
<u>1948 X</u>	ESE	180	9	20			250	<1.0	-		5.6
	ENE	145	7	21			255				
<u>1954 Edna</u>	ESE	260	28	9			250	(+1.3	+2		6.9
	ENE	175	10	18			265	(+1.3	+15		
1937 VIII	SSE	130	9	14			275	<1.0	-		6.2
	ESE	230	11	21			250				
	ENE	80	3	27			280				
<u>1938 IV</u>	ESE	240	9	27			255	Tide gage not operating at this time.			
	ENE	185	5	37			260				
<u>1944 I</u>	SSE	40	4	10			325	<1.0	-		6.7
	ESE	310	48	6			275				
<u>1951 Able (2nd Approach)</u>	ESE	255	21	12			275	<1.0	-		7.4
	ENE	160	12	13			280				
1943 II	ESE	200	14	14			290	<1.0	-		7.4
	ENE	65	5	13			310				
<u>1932 III</u>	SSE	115	16	7			305	<1.0	-		6.5
	ESE	195	20	10			300				
<u>1951 Jig</u>	ESE	160	15	11			325	+1.5	-15		7.0

Octants NNE or NNW, a few of them were in ENE but far off from Charleston. Consequently none of them lowered sea level at Charleston appreciably.

Tropical cyclone V 1927 caused a negative displacement of sea level of 1.0 foot seven hours after a positive displacement of 1.9 feet. The negative displacement occurred while the cyclone center was in Octant NNW although it continued into NNE; however, the minimum distance to Charleston in NNE was 270 miles so the storm may have been out of effective range of Charleston by the time it reached NNE. Two other cyclones I 1934 and Able 1952 passed through NNW also. Neither lowered sea level by a foot but V 1927 was closer to Charleston while in Octant NNW than either of them.

Tropical Cyclones in Octant WNW

As was true of tropical cyclones in the previous category, tropical cyclones coming closest to Charleston in Octant WNW will ordinarily have Charleston on the right side of their track and therefore will cause positive displacements of sea level at Charleston because they have passed through Octant WSW and possibly SSW. However since they contribute little to raising sea level while in WNW, a negative time lag is to be expected.

This is generally true of the cyclones listed in this category in the table. Four cyclones caused positive displacements of 2-1/4 to 4 feet with negative time lags of a few hours. Two others however, 1924 V and 1949 II, caused positive displacements of 2 feet with small positive time lags; these two were also the only cyclones in the group to cause subsequent negative sea level displacements. While the positive time lags may possibly be attributed to error introduced by inferring a constant speed between points of reference, there is no apparent reason why only these two cyclones should cause negative displacements. Tropical cyclone V 1924 was very close to Charleston while in Octants NNW and NNE, but a number of the other storms were closer than Hurricane II 1949 while in these octants. Perhaps the unusual severity of Hurricane II 1949 accounts for its effect.

The effect of Tropical Cyclone V 1924 was unusual too in that there was only a two hour difference in time between the maximum positive and negative displacements of sea level. This is shown on the marigram as a reversal of the tidal rise between 5 and 7 a.m. (75° W. time) on September 30. Immediately thereafter, the tide rose again at a somewhat accelerated rate. The eye of the cyclone almost passed over Charleston with strong winds first building up the level of the sea, the calm then releasing the accumulation and strong winds shortly thereafter driving the water from the coast. There was a change in sea level of 4.1 feet which took place in two hours that was directly attributable to meteorological conditions.

Hurricane XII 1933 caused a positive displacement of 1.0 foot with a time lag of -40 hours. The unusual time lag may be due in part to tide gage failure during the next eleven hours during which time the maximum recorded displacement may have been exceeded and in part to weakening of the hurricane as it approached Charleston; the storm dissipated shortly thereafter.

One hurricane 300 miles from Charleston had little effect on sea level. The Charleston tide gage was inoperative during two other storms.

Tropical Cyclones in Octant NNW

Those cyclones coming closest to Charleston in Octant NNW have Charleston on the right side of their tracks. They may have large positive displacements of sea level with negative time lags based on their effect in previous octants. They may also have negative displacements with positive time lags based on subsequent effects in Octant NNE.

Hurricane V 1928 caused a positive displacement of 3.8 feet followed by a negative displacement of 1.2 feet; the time lags corresponded to the above estimates. Hurricane I 1928 caused a displacement of +1.4 feet with a small negative time lag.

Hurricane II 1929 caused a positive displacement followed by a negative displacement but the time lag for the rise in sea level is +4 hours. Here again the apparent discrepancy may be due to inference of a uniform speed between two points on the travel path twenty-four hours apart. The time lag for the negative displacement puts the cyclone center in Octant NNE at the time.

Four other listed cyclones in this category had no appreciable effect on sea level at Charleston. Hurricane V 1941 is among these although it came within 20 miles of Charleston. Its failure to raise sea level is explained by its wide swing around Charleston in its clockwise motion but its failure to subsequently lower sea level while coming close to Charleston in Octants NNW, and NNE and ENE is not readily explained unless the hurricane lost its strength prior to approaching Charleston.

Tropical Cyclones in Octant NNE

Only one cyclone IV 1942, was closest to Charleston in Octant NNE. It was 240 miles away and had little effect on sea level at Charleston.

Tropical Cyclones in Octant ENE

Twelve tropical cyclones, all of hurricane intensity, were closest to Charleston in Octant ENE. Charleston was on the left side of the track of each.

There was a positive displacement of between one and two feet by six of these hurricanes, each with a negative time lag indicating that they were set up while the cyclone was in the ESE direction. The negative displacement of 1.5 feet for 1954 Hazel is interesting as it illustrates the behavior of a resurgence as defined by Redfield and Miller. There was a positive displacement followed consecutively by a negative, a positive and then a negative displacement, each about six hours apart. These oscillations are believed due to the free motion of the water in restoring the disturbed levels, augmented in some cases by the changed direction of the wind. The period of oscillation following this storm, roughly that of the semidiurnal tidal cycle, appears to be the usual pattern at Charleston. If this is so the resurgence at Charleston is not apt to attain substantially greater heights than the initial rise as it will occur at about the same tidal phase.

Tropical Cyclones in Octant ESE

There are twenty-four tropical cyclones listed as coming closest to Charleston in Octant ESE. Of these only two have Charleston on the right side of their tracks.

Although one of these raised sea level while the other lowered it, the data are not contradictory. Tropical cyclone III 1934 lowered sea level at Charleston by 1.2 feet. The negative time lag indicates it caused this while in Octant ENE. Hurricane V 1935 raised sea level 1.4 feet. The positive time lag indicates this occurred after the storm reached Octant SSE.

Theoretically, tropical cyclones in Octant ESE will set up currents parallel to the coast and have little effect on sea level at Charleston. This may be particularly true of cyclones with Charleston on the left side of their tracks. Some of the tropical cyclones listed in this classification caused positive displacements of sea level. In general these displacements are presumed to be due to their effect in octants previously traversed. The negative time lag or small positive time lag supports this suggestion.

The displacements attributed to several tropical cyclones are probably due to extraneous conditions. Sea level rose 1.3 feet when tropical cyclone XVI 1933 was near Charleston but this maximum displacement occurred about a half day after the cyclone had dissipated at its closest point to Charleston. There was a rise in sea level of 1.5 feet near the time Hurricane Jig 1951 was first reported but equal displacements of sea level were reported on the previous two days. In both cases, the displacements appear to be coincidental to the presence of the tropical cyclones or at best they are only partially responsible.

The two storms Hurricane II 1930 and Hurricane I 1945 illustrate the difficulty in the classification of storm intensity. Both cyclones are listed as attaining hurricane intensity and traveled over almost identical paths while in the vicinity of Charleston. The first had little effect on sea level at Charleston and the second raised sea level 2.6 feet. Further investigation disclosed that the first had lost most of its strength before reaching the Atlantic and the second retained its hurricane strength, thus explaining the difference in effect.

SUMMARY

While it has been demonstrated that the bearing of a tropical cyclone and the direction in which the cyclone is moving with respect to Charleston are important factors in determining sea level displacement at Charleston, too many other variables are involved to permit accurate quantitative forecasts at present. It is possible to predict that certain storms will have little or no effect. It is also possible to predict that other storms will raise sea level by an estimated amount with the extreme coming within a few hours of a certain time, provided, of course that there is an accurate forecast of the cyclone track.

As indicated previously, the intensity of a tropical cyclone at the time it can affect sea level at Charleston has not been adequately determined for the storms in this study. Similarly the dimensions of the effective diameters of most storms were not available although some data are published⁽²⁾ and more information of this kind will result from the current National Hurricane Research Project. The speed of the cyclone centers in the various octants

are given in the table but no apparent relationship to sea level displacement has been noted. A tropical cyclone moving slowly should have a greater effect on sea level because winds will blow from the same direction for a longer period of time. On the other hand, a tropical cyclone moving with rapid velocity (forty to fifty miles per hour) will augment the velocity of winds on the right side of the track and thus may strongly affect sea level. Presumably, heavy rainfall over the adjacent land area can raise the level of water in Charleston Harbor temporarily.

All these factors really need to be considered to a certain extent in forecasting sea level displacement. On the other hand, a study which classifies each cyclone according to each criteria may find that, with a limited sample, each storm is in a class by itself. In view of these variables, the fairly consistent results within each classification used in this study indicate the relative importance of the criteria used.

REFERENCES

1. Memorandum on Water Levels Accompanying Atlantic Coast Hurricanes, Alfred C. Redfield and A. R. Miller, Woods Hole Oceanographic Institution Reference No. 55-28. (Unpublished Manuscript)
2. Hydrometeorological Report No. 32, Characteristics of United States Hurricanes Pertinent to Levee Design for Lake Okeechobee, Florida, U. S. Weather Bureau and U. S. Corps of Engineers, March 1954.



Journal of the
HYDRAULICS DIVISION
Proceedings of the American Society of Civil Engineers

SYSTEMATIC CHANGES IN THE BEDS OF ALLUVIAL RIVERS^a

Walter C. Carey,¹ M. ASCE and M. Dean Keller,² J.M. ASCE
(Proc. Paper 1331)

ABSTRACT

This paper describes the sand wave formations present in alluvial rivers and discusses their variations with respect to river stage. The related rise and fall of crossings is also discussed. The illustrations are prepared from fathometer surveys and show the changes in the sand waves due to changes in stage.

INTRODUCTORY

Close association with various aspects of planning, constructing and operating works for the improvement of the Mississippi River, has gradually led to the conclusion that systematic changes take place in the river bed, and that these changes are a major factor in determining resistance to flow and in governing the general behavior of the river. Two somewhat over-lapping phenomena are involved; namely, (1) a rise and fall of the crossings between bends in sympathy with variations in discharge, and (2) a system of sand waves on the river bed, which varies as to general arrangement, and as to size and spacing of individual waves, in accordance with some controlling condition.

As to the first phenomenon, the variation in height of crossings with respect to discharge, it will be noted that its existence is well known to practical navigators, and engineers closely identified with the practical aspects of river work. Although obviously operating on all alluvial rivers, this phenomenon does not seem to be generally recognized among the hydraulicians,

Note: Discussion open until January 1, 1958. Paper 1331 is part of the copyrighted
Journal of the Hydraulics Division of the American Society of Civil Engineers,
Vol. 83, No. HY 4, August, 1957.

- a. Presented before American Society of Civil Engineers, at Annual Meeting, Jackson, Miss., on February 20, 1957.
1. Asst. to Chief of Eng. Div., New Orleans Dist., Corps of Engrs., U. S. Dept. of the Army, New Orleans, La.
2. Structural Engr., Bedell & Nelson, Cons. Engrs., New Orleans, La.

and its effects have received little, if any, attention in evolving the theoretical background of formal river hydraulics.

As indicated, crossing bars, rise and fall in a manner broadly related to changes in discharge: On the lower Mississippi, the magnitude, of these changes ranges from 25%, to even as much as 50%, of the change in water surface level. This phenomenon is so sensitive that even a small rise is immediately reflected by a rise of the crossing bar. When a period of high flow is succeeded by a fairly rapid fall, these built-up crossings cause a river to be a series of pools with steep crossing slopes: Under the influence of the resulting high velocities, the crossings rapidly scour, with a resultant lowering of the pools to "normal" low water. Such scour may be disorderly, however, and may fail to produce a good navigable channel; in fact, the more rapid the fall, the more likely it is that considerable dredging will be required at the crossings.

Closer study of this rise and fall of crossings, may throw new light on the movement of bed load material: It may develop that, in effect, the bends are "scoured out," at high stages, and that much of the "scoured" material is simply moved to the first crossing. During lower stages, this material is probably gradually removed from the crossing and deposited in the bend below. In addition to this source of "back fill," bends also receive back-fill from the extensive bank caving, which follows a falling river, after the supporting hydrostatic pressure is removed from the banks undermined at high stages. Consideration of these river bed "gyrations," prompts a remark about hydrographic surveys; namely, that new bed configurations will be found just as often as such surveys are made, and the only really "complete" survey, would be a continuous motion picture of the river bed.

This discussion of the rise and fall of crossings, in sympathy with changes in discharge, is presented for the purpose of relating it to the sand wave phenomenon, as one of the two major influences, affecting resistance to flow. It is hoped that the discussion will focus attention on a major hiatus in bed load studies; that is, the special nature of bed load movement in bends, which is so unlike bed load movement over crossings (or in glass sided troughs in laboratories), that it may be considered as virtually a completely different type of movement; that is, there may be an intermittent movement from bend to crossing (or vice versa depending upon stage) and a continuous "through freight" movement, going on in parallel.

The conclusion cited, concerning sand waves and sand wave systems, was influenced by several empirical sources: namely, (1) long experience in hydrographic surveys, originally by piano-wire lead-line and circle-sounding equipment, and, since the 1930's, by one of the early applications of sonic soundings; (2) routine sailing-line fathometer channel patrols for navigation, (3) evidence, from a steamboat pilot house, of uniformly spaced "reefs" on the convex side of bends, having (at this location) gradual upstream slopes, over which the water flows at high velocity, and short abrupt downstream slopes, forming comparatively deep and still pools, which sharply check the flow, and (4) experience in paddling a canoe, rowing a skiff, and swimming among such "reefs," when all these means of locomotion gave personal confirmation of the flow conditions described.

The final conclusion is that these "reefs" extend into the channel, as deeply submerged sand waves, where they continue to produce the same effects as in the shoal water near the sand-bar shore; that is, they generate turbulence. This paper deals principally with these "reefs" as constituting a "primary"

wave system; that is, the "secondary," and "tertiary" wave systems (both in evidence), are not given much consideration. The term "wave" will be restricted to these primary waves, and the secondary and tertiary waves will be referred to as "ripples."

Preliminary Field Investigations

Continued speculation on the sand waves, led to the decision to make a preliminary field investigation: If the results warranted it, more extensive investigations could then be made, and any such preliminary work would determine the nature and direction of the more extended study.

It should be noted here, that such investigations would be entirely impractical except by the use of the fathometer to obtain a continuous profile along the path of travel; that is, no amount of conventional hydrographic surveying could yield the continuous detailed data necessary to study these sand waves. For this reason, previous "sand wave" studies, on the Mississippi, by McMath (around 1880) and Ockerson (about the turn of the century) are of little interest.

A preliminary field investigation was arranged late in 1952: Advantage was taken of a regular Navigation Channel Patrol trip of the stern-wheel Steamer General John Newton to obtain a continuous fathometer profile of the "sailing-line" from New Orleans to Old River, a distance of some 200 miles. The horizontal scale ranged from 30 to 40 inches to the mile, and the vertical scale was one inch to 10 feet. The observations, on this trip, confirmed the general occurrence of sand waves over the crossings and around the bends.

Hypothesis

The following 4-point hypothesis was formulated on the basis of accumulated empirical experience and the results of the first fathometer "sailing-line" profile.

Point (1)

Sand waves occur generally on the bed of a river in a systematic manner, and they vary in a systematic manner with changes in discharge.

Point (2)

The sand waves tend to become larger with increases in discharge and smaller with decreases in discharge.

Point (3)

There is a lag in the rate of change of sand waves, and, on a continuously rising river, the waves are somewhat "smaller than they should be," and, on a falling river, they are somewhat "larger than they should be."

Point (4)

These waves constitute a major element of resistance to flow.

Corollaries

These corollaries proceed from the hypothesis:

Corollary (1)

Roughness, or resistance to flow, is not an accident or an attribute of the soil formations through which a river flows, but is rather a property, or condition, of the river bed, controlled by the river itself.

Corollary (2)

The fact that the "rating curve," at any given station, is a "loop" (Fig. 1) rather than a "curve" may be partially explained on the basis of a "lag" in sand wave adjustment; that is, the smaller waves present, on a rising phase, offer less resistance to flow, and the larger waves present, on a falling phase, offer more resistance to flow.

The over-lapping phenomenon, of rise and fall of river crossings, also operates to produce the conditions recorded by the "loop" rating curve.

Corollary (3)

Slope itself (in a local sense) tends to become a "result" rather than a "cause."

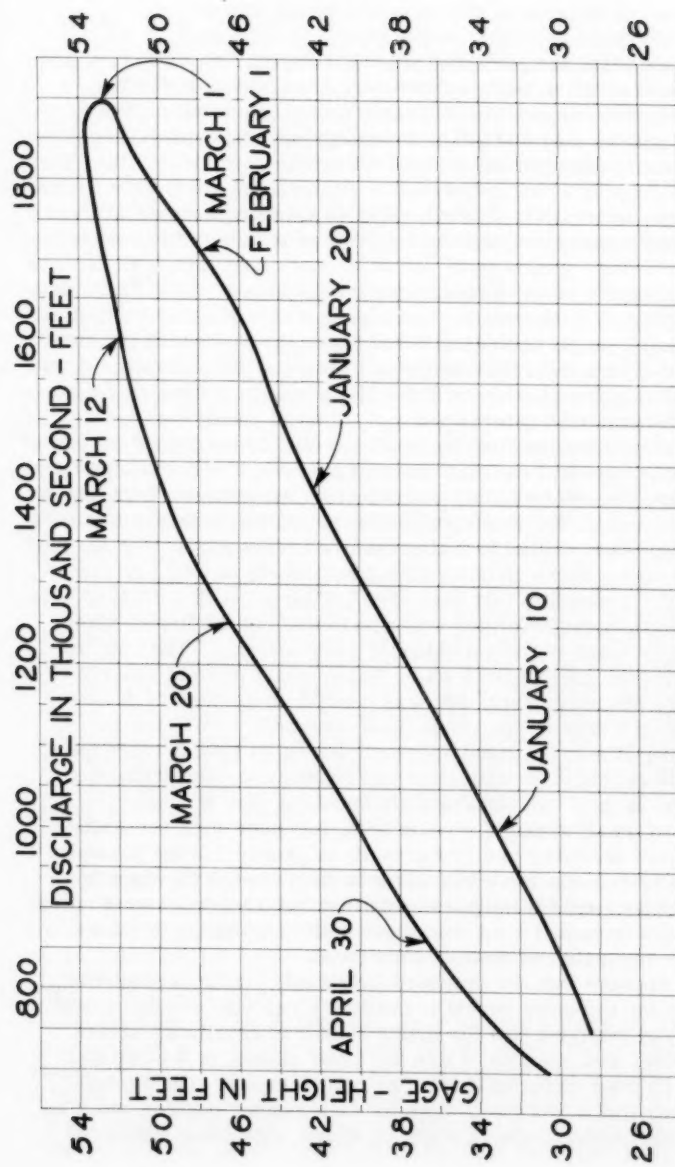
Underlying all this discussion, is the assumption that, with discharge and other governing conditions constant, a stream will produce a system of sand waves, which remains constant, as to size and shape of individual waves, and as to the wave "system." The implication is that, during a cycle of rise and fall, bed adjustment cannot take place, with sufficient rapidity, to be, at all times, in accord with the instantaneous demands of the varying discharge.

Extended Field Observations

Since the initial field observation in 1952, observations, on an extended basis, have fully confirmed that sand waves exist in a systematic manner, and vary in accordance with some orderly influence. Although the "systematic" occurrence is clear from visual inspection of the profiles, the influences governing the "system" are less clear. There are, however, definite indications that "individual waves" and "wave systems" vary in sympathy with changes in discharge, and there is some likelihood that a certain type of wave and wave system will be found to be associated with the horizontal alignment at any location.

As to the effect of increased discharge in increasing wave size, there was early evidence of an "anomaly;" that is, it was noted on two occasions, when the river rose to nearly bankful, that the "tops" of some crossings became perfectly smooth: The word "anomaly" is employed because waves were still present, on the upstream and downstream slopes of the crossings and around the bends, and the waves, where present, were larger than at low water. This behavior, of the tops of crossings, will be an interesting facet of study to pursue further, when high over-bank river stages again occur.

As a first result of these field observations, the following tentative deductions are advanced: The direct effect on resistance to flow, of the size and shape of the particles on the river bed (i.e., those on the immediate surface at a given instant), may be small in comparison with the effects of the successive orders of waves and ripples. Since the "primary" sand waves are so large, as to virtually constitute major river-bed "topography," it appears possible that their frictional effect is great as compared with, either the effect contributed by the lesser orders of waves (i.e., "ripples"), or the theoretical "drag" effect. Finally, it may be that the sizes and shapes, of the grains, are ultimately significant, not because of their direct effect upon friction, but because of their indirect effect, in governing the formation, size and systematic variation of the primary sand waves and "ripples" on the river bed. It also appears likely that the size range of particles, present on the river-bed surface, at any given time, is subject to control by the river, itself,



MISSISSIPPI RIVER
TARBERT LANDING, MISS.
RATING CURVE
1950 FLOOD

as seems to be the trend of opinion in recent papers, based on laboratory and field measurements, and analytical studies.

The observations, on which this paper is based, were entirely fathometer profiles; that is, no studies were made of sand sizes, the manner of adjustment of the waves, their speed of movement, or other associated phenomena.

Views on Sources of Friction in Alluvial Rivers

Various hydraulic texts and published papers, treating flow of rivers, bed load movement, and related questions, have been examined in order to develop the thinking with respect to systematic variations in the river bed (i.e., sand waves, and the rise and fall of crossings) as major phenomena governing resistance to flow and the general behavior of alluvial rivers. In general, the broad subject, of such systematic changes, does not seem to enter into formal river hydraulics: Rather, there is extended consideration of friction as such, and a change in attitude, over the years, as to the causative factors.

The generally accepted view, of earlier writers, appears to have been that "roughness" is a property, inherent in the channel, and ultimately related to the nature of the soils, or the geological formations, through which the river carves its channel. The impression seems to have been that, whatever it was that controlled friction, it was constant for a given reach, or even an entire river, once its value had been determined.

Another group of writers, relates the friction to the "sand paper" or "drag" effect of the particles, present on the surface of the bed. Some go further and indicate a belief that the river exercises a selective influence over the sizes of grains, actually present under any particular condition. Still other writers take a position, somewhat related to that presented in this paper; that is, sand waves and ripples, are a factor in determining resistance to flow. At least one has indicated the possibility that the waves get larger with increased discharge. Another thought the river bed would be smooth at the lowest stage.

Still other writers make river bed behavior very complex: They put unlimited trust in involved mathematics which finally rests on field observations, or laboratory measurements, that may contain an element of dubiousness. By insisting on a detailed particularized approach, they implicitly reject the possibility of a generalized approach, based on laws or principles, perhaps susceptible of initial identification and subsequent measurement on an empirical basis. It may be, figuratively speaking, that microscopic work on sand grains, and small areas of stream beds, has prevented recognition of (1) the need to view the river bed continuously in profile; (2) the possible significance of the systematic river bed changes discussed in the opening paragraph of this paper, and (3) the possibility that bed-load movement in the bends, is so different from bed-load movement in the crossings, that they constitute virtually separate and distinct phenomena.

Summing up, it appears that the proposed hypothesis conflicts somewhat with both the older and the more recent prevailing views concerning causes of flow resistance, by implying that the major source of resistance arises from systematic river-bed changes, which the river makes, of its own volition, and modifies to meet changing discharge requirements. The overall conception is a river which lets itself down its valley under control, much as a person controls his descent, down a flight of stairs, with some additional

control obtained by sliding his hand down the bannister. Final support, or partial refutation, of the four-point hypothesis, awaits additional fathometer observations at overbank stages, and comparisons of the resulting profiles with similar profiles, taken at lower stages. Because of the prolonged low stages, due to the drouth, no overbank stages have occurred in the five years, since interest in this subject came to a head.

Comparisons of Fathometer Sailing-Line Profiles

Successive sailing-line profiles were run, over several years, under various conditions of discharge. These profiles have been studied to detect systematic variations, and to select half-mile "study-reaches" for comparing such variations. The results of these studies have been incorporated in the figures, now to be discussed:

Each figure has a vicinity map to show the river configuration above and below the selected "study-reach." There is also a condensed "sailing-line" profile, extending above and below the study-reach. The location of the study-reach itself is shown on the map and on the profile. Finally, the half-mile study reach itself is shown to full scale, for each of the conditions, to be compared.

In viewing the full scale study-reach profiles, it should be noted that the sand waves are somewhat distorted: This is due to the fact that the "vertical" axis of the fathometer chart is a curve; hence, it is "vertical" only at the center of the chart, is inclined up and to the left on the lower half, and is inclined up and to the right in the upper half of the chart. The vertical scale is as indicated by the depth numerals, and the horizontal scale is as indicated by the marks, which set off 20ths of a mile, or roughly 250 feet.

Figs. 2, 3, and 4

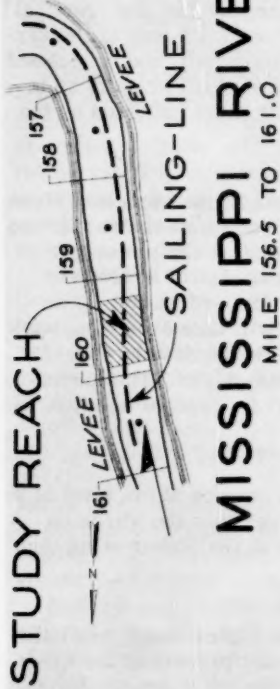
A fairly typical crossing: In fig. 2, at the higher stage, the upstream slope has smoothed off, but there is a well developed wave system on the rest of the crossing, and the waves are larger at the high stage than at the low stage. Note that the amplitude of the waves, on figs. 3 and 4, is nearly 30 feet and that the normal primary waves have formed on these "Super" waves. It is suspected that the "Super" waves, just forming here, will take over completely at higher than bankful stages. In fig. 4, the waves, on the downstream crossing slope, are of about the same amplitude at both stages. This deviation from the hypothesis, cited earlier, does not affect its general validity, as will appear in due course.

Figs. 5 and 6

Both of these figures deal with the lower end of a crossing at the start of a bend. In fig. 5, the waves on the higher stage are larger than the waves on the lower stage. In fig. 6, the waves are much larger at the higher stage than at the lower stage.

Figs. 7, 8, 9, and 10

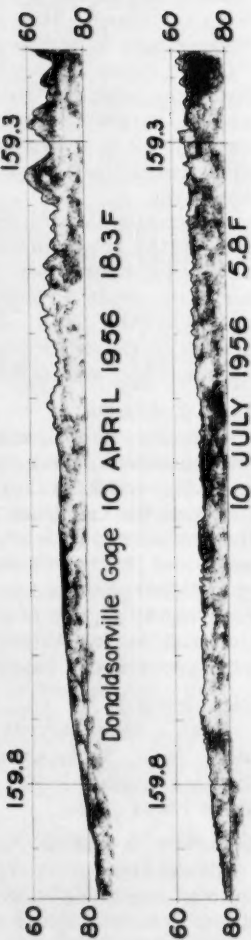
To the right of fig. 7, the Sand Wave System for the higher stage, has built up to an amplitude of about 10 feet. These waves are not present at the lower stage. Note that the crossing has smoothed off at the higher stage. In fig. 8, a "Super" Sand Wave System has attained an amplitude of over 20 feet, at the higher stage. Note that the normal primary waves are superimposed on the "Super" system. At the lower stage there is no significant wave system. In



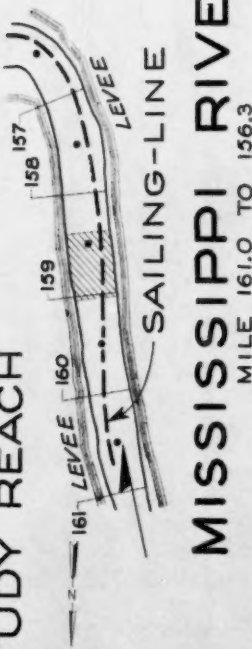
SAILING-LINE PROFILE 10 APRIL 1956



SAND WAVE SYSTEMS



STUDY REACH



SAILING-LINE PROFILE 10 APRIL 1956



SAND WAVE SYSTEMS

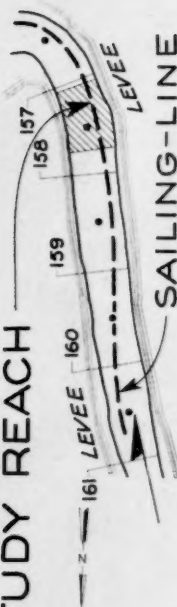


Donaldsonville Gage 10 APRIL 1956 18.3F



Depths: Feet Below W.S.

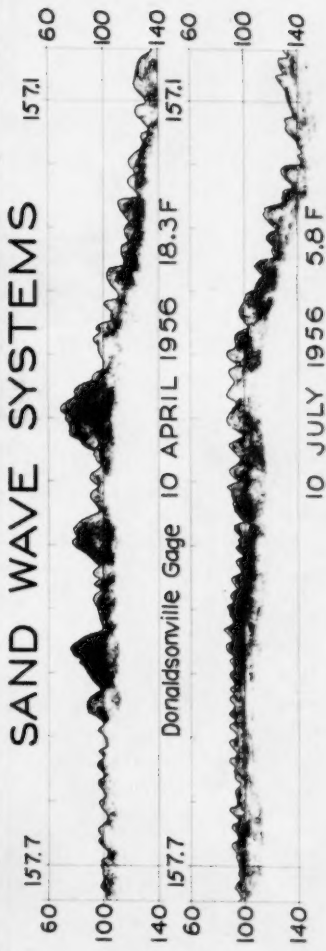
STUDY REACH



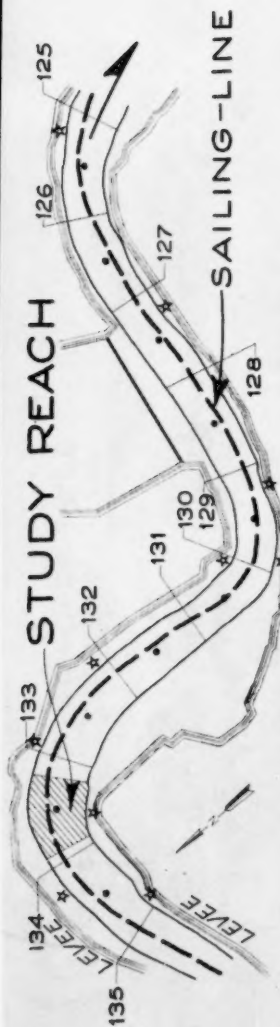
MISSISSIPPI RIVER

MILE 161.8 TO 156.3

SAILING-LINE PROFILE 10 APRIL 1956



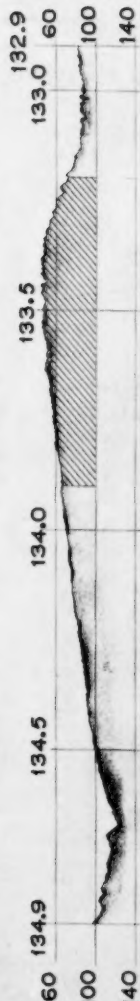
Depths: Feet Below W.S.



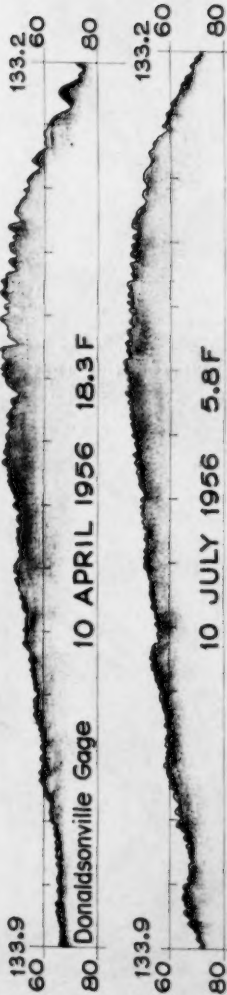
MISSISSIPPI RIVER

MILE 135.0 TO 125.0

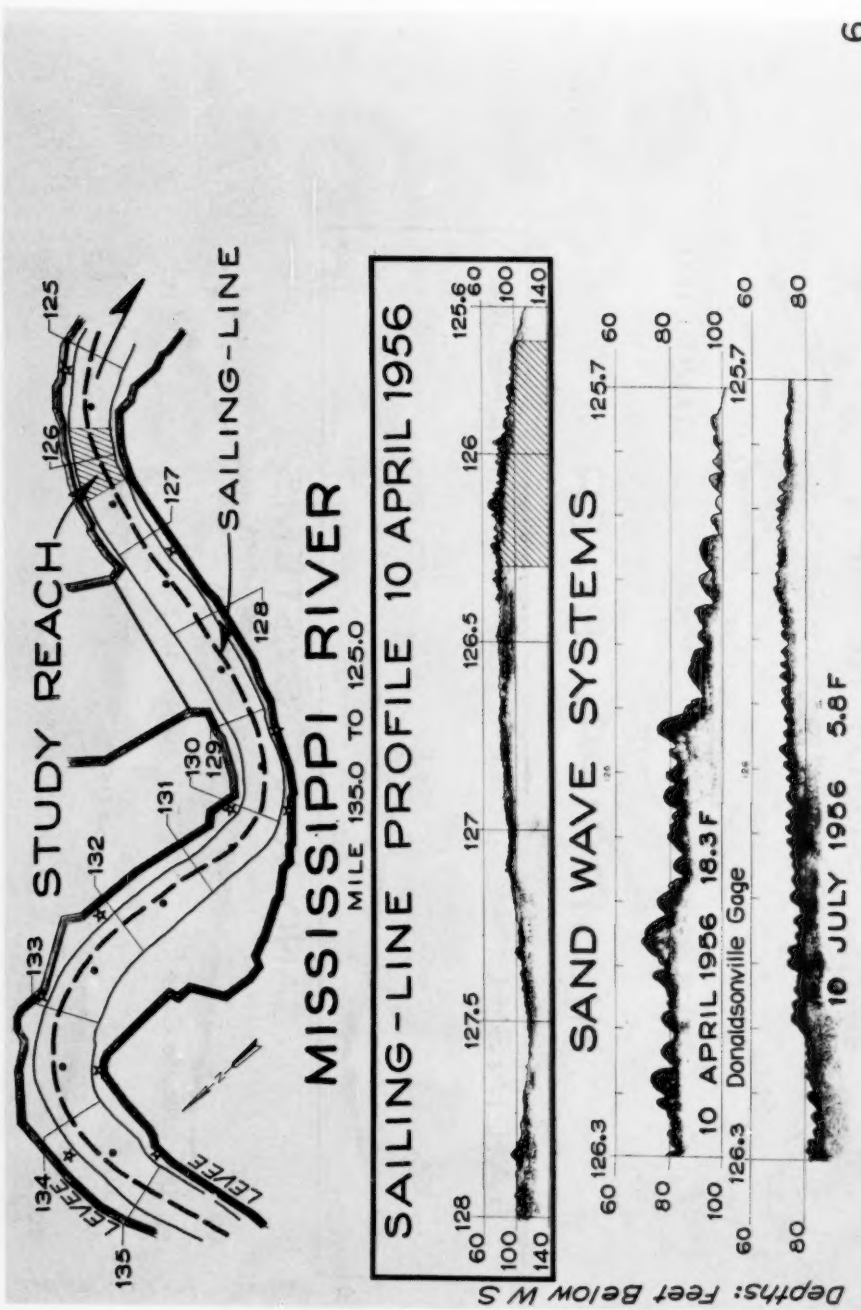
SAILING-LINE PROFILE 10 APRIL 1956

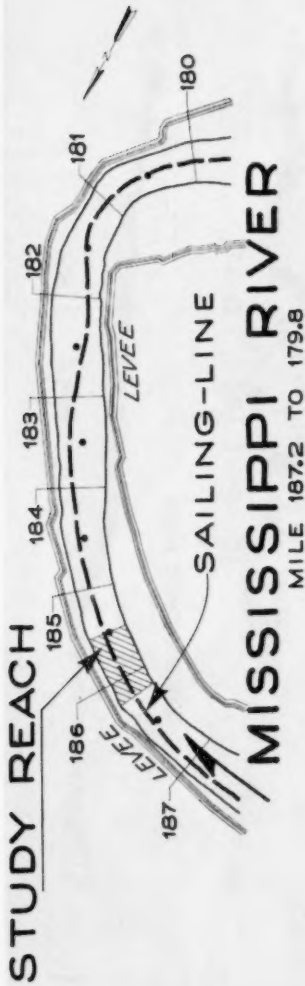


SAND WAVE SYSTEMS



Depths: Feet Below R.S.

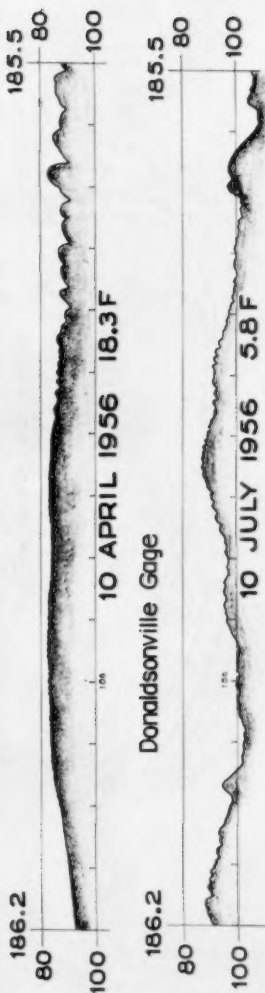


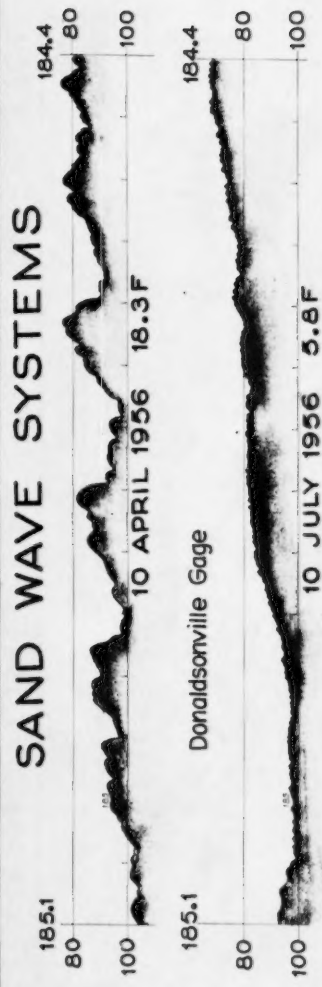
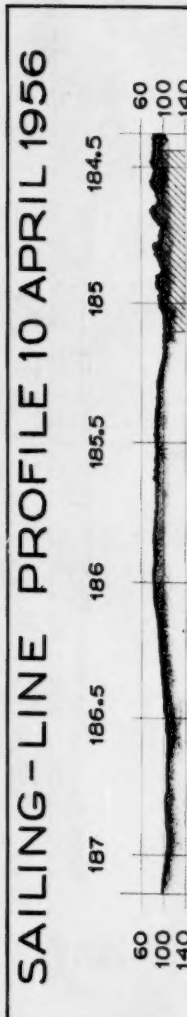
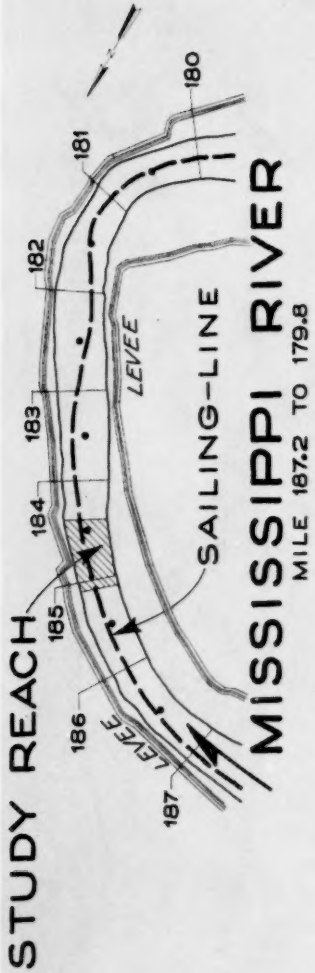


SAILING-LINE PROFILE 10 APRIL 1956

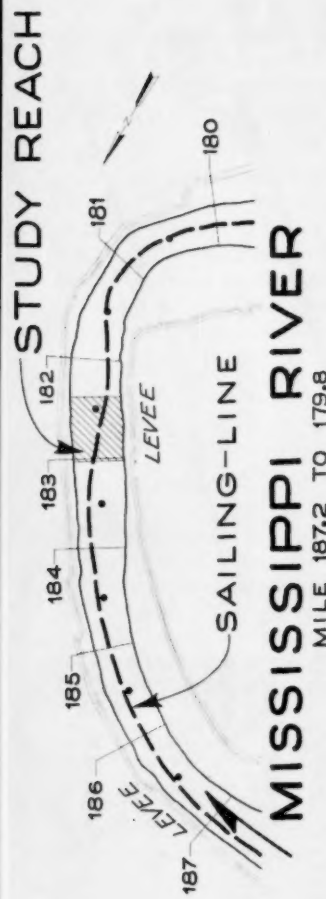


SAND WAVE SYSTEMS





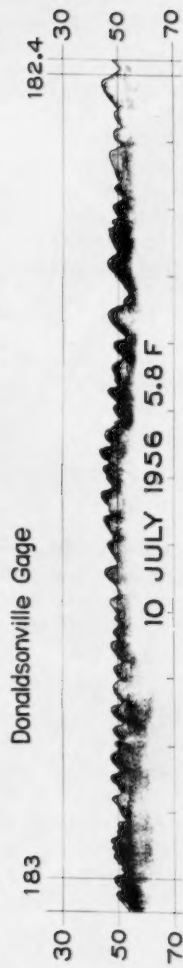
Depths: Feet Below Ws



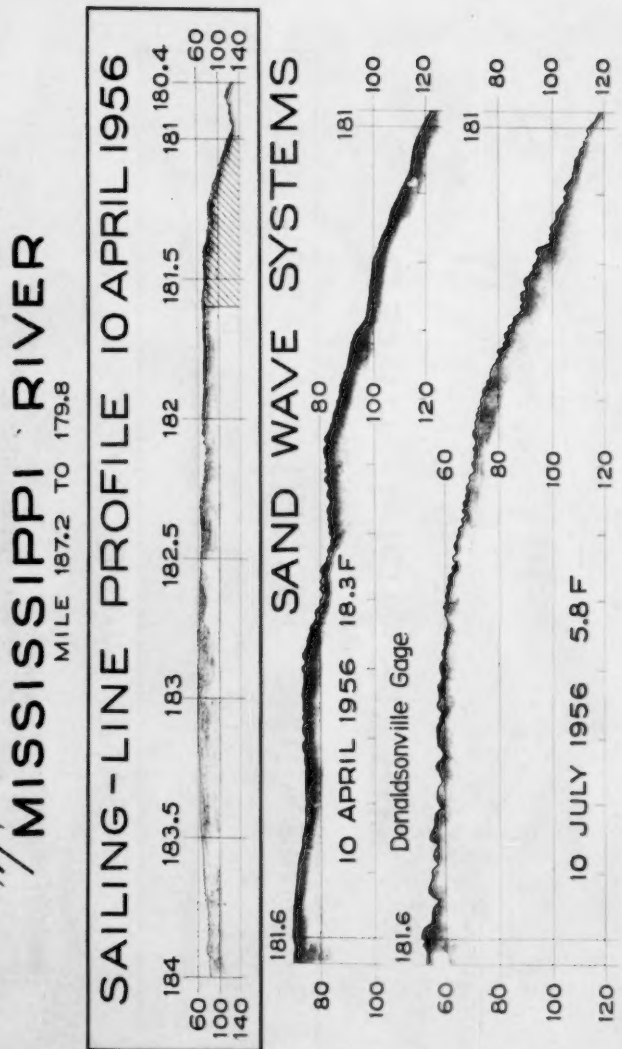
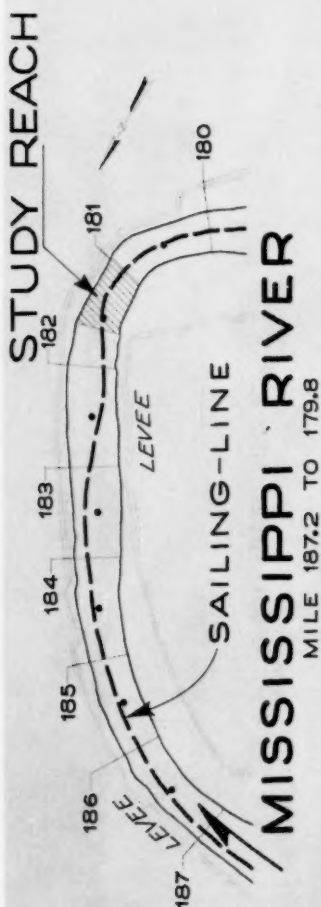
SAILING-LINE PROFILE 10 APRIL 1956



SAND WAVE SYSTEMS



Depths: Feet Below WS



Depths: Feet Below WS

fig. 9, the explanation for the system of large waves, at the lower stage, is that this is the same system of large waves, as shown in fig. 8, moved downstream. As the stage drops, it is possible that the waves migrate downstream, decreasing in size as they move. In fig. 10, the waves in these two systems are not too different; possibly because of the equalizing effect of the wave migration, as indicated in figs. 8 and 9. Note that the downstream crossing slope has been somewhat smoothed off, at the higher stage.

Fig. 11

This figure shows "Grandview Reach," a long "reach" that has been historically stable. At the far left, for the highest stage, there is a well developed wave system with an amplitude of about 10 feet; at the middle stage, the wave system has migrated to the center of the study reach and the amplitude has decreased to about 4 feet; and, at the lowest stage, the major wave system has migrated further downstream and the amplitude has decreased to 2 or 3 feet.

Fig. 12

This figure shows a rapidly caving bend above Baton Rouge: This bend is composed almost entirely of sand to the top of the bank. The unusual shape of the waves at the high stage is due to the reduced horizontal scale of this figure. The steep slope from the lower end of the crossing to the head of the bend has smoothed off at the high stage. This bend has caved at the average rate of 5,000,000 cubic yards per year for the last 16 years and has moved back 70 feet per year at the point of greatest caving.

Figs. 13 and 14

Note the unusual alignment of the river in this vicinity. The waves are larger on the higher stage. In fig. 14, there are indications of "Super" waves, on which the normal primary waves are superimposed.

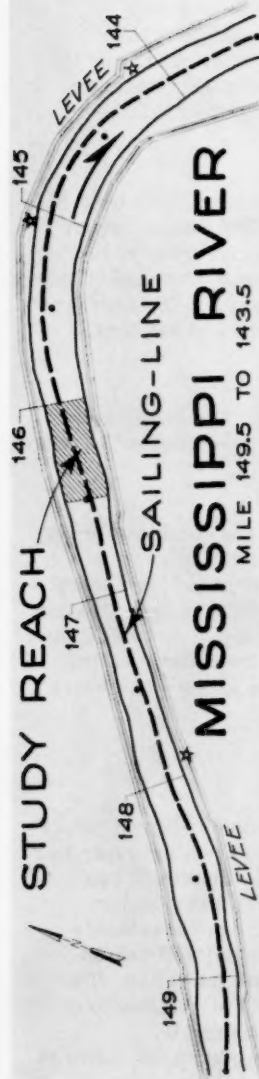
Figs. 15 and 16

These figures show a typical crossing: Fig. 15 shows the upstream crossing slope, and fig. 16 the downstream crossing slope. In fig. 15, there is a well developed "Super" wave system, on which are superimposed the normal primary waves. However, at the lower stage, only the normal primary waves are present. Fig. 16, shows rather symmetrical and consistent wave systems, at both stages. There are also indications that there has been an "equalization" of the wave systems, at higher and lower stages, due to the migration of the larger waves from the upstream crossing slope.

CONCLUSIONS

These studies afford substantial support for three of the component points of the hypothesis; namely, (1) that sand waves exist generally on the river bed in a systematic manner; (2) that sand waves tend to vary in amplitude and spacing, in accordance with variations in discharge; and (3) that a major source of resistance to flow, in an alluvial river, is provided by a primary system of sand waves, which, in turn, is created by the river itself and operates as a means of controlling its orderly progression down its valley. The fourth "point," that the waves constitute a major component of resistance to flow, has not been confirmed, although it still appears reasonable.

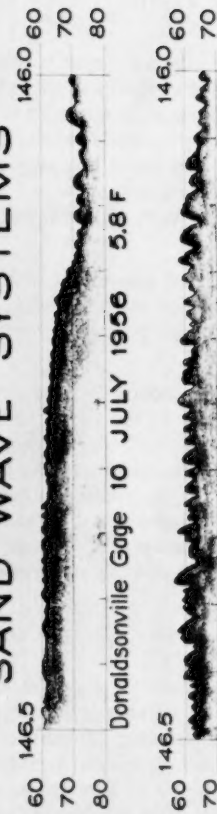
The fathometer profile observations, on which this paper is based, covered



SAILING-LINE PROFILE 10 JULY 1956



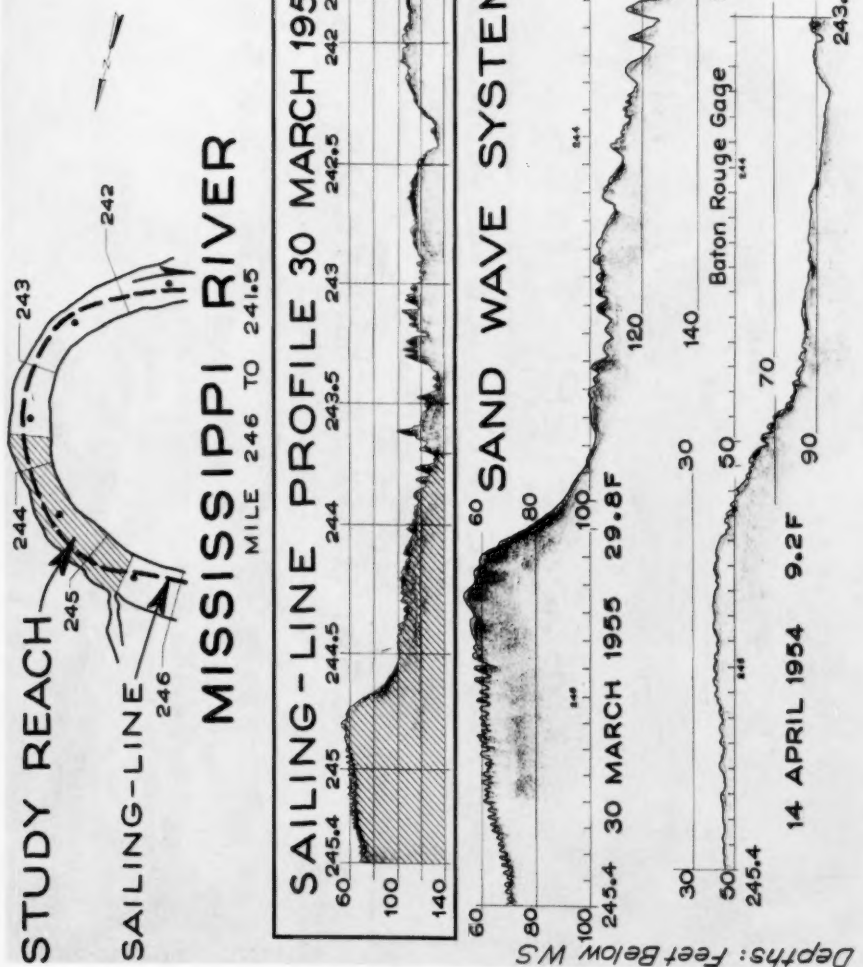
SAND WAVE SYSTEMS



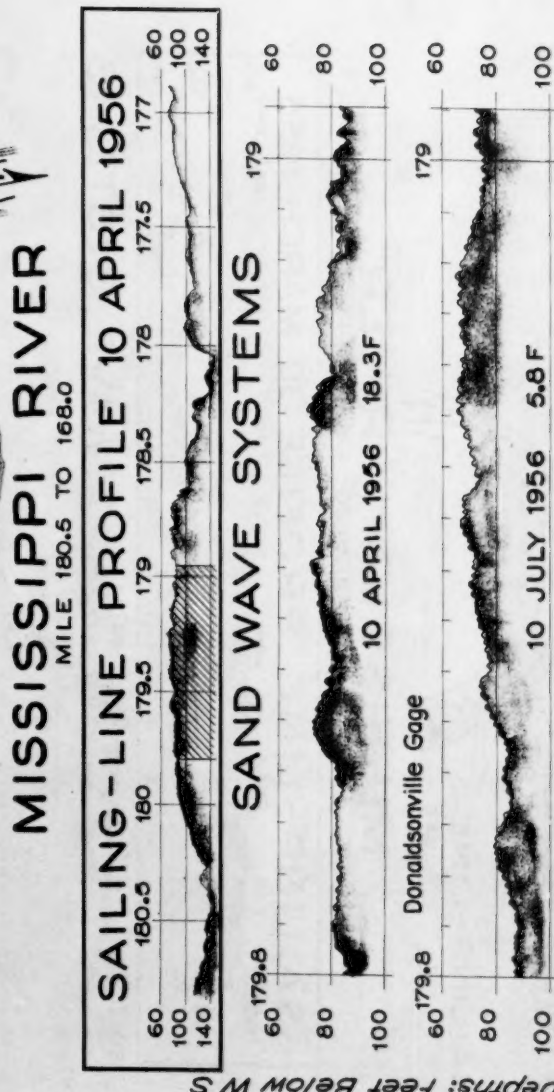
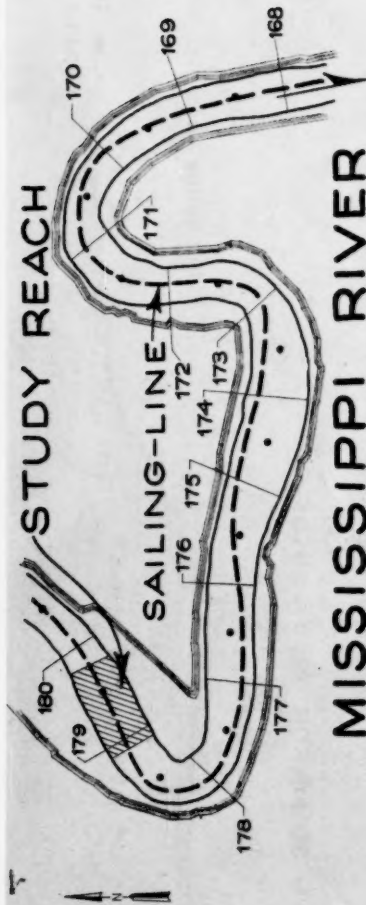
11 MAY 1956 13.4 F



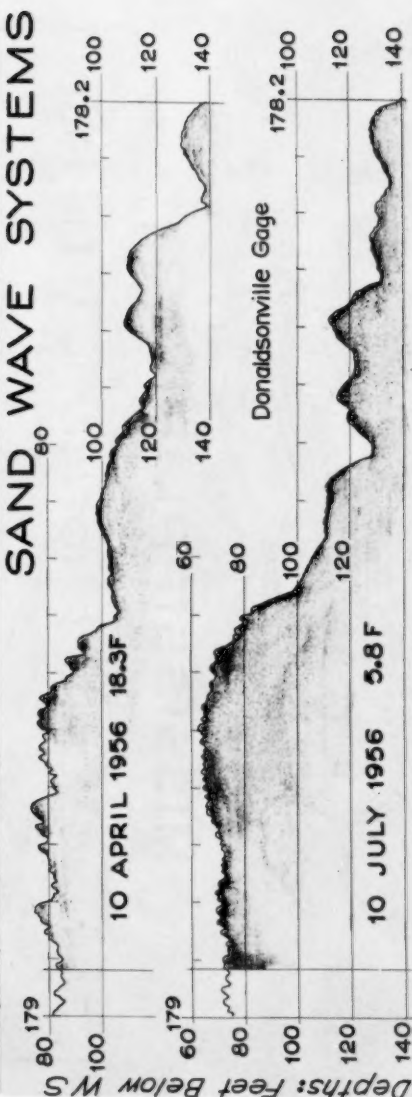
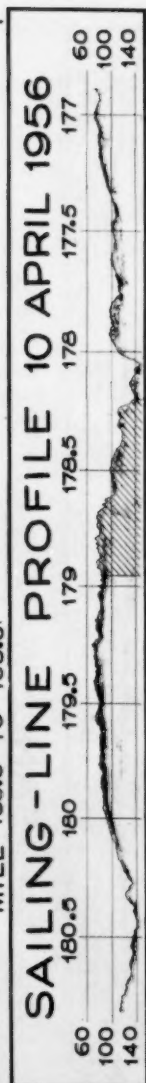
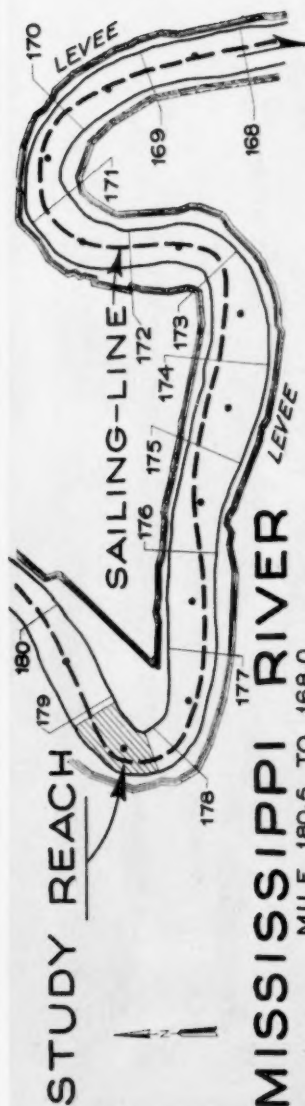
Depths: Feet Below W.S.

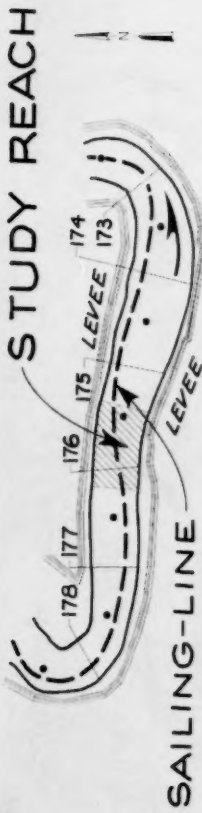


Depths: Feet Below W.S.



Depths: Feet Below W.S.





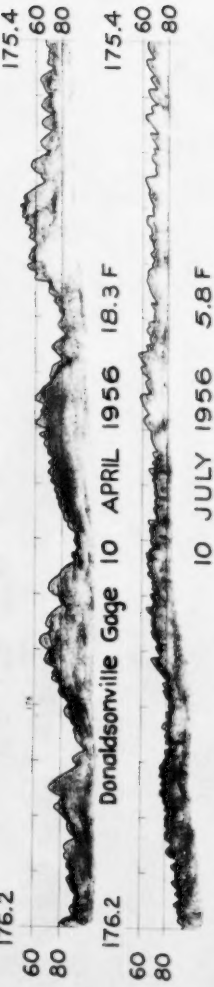
MISSISSIPPI RIVER

MILE 178.5 TO 172.5

SAILING-LINE PROFILE 10 APRIL 1956



SAND WAVE SYSTEMS

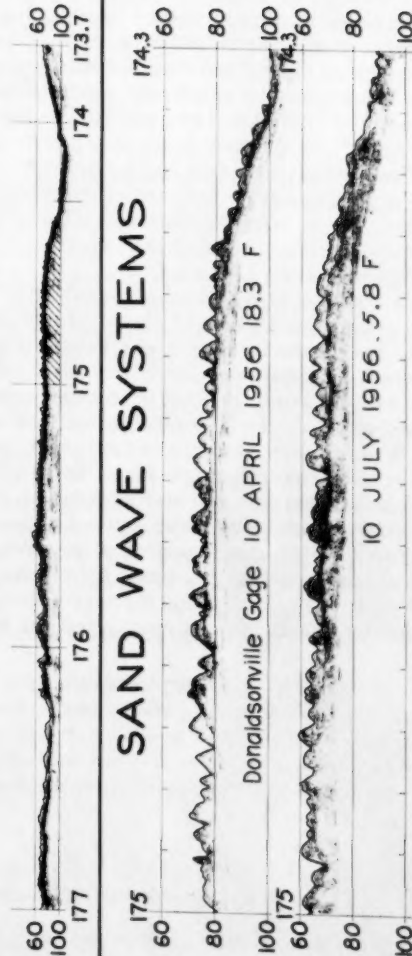


Depths: Feet Below W.S

10



MISSISSIPPI RIVER
MILE 176.5 TO 172.5
SAILING-LINE PROFILE 10 APRIL 1956



Depths: feet Below W.S.

a limited range of river stages, and the value of the conclusions, derived therefrom, is correspondingly limited. The paper will serve its purpose if it demonstrates the existence of a practical field of investigation that may lead to useful knowledge concerning; (1) the adjustment of sand wave formations, (2) the rise and fall of crossings, (3) the special character of bed load movement in bends, and (4) the joint bearing which these phenomena have upon resistance to flow.

Federal Agencies, engaging in planning, constructing and operating water resources projects, can often gather data on river bed conditions at little expense over that of the fathometer paper involved; as, for instance, in the case of channel patrols for navigation. In general, observations can be made at full cruising speeds on trips for other purposes, or on the idle return trips from other missions. Either the "sailing-line," the "thalweg," or the river "center-line," can be followed, as may be convenient, and it is not necessary to cover an "area" in order for the data to be useful. Working up the data, can conceivably be relatively inexpensive. A point to note is that studying "lines" or "profiles," has much to be said for it, as against studying "cross-sections": In the first place, the key to studying these river bed phenomena is "continuity," and this is something "cross-sections" cannot supply, despite the great amount of field and office work involved; in the second place, a "line" can be taken as representative of a "volume" within certain limits, if proper lateral-control of the line is provided, and known points are selected for linear-control "fixes."

After a certain amount of "qualitative" study of "lines," to determine the manner and magnitude of river bed adjustments, ways and means will probably be evolved to use the same data to make "quantitative" determination of the bed-load material movement involved in the sand waves and in the rise and fall of crossings; that is, the material that probably has the most profound effect on the hydraulic properties of streams.

In conclusion, it appears likely that organized study of these phenomena of river bed behavior, might have these effects: (1) throw new light on some theoretical aspects of river hydraulics, (2) indicate a better approach to planning and constructing bridge piers, pipe-line crossings, etc., and (3) point the way to a better understanding of the hydraulic results of comprehensive river stabilization and lay the basis for extending the claimed economic benefits, for such work, far beyond the mere protection of lands and improvements from the effects of bank caving and bar building.

Journal of the
HYDRAULICS DIVISION
Proceedings of the American Society of Civil Engineers

SYNTHETIC STORM PATTERN FOR DRAINAGE DESIGN

Clint J. Keifer¹ and Henry Hsien Chu,² Associate Members ASCE
(Proc. Paper 1332)

SYNOPSIS

The City of Chicago has been engaged in an extensive auxiliary outlet sewer construction program since the end of World War II. Bond issues totaling more than \$88,000,000.00 have been passed to finance this program. The engineers of the Sewer Planning Division felt it worthwhile to make a comprehensive study of the principles involved in the rainfall-runoff relationship in order to economically utilize this expenditure. The development of a synthetic storm pattern, for use in the hydrograph method of sewer design, is one phase of this research, and is the theme of this paper.

INTRODUCTION

It is the purpose of this paper to present a method of determining a storm pattern which may be used in the hydrograph method of sewer design.^(1,2,3) This storm pattern will be developed from a rate-duration-frequency curve selected for use in design. It will also be shown that although this storm pattern will include the average intensities of the rate-duration curve for all durations, it will produce no greater runoff peaks than that of the rainfalls of the separate durations.

The chronological location of the peak period of rainfalls with reference to the total storms period and the amount of antecedent precipitation immediately preceding the maximum period of any durations will be derived from the statistical average of rainfall records. The importance of this antecedent rainfall in affecting the peak of the runoff hydrographs will be illustrated.

Note: Discussion open until January 1, 1958. Paper 1332 is part of the copyrighted
Journal of the Hydraulics Division of the American Society of Civil Engineers,
Vol. 83, No. HY 4, August, 1957.

1. Senior Sewer Designing Engr., City Bureau of Eng., Chicago, Ill.
2. Civ. Engr., City Dept. of Public Works, Chicago, Ill.

Rainfall Characteristics Affecting Runoff

The rainfall and resulting runoff hydrograph should be analyzed in order to determine what other characteristics, besides the average rate of water falling within a given time period, would tend to affect the peak rate of runoff. If in one rainfall, some precipitation preceeded the maximum period, filling many of the surface depressions, wetting all surfaces and satisfying the greater infiltration capacity of the soil, the peak runoff rate would be higher than from another rainfall having the same intensity during the maximum period but lacking the antecedent rainfall. In the development of a synthetic storm pattern for use in the hydrograph method, the right amount of antecedent rainfall must be replaced in front of the statistical volume of rainfall occurring within the maximum period.

Another important characteristic that affects the peak rate of runoff with a given volume of water falling in a specific period, is that of the variation of rainfall intensities within that time period. Consider a long duration rainfall in which most of the precipitation falls in the early part of the period. In this case, the greater infiltration capacity at the beginning and the surface depression storage would absorb much of the peak rainfall, thus making the runoff rate approach a lower value of equilibrium. On the other hand, if the bulk of precipitation occurred in the latter portion of the period, most of the previously mentioned losses would be already satisfied before the time of peak rainfall intensity, and a higher peak rate of runoff would result.

To sum up briefly, the three most important characteristics affecting the peak runoff rate for a specific period or duration are as follows:

1. Volume of water falling within the maximum period,
2. Amount of antecedent rainfall,
3. Location of the peak rainfall intensity.

A synthetic rainfall encompassing the statistical average of these three characteristics should then be adequate for use in the hydrograph method as the design storm pattern for any given duration, see Figure (1).

Evaluation of the First Characteristic for Single Storm Pattern

The volume of water falling within the maximum period can be taken from the rate-duration curve of a given frequency selected for design purposes. The equation for this rate-duration curve may take the following form:

$$i_{av} = \frac{a}{t_d^b + c} \quad (1)$$

where i_{av} is the average intensity in inches per hour, t_d is the duration of the maximum period in minutes, and a , b and c are constants. The volume of water falling, or mass rainfall for any duration is graphically represented by the area of a rectangle of which the upper right-hand corner touches the rate-duration curve, see Figure (2). This rainfall mass, in inches, can then be expressed by

$$P = i_{av} \frac{t_d}{60}$$

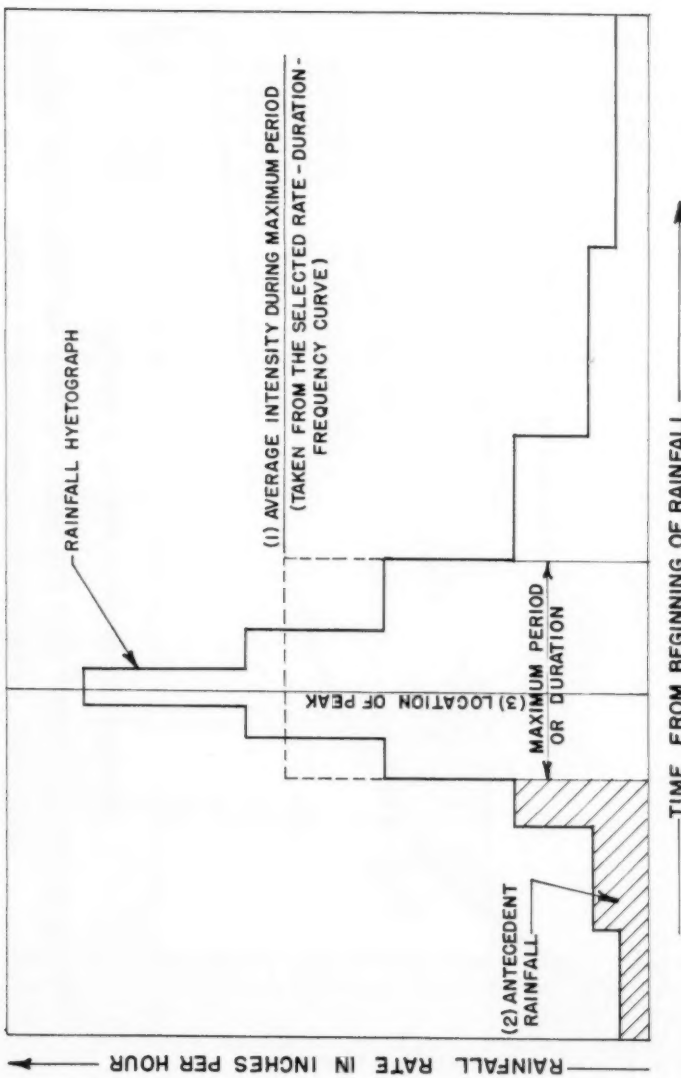


FIGURE 1-A RAINFALL HYETOGRAPH SHOWING THE THREE MOST IMPORTANT CHARACTERISTICS AFFECTING THE PEAK RATE OF RUNOFF.

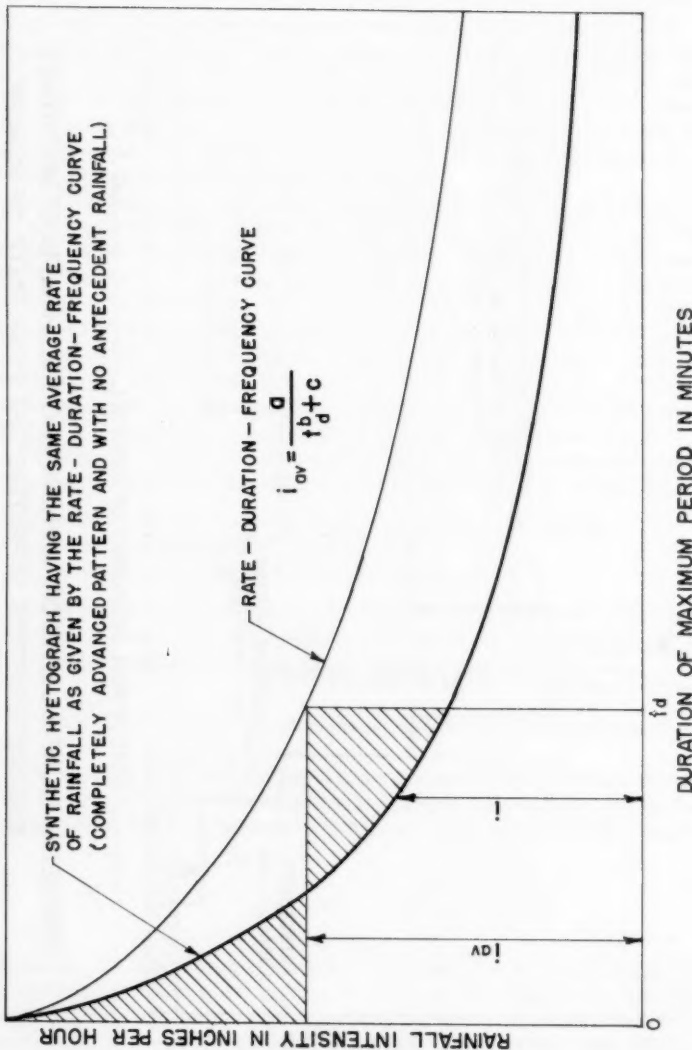


FIGURE 2 - DEVELOPMENT OF A SYNTHETIC STORM PATTERN FROM THE ACCEPTED RATE-DURATION-FREQUENCY CURVE.

Substituting Equation (1) for i_{av}

$$P = \frac{a}{t_a^b + c} \cdot \frac{t_a}{60} \quad (2)$$

First, a completely advanced type rainfall pattern can be developed which has the peak occurring at the beginning, and with no antecedent rainfall. A curve representing the hyetograph of this type of rainfall must have the same average intensity for any maximum period as that given by the rate-duration curve, as shown in Figure (2). The area under the curve of the hyetograph can be expressed mathematically by

$$P = \frac{1}{60} \int_0^{t_a} i \, dt_a$$

where i is the ordinate of the hyetograph in inches per hour.

Differentiating with respect to t_a

$$\frac{dP}{dt_a} = \frac{i}{60} \quad (3)$$

But from Equation (2)

$$P = \frac{a}{60} \cdot \frac{t_a}{t_a^b + c}$$

Differentiating

$$\frac{dP}{dt_a} = \frac{a}{60} \cdot \frac{[(1-b)t_a^b + c]}{(t_a^b + c)^2} \quad (4)$$

Combining Equations (3) and (4)

$$i = \frac{a[(1-b)t_a^b + c]}{(t_a^b + c)^2} \quad (5)$$

Equation (5) then represents a completely advanced type storm having for all durations, the same average intensities as those given by the rate-duration curve. For Chicago area, the accepted rate-duration curve developed by Eltinge and Towne of the Sanitary District of Chicago,⁽⁴⁾ for a five-year frequency, is

$$i_{av} = \frac{90}{t_a^{0.9} + 11} \quad (6)$$

Therefore, the constants in Equation (1) are $a = 90$, $b = 0.9$, and $c = 11$.

Substituting these values into Equation (5), one obtains

$$i = \frac{90(0.1 t_d^{0.9} + 11)}{(t_d^{0.9} + 11)^2} \quad (7)$$

By assuming different values for t_d , Equation (7) represents a storm starting with the rate of 8.18 inches per hour at the first instant and decreasing steeply to 4.42 inches per hour at the end of the 5th minute, to 1.13 inches per hour at the end of the first half hour and so on.

To make Equation (5) applicable to any intermediate type storm pattern the following modifications shall be made: Within the maximum period of any rainfall, the duration t_d can be split up into that part occurring before the most intense moment and that part after the most intense moment. Introduce the symbol "r" to represent that portion of any duration occurring before the most intense moment, expressed as a ratio to the entire duration, refer to Figure (3), and set

$$t_b = r t_d \quad \text{and} \quad t_a = (1-r) t_d \quad (8)$$

where t_b is the time before the peak in minutes, and measured from the peak to the left and t_a is the time after the peak in minutes measured to the right of the peak. The ratio "r" is then a measure of the advanceness of the storm pattern. If $r = 0$, the storm is of the completely advanced type as discussed in the last paragraph. If $r = 1$, the storm is of the completely delayed type, that is, it has its peak at the end of each and every duration and has considerable antecedent rain falling before each and every maximum period. For intermediate type storm patterns, the "r" value will range between zero and one.

Solving the first part of Equation (8) for t_d and substituting in Equation (5)

$$(\text{Before The Peak}) \quad i = \frac{a \left[(1-b) \left(\frac{t_b}{r} \right)^b + c \right]}{\left[\left(\frac{t_b}{r} \right)^b + c \right]^2} \quad (9)$$

Solving the second part of Equation (8) for t_d and substituting in Equation (5)

$$(\text{After The Peak}) \quad i = \frac{a \left[(1-b) \left(\frac{t_a}{1-r} \right)^b + c \right]}{\left[\left(\frac{t_a}{1-r} \right)^b + c \right]^2} \quad (10)$$

A synthetic hyetograph plotted from Equations (9) and (10) will have, for all durations taken during the most intense period, the same average intensity as the rate-duration curve from which the constants a, b and c are derived.

Using the above mentioned constants for the Chicago area,

$$(\text{Before The Peak}) \quad i = \frac{90 \left[0.1 \left(\frac{t_b}{r} \right)^{0.9} + 11 \right]}{\left[\left(\frac{t_b}{r} \right)^{0.9} + 11 \right]^2} \quad (11)$$

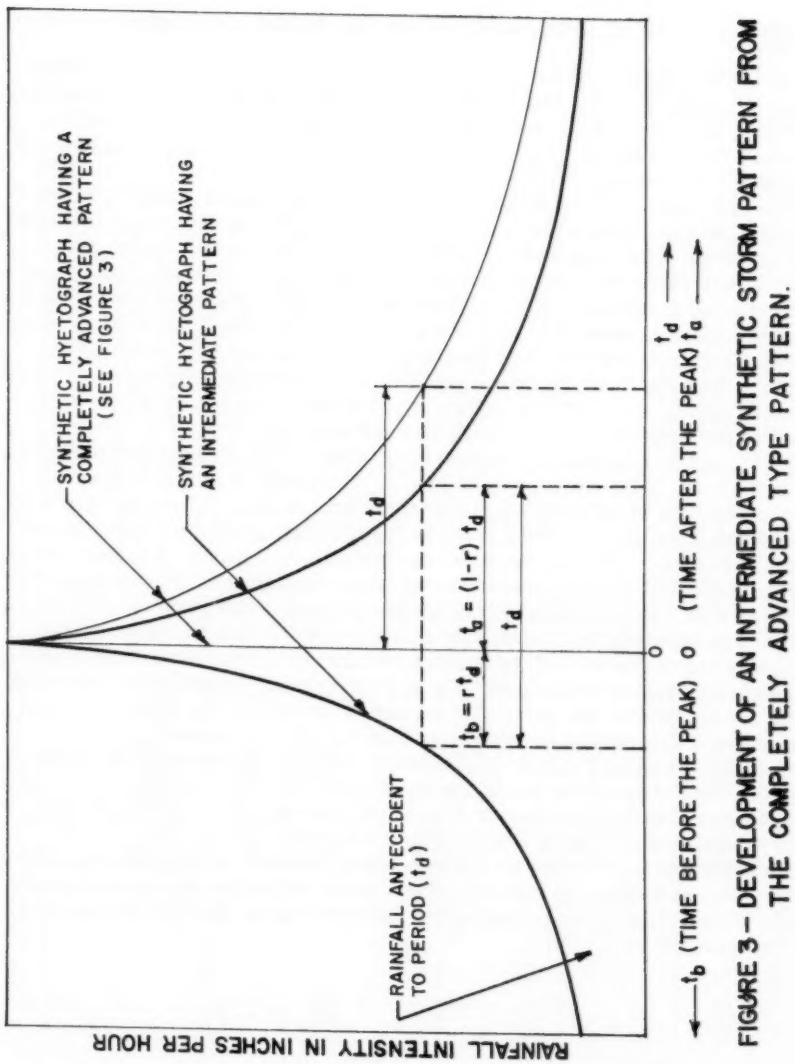


FIGURE 3 - DEVELOPMENT OF AN INTERMEDIATE SYNTHETIC STORM PATTERN FROM THE COMPLETELY ADVANCED TYPE PATTERN.

$$(After \text{ The Peak}) \quad i = \frac{90 \left[0.1 \left(\frac{t_d}{1-r} \right)^{0.9} + 11 \right]}{\left[\left(\frac{t_d}{1-r} \right)^{0.9} + 11 \right]^2} \quad (12)$$

Determination of "r" Conforming with the Second and Third Characteristics

The first characteristic has been evaluated by the development of Equations (11) and (12) from the accepted rate-duration curve. It remains to determine, from records of excessive rainfalls, the best value to assign the constant "r" so that the other two characteristics of the synthetic storm pattern will conform approximately to the statistical data.

Rainfall records were obtained from the Metropolitan Sanitary District of Greater Chicago, where the records of heavy storms from seventeen automatic recording rainfall gauges located in the Chicago area are compiled. Four widely separated stations were selected so as to retain the individuality of each station-rainfall. The four stations were at Loyola University (Station 10), Springfield Avenue Pumping Station (Station 14), The West Side Treatment Works (Station 7) and Roseland Pumping Station (Station 15). Only those rainfalls which at least for some duration are considered excessive, were recorded. Eighty-three station-rainfalls are given, with data taken from the records for durations of 15, 30, 60, and 120 minutes.

In Table 1, the following information is given: For example, at Station 14 on May 11-12, 1935, the maximum rainfall occurring in a fifteen minute period was 0.39 of an inch, while the antecedent rainfall occurring before that period was 1.40 inches. Since the maximum fifteen minute period contains three five-minute periods, the most intense was the second. Likewise, in the same storm at Station 14, the maximum mass occurring in the 120 minute duration was 1.82 inches, only 0.05 inches fell antecedent, and out of the 120 minute duration the twentieth five-minute period was the most intense, therefore the storm was of the delayed type pattern. The blanked spaces indicate those durations within which the maximum mass rainfall was not excessive. These figures are purposely deleted in order that the statistical average obtained will reflect the characteristics of only the excessive storms concerned. The mean values of antecedent rainfall and the location of the peak for each of the given durations were obtained. The mean values of mass antecedent rainfall are plotted in Figure (4), and the mean values for the locations of peak are plotted in Figure (5).

An analytical expression for the antecedent rainfall of the synthetic storm pattern can be derived as follows: For a given "r" value, the mass rainfall within the duration t_d occurring before the peak can be obtained by multiplying Equation (2) by "r," or

$$P_b = r P = r \frac{a}{60} \frac{t_d}{t_d^{0.9} + c}$$

where P_b is the mass rainfall before the peak in inches.

For the Chicago five-year frequency rainfall

$$P_b = r \frac{1.5 t_d}{t_d^{0.9} + 11}$$

TABLE I - RAINFALL RECORDS FROM FOUR STATIONS IN THE CHICAGO AREA

Sta.	Date	15 MIN. DURATION			30 MIN. DURATION			60 MIN. DURATION			120 MIN. DURATION		
		Max. Mass.	Ante- cedent Mass	Peak* Five Min.	Max. Mass	Ante- cedent Mass	Peak* Five Min.	Max. Mass	Ante- cedent Mass	Peak* Five Min.	Max. Mass	Ante- cedent Mass	Peak* Five Min.
14 17 15	May 11-12 1935	.39 .44 .49	1.40 1.01 .46	2 3 2	.67 .76 .83	.67 .65 .46	6 6 2	1.14 1.26 1.44	.44 .60 .31	11 7 4	1.82 1.76 1.76	.05 .10 .20	20 19 6
	14 17 15	.70 .56 .84	.54 .06 .14	2 2 1	.97 .71 1.07	.36 .01 0	3 3 2	1.05 1.22 1.21	.29 0 0	4 2 3			
		.81 .51 1.26	.05 .21 1.57	3 2 1	.90 1.22 2.19	.05 .04 .50	3 3 4	1.02 1.35 2.90	.03 0 .08	7 4 9	1.45 2.99	.01 0	6 16
10 14 15	June 20-21 1937	.51 .51 1.26	0 .23 1.57	2 2 1	.56 1.22 2.19	0 .04 .50	2 3 4	.81 1.19 1.84	0 .05 .01	2 5 3	1.88	0	9
	14 17 15	.51 .40 .91	0 .25 .19	2 2 2	.56 1.22	0 .01	2 3	.81 1.19 1.84	0 .05 .01	2 5 3	1.88	0	9
		.62 .46 .56	.28 .07 .77	2 2 3	.50 .78 .99	.16 .12 .48	3 5 5	.96 1.06 1.29	.06 6 .16	6 1.40	.06	6	
10 14 15	Oct. 3-4 1941	.62 .46 .56	.01 .07 .77	2 2 3	.66 .51 .34	5 2 6	1.06 1.22 1.29	.28 10 10	1.61 1.54 1.54	0 0 .04	3 15		

* The numbers in these columns indicate the ordinal position of the five-minute period, within the duration, containing the most intense rainfall.

TABLE I - CONTINUED

10	July 6	1.09	.60	1	1.86	.60	2	3.61	.60	2	4.83	.10	6
14		1.51	1.58	1	1.27	1.58	1	2.10	.42	9	3.05	0	12
7		1.75	1.17	3	1.91	.17	3	2.55	.17	3	3.38	.01	5
15		1.75	1.38	2	1.02	1.32	3	1.78	.48	10	2.64	0	15
10	June 12	.62	.26	2	.78	.08	5	.89	.01	8	1.43	0	21
14		.97	.45	2	1.00	.42	3	1.04	.42	3	1.43	0	21
7		.72	.04	1	.90	.01	2	.94	0	3	1.43	0	21
15		.80	.17	3	1.06	0	5	1.08	0	5	1.43	0	21
10	August 9	.48	.05	2	.57	.05	2	1.25	0	3	1.54	0	3
14		.90	.14	1	1.17	.01	2	1.25	0	3	1.54	0	3
7		.89	.10	1	1.05	.04	2	1.12	0	3	1.50	0	3
15		.65	.30	2	.81	.30	2	.91	.20	8	1.50	0	3
10	April 4	.46	.20	3	.56	.10	5						
14		.35	.38	2	.51	.22	5						
7		.56	.33	1	.63	.25	2						
15		.45	.48	1	.79	.27	2						
10	April 5	.46	.20	2	.56	.10	5						
14		.38	.82	2	.63	.30	2						
7		.56	.33	2	.71	.32	2						
15		.48	.46	1	.79	.32	2						
10	Sept. 21	.43	1.01	2	.62	1.01	2	1.31	.90	3	1.81	.40	15
14		.48	.79	2	.71	.57	5	1.27	.57	5	1.73	.38	10
7		.39	.54	2	.67	.54	2	1.09	.33	4	1.63	.12	10
10	March 18-19	.60	1.04	3	.90	1.04	3	1.52	.42	9	1.76	.33	15
14		.41	.32	2	.73	.32	2	1.40	.34	2	1.82	.30	4
7		.37	.87	1	.63	.87	1	1.10	.87	1	1.45	.67	10
10	June 2-3	.40	1.03	2	.58	.82	4	1.03	.42	11	1.44	.24	18
14		.57	.58	2	.60	.57	3	1.13	.65	7	1.44	.24	18
15		.57	.78	1	.94	.71	3	1.13	.65	7	1.44	.24	18

TABLE I - CONTINUED

15	June 24	.84	.02	2	.94	0	3	.96	0	3	
10	1950	.40	0	2	.54	0	2				
14	July 8	.42	.06	1	.55	.06	2				
7	1951	.35	.24	1	.61	.10	4				
15		.56	.39	2	.67	.39	2				
14	June 10	.49	.23	1	.72	.09	3	.81	0	6	
7	1953	.36	.29	2	.65	0	5	.80	.10	4	
15		.52	.10	1	.63	.01	3				
10	March 25	.80	.66	1	1.47	.23	3	2.16	.23	3	2.76
14	1954	.38	.34	3	.60	1.00	2	.81	.91	4	.20
15	July 2	1.01	0	2	1.15	0	2	1.37	0	2	1.41
10		.65	0	2	.68	0	2	1.02	0	3	
14	July 3	.91	.01	2	.96	.01	2	.84	0	2	
7	1954	.70	.02	1	.78	0	2	.87	0	2	
15		.69	0	2	.78	0					
10	July 6 A.M.	.74	.03	1	.95	.03	3	1.03	0	4	
10	July 6 P.M.	.45	.32	1	.69	.19	2	.91	0	7	
14	1954	.50	.03	2	.66	.03	2				
10	August 18	.90	1.11	2	.51	.19	5	2.49	0	2	2.66
14	1954	.99	.22	2	1.60	.63	4	1.44	.07	5	1.63
7		.77	.97	3	1.26	.22	2	1.91	0	9	.05
15					1.47	.27	3			0	9

TABLE I - CONTINUED

10	October 3	.45	.30	2	.67	.08	5	.82	.24	3	1.41	.02	7
14		.66	.10	2	.92	0	3	.99	0	4	2.18	0	4
7		.56	.33	2	.97	0	4	1.31	0	2	3.32	.19	24
15		.65	2.13	1	1.08	2.43	6	1.74	.19				
10	October 9	.42	.39	2	.64	.29	3	.95	.21	5	1.43	.21	5
14		.43	1.31	3	.55	1.28	4	1	1.33	.48	1	2.12	.33
15		.46	.48	1	.92	.48							4
10	October 10	.56	.29	2	.84	.29	2	.99	.26	3			
14		1.14	.23	2	1.56	.23	3	1.83	.19	4	1.92	.14	15
7		.97	.11	2	1.32	.34	1	1.74	.10	3	1.85	.10	3
15		.99	.15	2	1.26	.01	4	1.30	0	5	1.40	0	5
10	May 24	.35	.24	2									
	1955												
Number of Excessive- ive Station Rain- falls													
Summation		81		80		61		60		56			
Mean		33.73		151		25.95		239		12.40		4.25	
Mean Location of Peak within Rainfall Duration		.410		1.86		.324		2.99		.203		4.78	
		.453				.415				.356			

*Mean location of peak within 15 minute duration derived from (1.86-0.50) 5/15 = .453;
similarly for other durations.

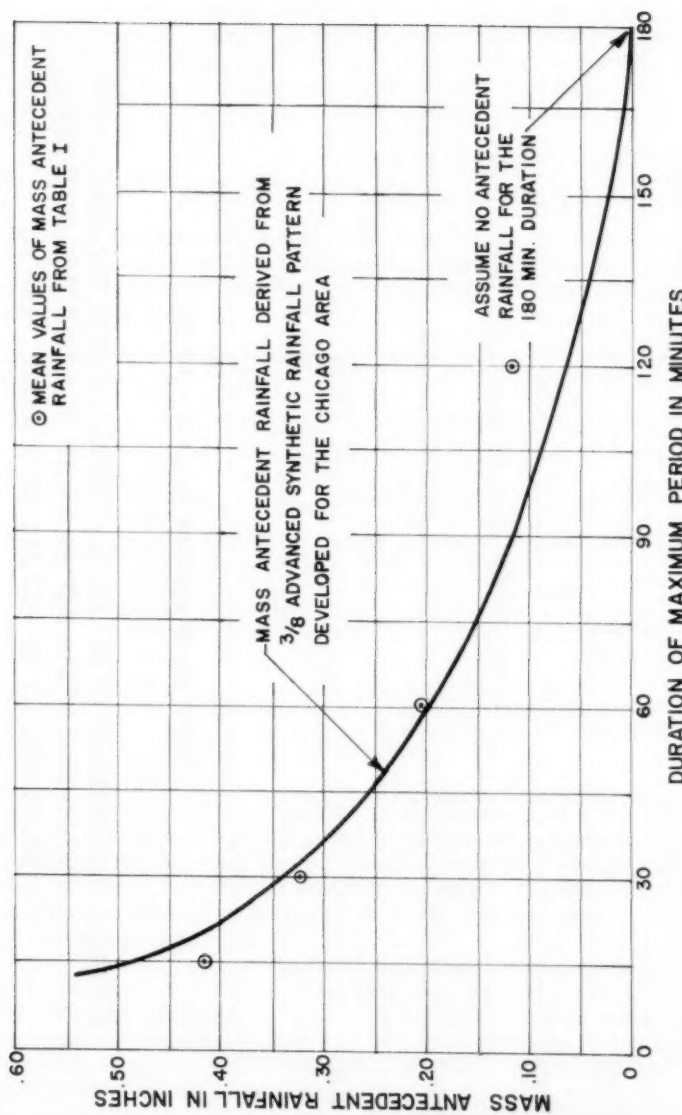


FIGURE 4 - COMPARISON OF THE MASS ANTECEDENT RAINFALL OCCURRING IN THE SYNTHETIC STORM PATTERN WITH THAT OF THE STATISTICAL MEAN VALUES OF ACTUAL RAINFALLS.

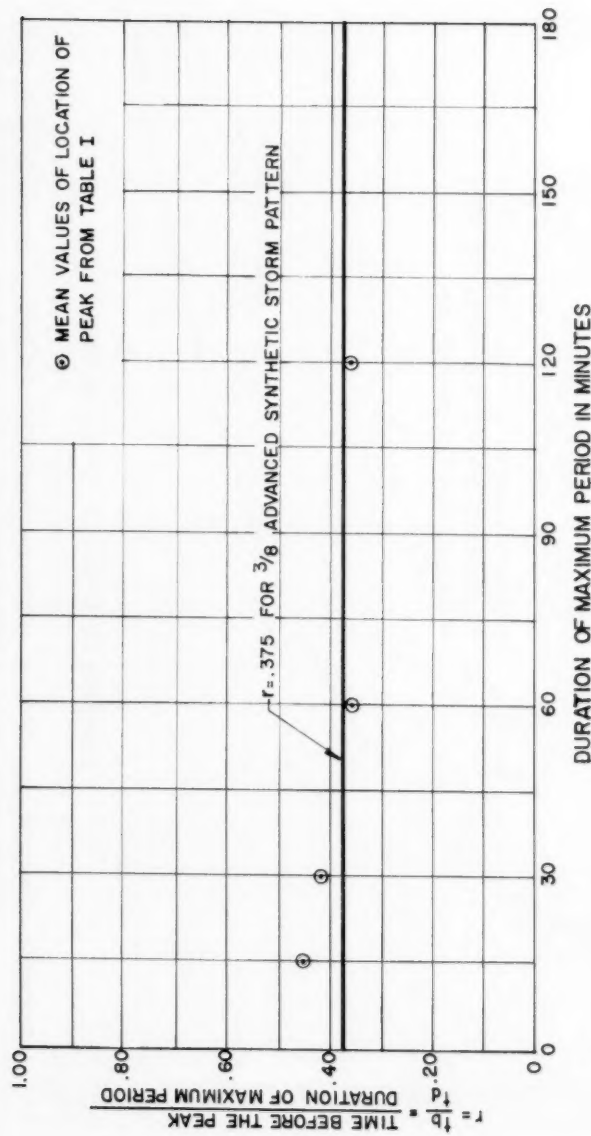


FIGURE 5 – COMPARISON OF RELATIVE LOCATION OF PEAK OCCURRING IN THE SYNTHETIC STORM PATTERN WITH THAT OF THE STATISTICAL MEAN VALUES OF ACTUAL RAINFALLS.

Then the total duration of the synthetic storm pattern is set equal to the longest time of concentration of any sewer system to be designed. For Chicago the total duration of the synthetic storm pattern was set at 180 minutes. Also, since this duration was quite long for storm sewer design, it was assumed that any small amount of rainfall preceding this period would produce little effect on the rate of runoff, therefore no antecedent rain was assumed before this 180-minutes-long synthetic storm pattern; then the amount of antecedent rainfall preceding the duration t_d , can be expressed as

$$A = [P_b]_{t_d=180} - [P_b]_{t_d=t_d} = r \frac{1.5(180)}{(180)^{0.9} + 11} - r \frac{1.5 t_d}{t_d^{0.9} + 11} = r \left(2.29 - \frac{1.5 t_d}{t_d^{0.9} + 11} \right) \quad (13)$$

where A is the mass antecedent rainfall in inches. Solving Equation (13) for "r" and substituting the statistical mean values of antecedent rainfall for A and the corresponding duration t_d , the value of "r" for each duration can be computed, see Table II.

t_d	$t_d^{0.9}$	$t_d^{0.9} + 11$	$\frac{1.5 t_d}{t_d^{0.9} + 11}$	$\frac{A}{r}$	A	r	Ar
15	11.5	22.5	1.000	1.290	.416	.322	.1340
30	21.4	32.4	1.388	.902	.324	.360	.1168
60	39.8	50.8	1.769	.521	.203	.390	.0792
120	74.4	85.4	2.110	.180	.118	.655	.0771
				$\sum A = 1.064$		$\sum (Ar) = .4115$	
				Weighted Value of "r" = .386			

Table II - Determination of the Value of "r" from Mass Antecedent Rainfall.

Since the "r" is to be constant through all durations, and the antecedent rainfall for the shorter durations is much greater and of greater importance in affecting runoff than that for the longer durations, it seems that the "r" computed for different durations should be weighted in proportion to the mass it reflects in obtaining the average "r" value. The weighted average value of "r" thus obtained is 0.386.

The location of peak within each duration provides another direct approach in evaluating the "r" value. In the last line of Table I, "Mean Location of Peak within Rainfall Duration" or mean "r" for each duration, is calculated on the basis that the momentary peak of every recorded rainfall happened exactly at the middle of the recorded "Peak Five-Minute." Then these "r" values of each duration were weighted proportionally to the time of duration in obtaining the average "r" for all durations. This was done because the shorter durations contain so few five-minute periods that the mean location of the peak is not so well defined as in the cases of longer durations. The value of "r" thus derived by considering the location of the peak is

$$\frac{15(.453) + 30(.415) + 60(.356) + 120(.366)}{15 + 30 + 60 + 120} = 0.376$$

An even fraction 3/8 or 0.375 which is close enough to the above findings was assigned to "r," thus establishing a synthetic storm pattern with a three-eighths advanced type. The mass antecedent rainfall for "r" = 0.375 is plotted in Figure (4) by the use of Equation (13). Also in Figure (5) a horizontal line with "r" = 0.375 is drawn. Comparison of these curves with the statistical mean values indicate fairly close agreement in antecedent rainfall with the shorter durations and in the location of peak with the longer durations.

Substituting the value of "r" = 3/8 into Equations (11) and (12) they become

$$(\text{Before the peak}) \quad i = \frac{90 \left[0.1 \left(\frac{8}{3} t_b \right)^{0.9} + 11 \right]}{\left[\left(\frac{8}{3} t_b \right)^{0.9} + 11 \right]^2}$$

$$(\text{After the peak}) \quad i = \frac{90 \left[0.1 \left(\frac{8}{5} t_a \right)^{0.9} + 11 \right]}{\left[\left(\frac{8}{5} t_a \right)^{0.9} + 11 \right]^2}$$

The synthetic storm pattern plotted according to the above equations satisfies best the three characteristics outlined in the beginning of this treatise and therefore can be used as the design storm pattern for the hydrograph method of storm sewer design in the Chicago area. Since the total duration of the synthetic storm pattern is limited to 180 minutes, the time before the peak is limited to 3/8 of 180 minutes or 67 1/2 minutes and the time after the peak to 5/8 of 180 minutes or 112 1/2 minutes. A hyetograph of the synthetic storm pattern is shown in Figure (6).

Also shown for comparison, in Figure (6), is a hyetograph for a one-year frequency synthetic rainfall, based upon the Eltinge-Towne formula for a "One-year frequency" rate-duration curve, namely

$$i_{av} = \frac{49}{t_d^{0.9} + 7}$$

and the value of "r" is assumed to remain at 0.375.

CONCLUSION

The "Synthetic Storm Pattern," having been derived from the accepted rate-duration curve, and fitted to the statistical values of antecedent rainfall and location of the peak, may now be used in the "Hydrograph Method" of sewer design. The advanced type pattern with "r" = 3/8, found to be acceptable in the Chicago area, might not be suitable in other localities. The authors believe that setting the "r" value is of considerable importance since it determines the amount of antecedent rainfall for all durations. In Figure (7), it is shown for comparison, the affect of the change in the "r" value on the runoff hydrograph of a 70 foot length of turf strip after subtracting losses due to infiltration, depression storage and surface detention. It can be seen

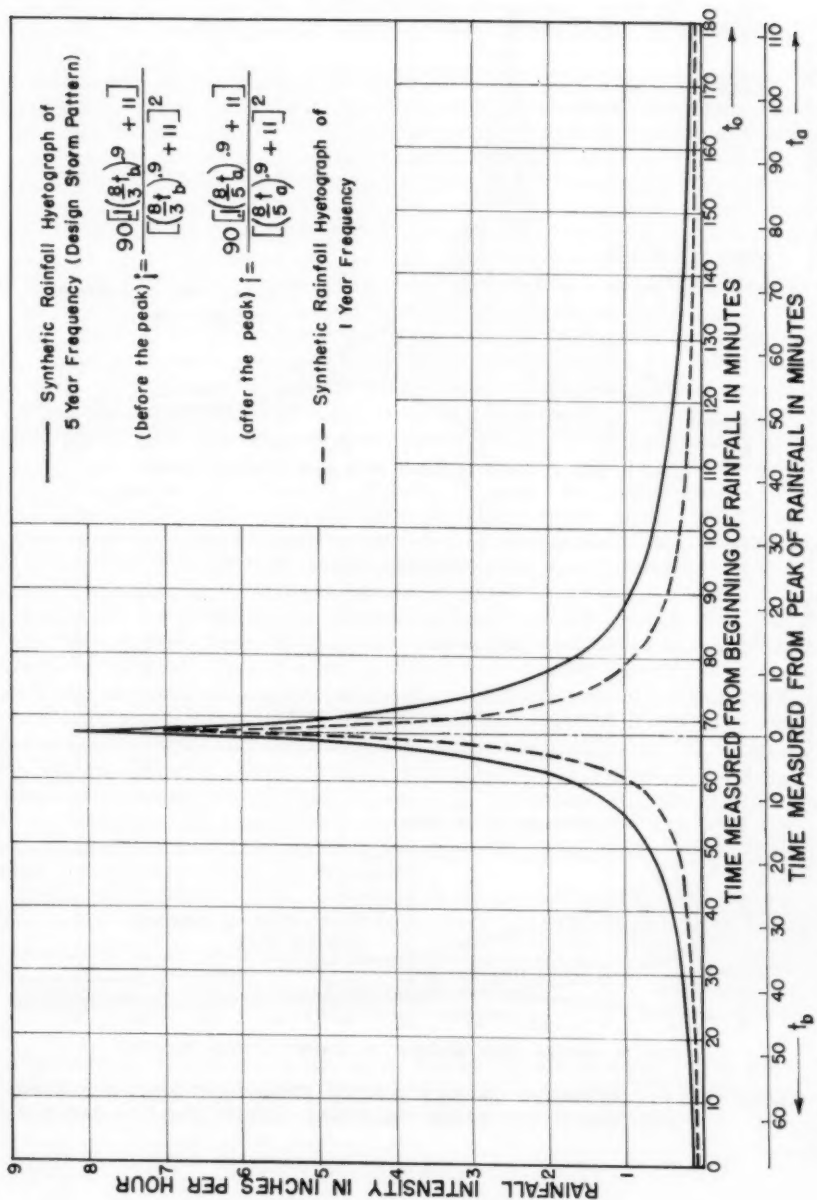


FIGURE 6 - SYNTHETIC STORM PATTERN HYETOGRAPHS OF THREE-EIGHTH ADVANCED TYPE

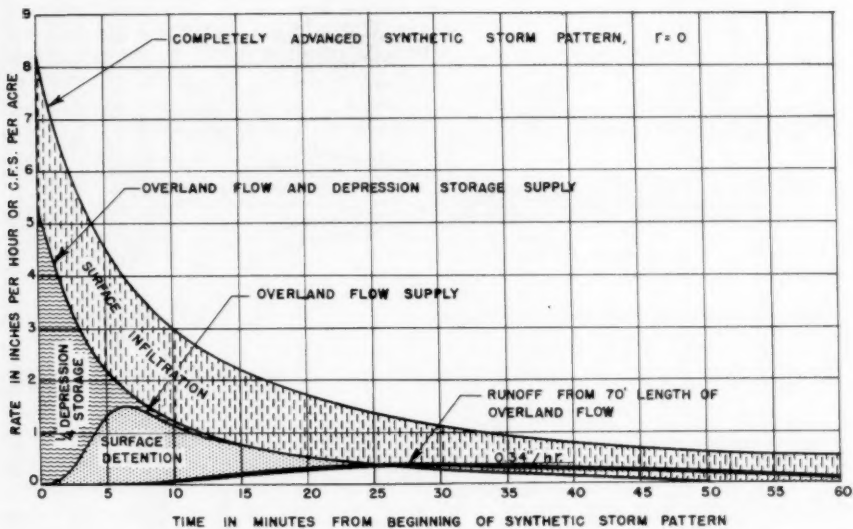
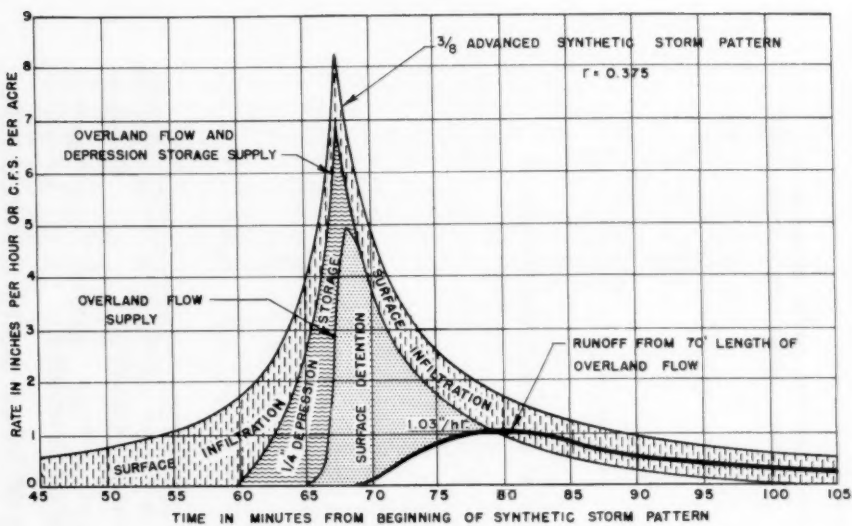


FIGURE 7 - COMPARISON OF NET RUNOFF FROM TURF AREA RESULTING FROM SYNTHETIC STORM PATTERNS HAVING $R = 0.375$ AND $R = 0$

that for the completely advanced storm pattern, the peak runoff rate is only a third of that for the 3/8 advanced storm pattern. Figure (8) shows a comparison of the runoff hydrographs from a typical residential area in Chicago, with 36 percent imperviousness, resulting from synthetic storm patterns having "r" = 0.375 and "r" = 0.

The Synthetic Storm Pattern having the same average intensities as that given by the rate-duration curve for all durations, would not be likely to occur at the same frequency as the rate-duration curve from which it was derived. It would undoubtedly have a greater return period, that is, less frequent occurrence. The use of the Synthetic Storm Pattern, however, should not produce greater runoff peaks than the use of a separate uniform intensity rainfall for every location in the sewer system, if the uniform intensity rainfalls have the correct antecedent precipitation. In Figure (9), the synthetic storm pattern has been used as a supply hydrograph at intervals along a sewer, and routed by the time-offset procedure to produce hydrographs at various times of travel. This use of the synthetic storm pattern, and subsequent use of uniform rainfalls as the supply hydrographs, is only illustrative and would occur only if the area was entirely impervious and had no losses or reductions before entering the sewer. Figures (10) and (11) show various duration uniform intensity rainfalls, with antecedent precipitation equal to that of the 3/8 advanced synthetic storm pattern, being routed by time-offset to produce hydrographs at various times of travel. Figure (12) shows the comparison of the peaks of the hydrograph derived from the synthetic storm pattern and those derived from the uniform intensity rainfalls. It can be seen that the attenuation of the hydrograph peaks of the synthetic storm pattern envelope those of the uniform rainfalls of separate durations, and would produce no greater quantities for use in design. In a more rigorous analysis of comparing the design rates derived from the synthetic storm pattern to those derived from rainfalls of separate durations, it was found that the peak rate of runoff is directly proportional to the net volume of the supply curve in the maximum period equal to the routing time. Then, since the synthetic storm pattern has the same volume of rainfall up to the end of any duration as the uniform intensity rainfall of the same duration with antecedent precipitation, they would both produce the same runoff peaks. If infiltration, depression storage and surface detention were subtracted chronologically from these two rainfalls, the same net volume of supply would result. Thus after routing, they would again produce equal runoff rates.

From the foregoing, it is concluded that the synthetic storm pattern can be used as the "Design Storm Pattern" in the hydrograph method of sewer design for all locations in a sewer system.

ACKNOWLEDGMENT

The authors wish to thank Mr. A. L. Tholin, M. ASCE, Chief Sewer Engineer, Sewer Planning Division, Bureau of Engineering, City of Chicago, for his encouragement and leadership in making this study possible.

REFERENCES

1. "Surface Runoff Determination from Rainfall without Using Coefficients," by W. W. Horner and S. W. Jens, Transactions ASCE, Vol. 107, pp. 1039-1117 (1942).

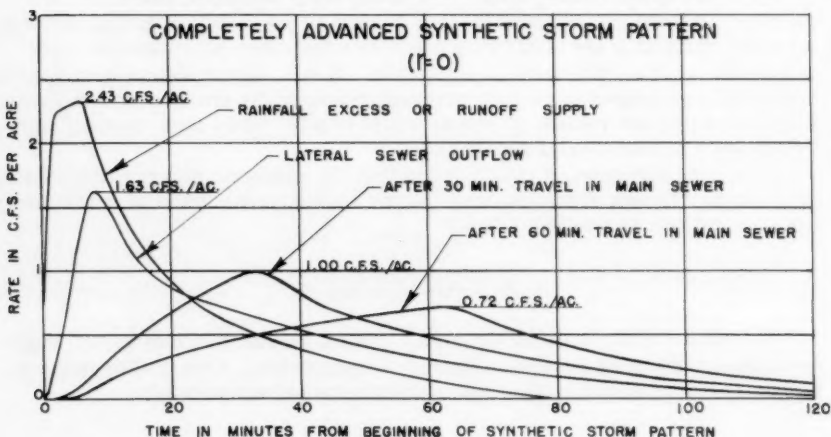
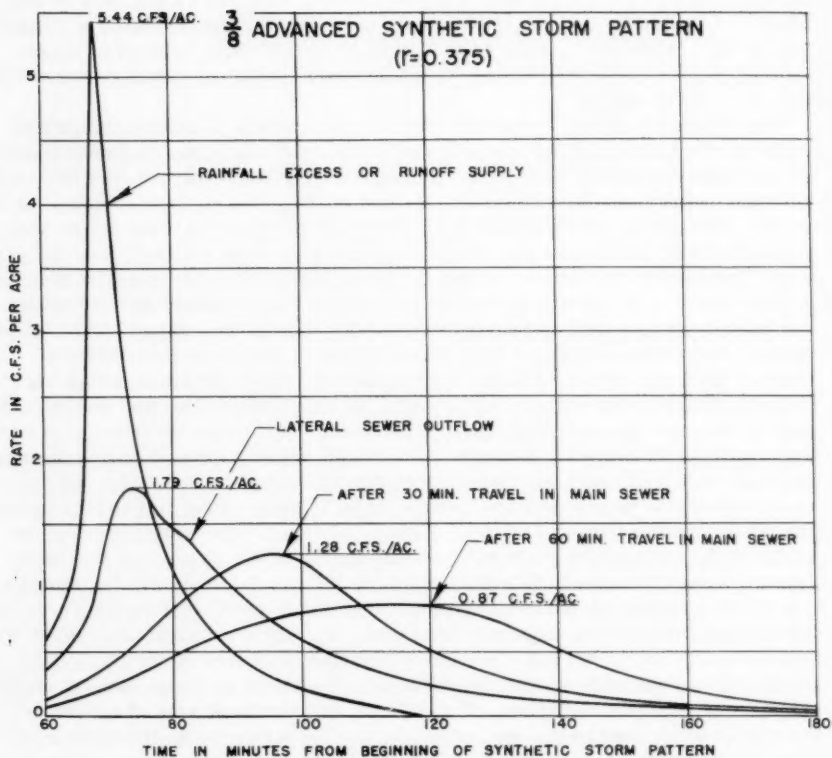


FIGURE 8 - COMPARISON OF RUNOFF HYDROGRAPHS, FROM SEWERS IN RESIDENTIAL AREAS, RESULTING FROM SYNTHETIC STORM PATTERNS HAVING $r=0.375$ AND $r=0$.

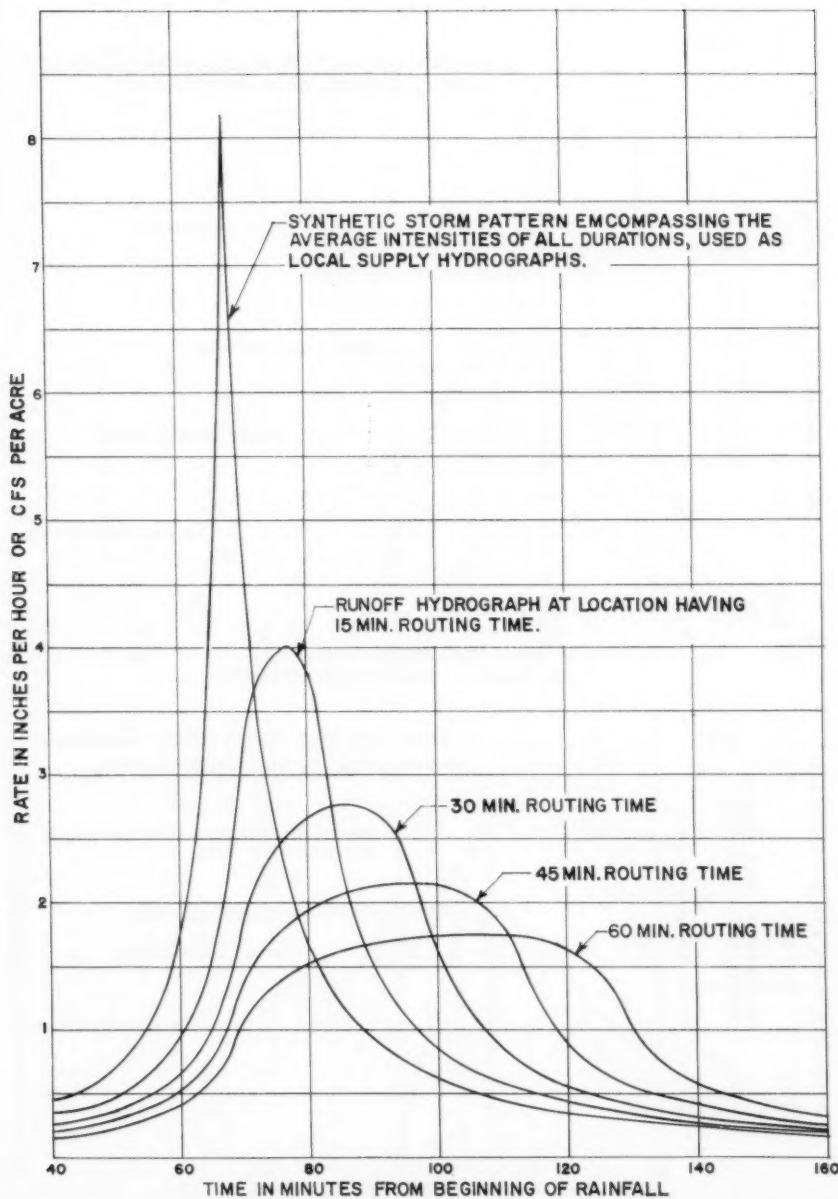


FIGURE 9 - SYNTHETIC STORM PATTERN ROUTED BY TIME OFFSET TO OBTAIN RUNOFF HYDROGRAPHS AT LOCATIONS HAVING VARIOUS TIMES OF TRAVEL.

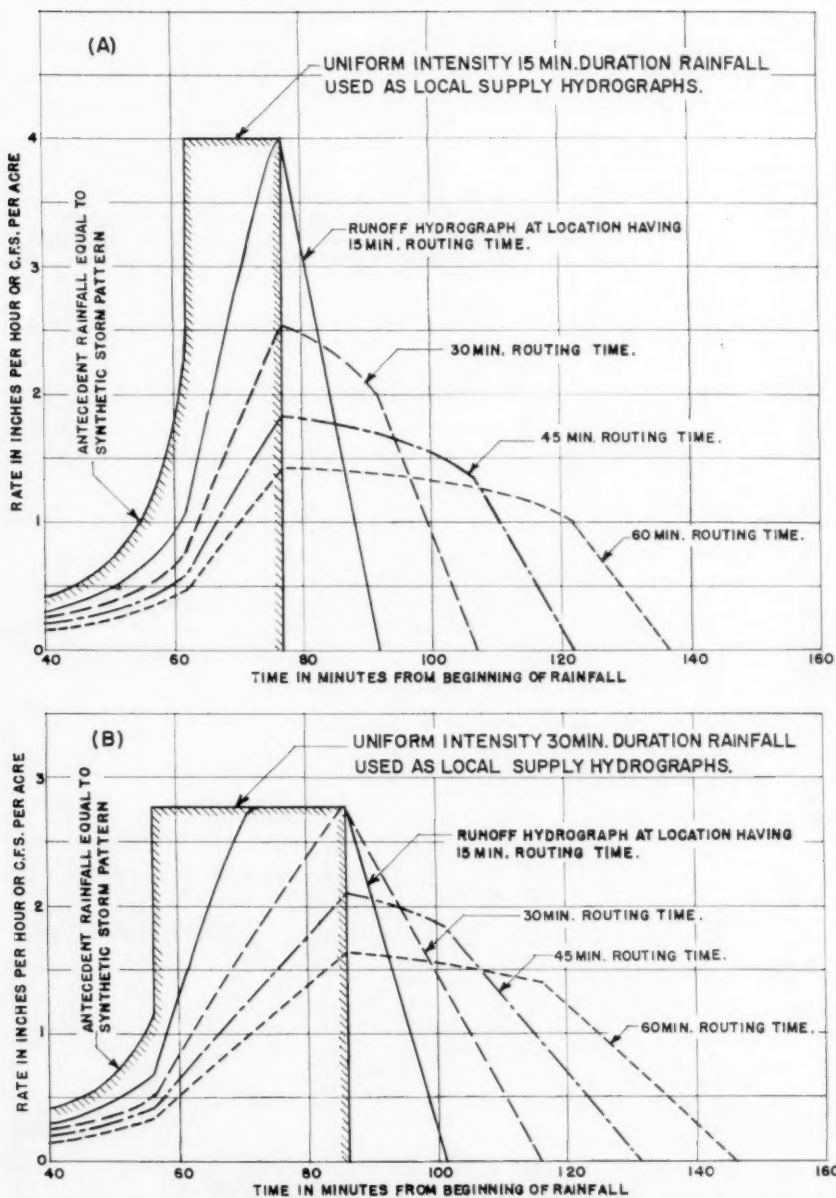


FIGURE 10 - UNIFORM INTENSITY 15 MIN. AND 30 MIN. RAINFALLS ROUTED BY TIME OFFSET TO OBTAIN RUNOFF HYDROGRAPHS AT LOCATIONS HAVING VARIOUS TIMES OF TRAVEL.

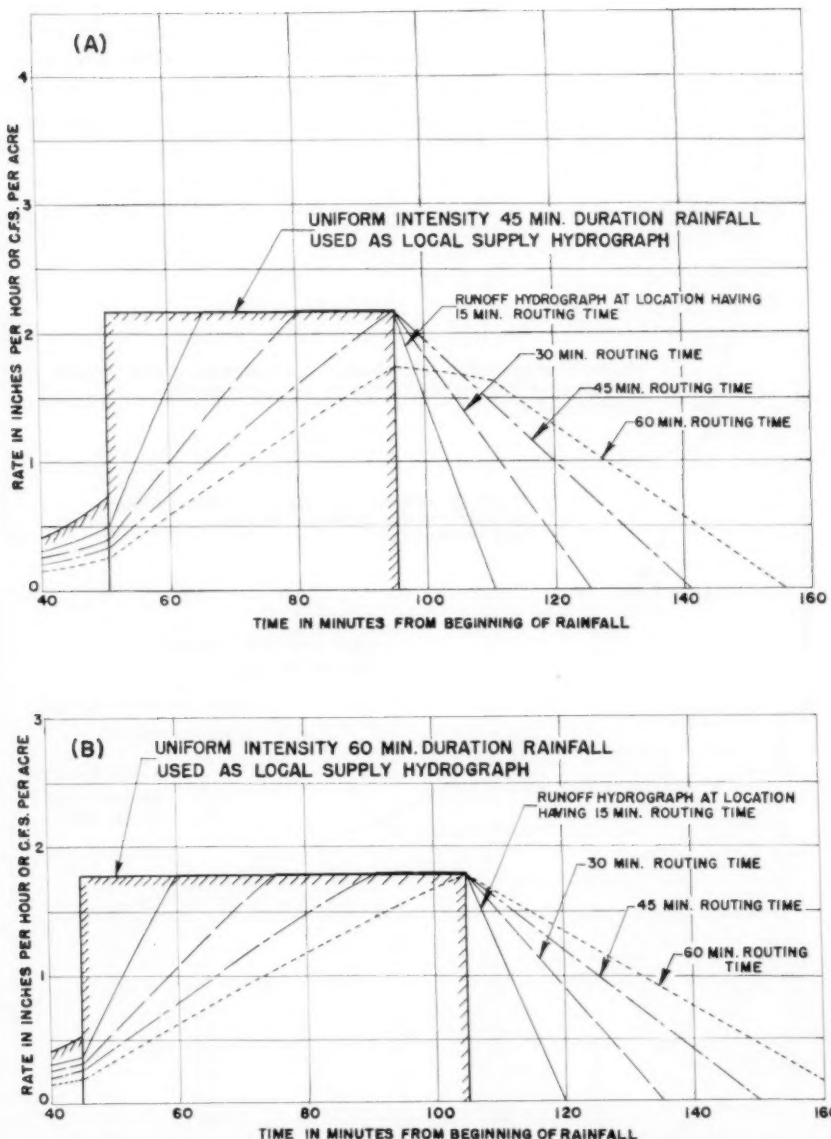


FIGURE 11 - UNIFORM INTENSITY 45 MIN. AND 60 MIN. RAINFALLS ROUTED BY TIME OFFSET TO OBTAIN RUNOFF HYDROGRAPHS AT LOCATIONS HAVING VARIOUS TIMES OF TRAVEL.

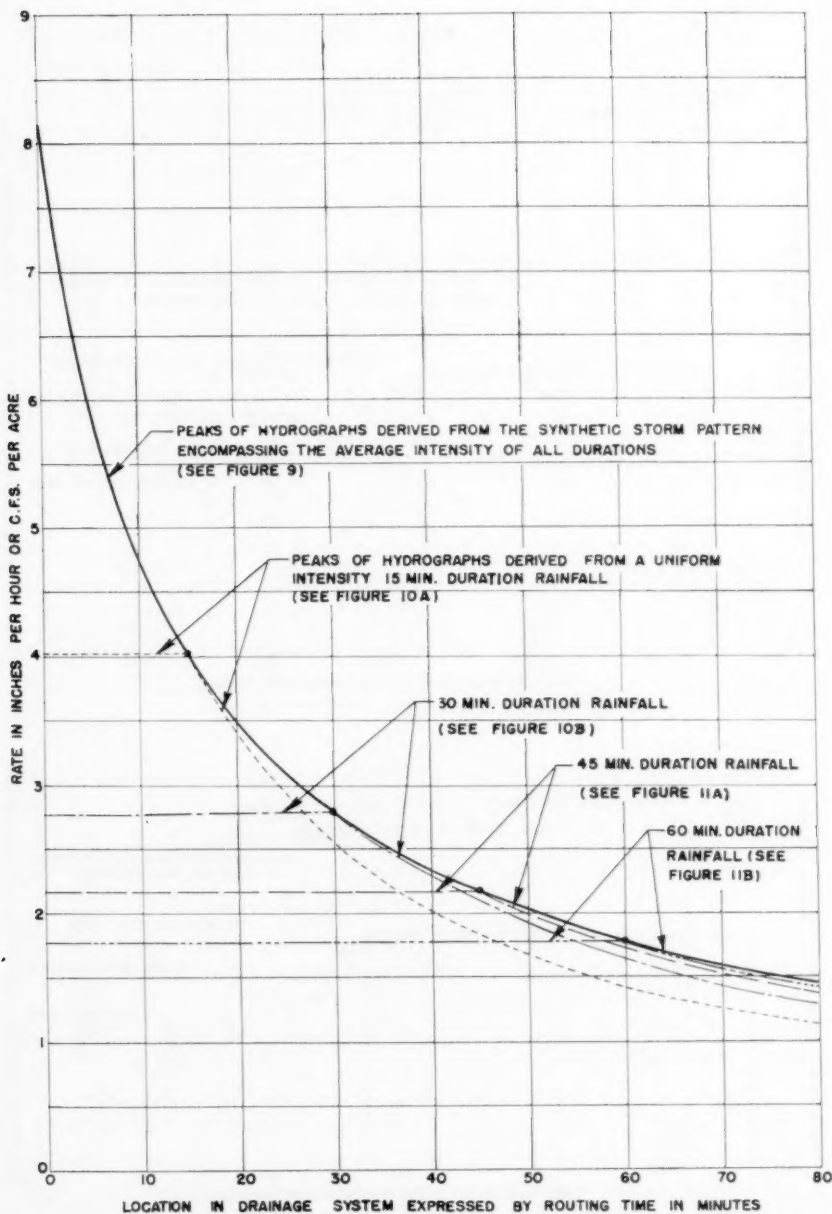
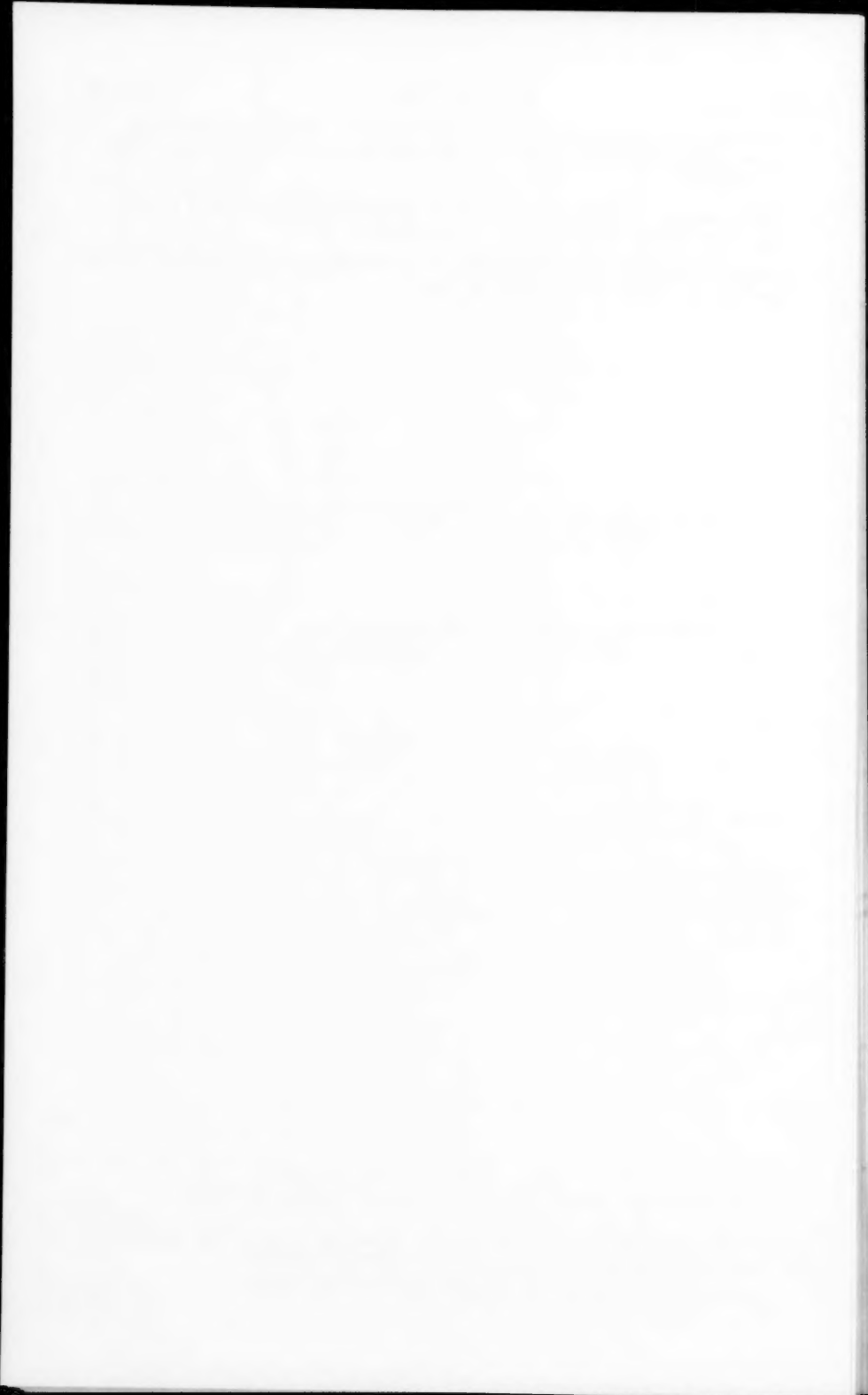


FIGURE 12 - CURVE OF PEAK RUNOFF RATES DERIVED FROM SYNTHETIC STORM PATTERN ENVELOPING THOSE CURVES DERIVED FROM UNIFORM RAINFALLS OF VARIOUS DURATIONS.

2. "Hydraulics of Runoff from Developed Surfaces," by C. F. Izzard, Proceeding Highway Research Board, National Research Council, Dec. 1946, pp. 129-150.
3. "The Drainage of Airports," by W. W. Horner, University of Illinois, Eng. Exp. Station Bulletin Vol. 42, No. 14, Nov. 1944.
4. Eltinge-Towne formula, "Handbook of Applied Hydraulics," by C. V. Davis 2nd Edition, McGraw-Hill 1952, p. 1034.



Journal of the
HYDRAULICS DIVISION

Proceedings of the American Society of Civil Engineers

CHARACTERISTICS OF FLOW OVER TERMINAL WEIRS AND SILLS

P. K. Kandaswamy,¹ A.M. ASCE and Hunter Rouse,² M. ASCE
(Proc. Paper 1345)

ABSTRACT

Generalized experimental results are presented to show the variation in both the discharge coefficient and the nappe profile for two-dimensional flow over a vertical sharp-crested weir at the end of a horizontal channel as the ratio of head to depth of flow changes continuously from zero to unity.

SYNOPSIS

Whereas most existing weir formulas lose significance as the ratio of head to height of weir becomes great, it is known that the rate of flow over a sill at the end of a channel can be estimated from the basic weir equation by assuming the velocity of approach to have its critical magnitude. This gives rise to a discharge function for sills which meets that for weirs in a sharp peak when the head is about ten times the weir height. There are related indications that the nappe attains a maximum elevation and thickness at the same head-height ratio. Laboratory tests to determine quantitatively the variation in discharge coefficient and nappe profile over the entire range are described, and the experimental results are presented in generalized form for design purposes.

Historical Background

Poleni,(1) in 1717, was the first to publish an equation for weir discharge obtained by integrating over the outlet section an expression for the velocity in terms of the square root of distance below the free surface. Although he

Note: Discussion open until January 1, 1958. Paper 1345 is part of the copyrighted Journal of the Hydraulic Engineering Division of the American Society of Civil Engineers, Vol. 83, No. HY 4, August, 1957.

1. Iowa Inst. of Hydr. Research, State Univ. of Iowa.
2. Prof., Fluid Mechanics & Div., Inst. of Hydr. Research, State Univ. of Iowa.

neither took account of the nappe contraction nor explicitly introduced the gravitational acceleration g , Poleni's name continues to be associated with the elementary discharge equation

$$q = \frac{2}{3} C_c \sqrt{2g} h^{3/2} \quad (1)$$

in which q is discharge per unit width of flow section, C_c the coefficient of contraction, and h the head on the crest. Contraction of the nappe was taken indirectly into consideration by Du Buat⁽²⁾ sixty years later in setting as arbitrary limits of integration the crest level and a level the distance $h/2$ above the crest; it was also Du Buat who introduced present-day methods of estimating the effect of submergence. Bidone,⁽³⁾ better known for his study of the hydraulic jump, appears to have been the first to show an interest in expressing algebraically the geometry of the weir nappe.

Not until about the middle of the 19th century was attention focused upon the velocity-of-approach "correction" for weir discharge, which was to dominate certain branches of the literature for another century. In 1845 Weisbach⁽⁴⁾ published the familiar integral form

$$q = \frac{2}{3} C_c \sqrt{2g} \left[\left(h + \frac{v_0^2}{2g} \right)^{3/2} - \left(\frac{v_0^2}{2g} \right)^{3/2} \right] \quad (2)$$

Since the solution of this equation has to proceed by successive approximation because of the implicit presence of the approach velocity v_0 on the left side of the equation, the impression has persisted that this velocity is independently variable. Weisbach himself appreciated the fact that a unique solution existed for any ratio of head h to depth of approach $h + w$, as he proposed an empirical formula for its evaluation:

$$q = \frac{2}{3} \left(C_c \right)_0 \left[1.041 + 0.3693 \left(\frac{h}{h+w} \right)^2 \right] \sqrt{2gh^3} \quad (3)$$

Bazin⁽⁵⁾ in 1888 adopted the same form of function, with specific evaluation of the limiting coefficient of contraction $(C_c)_0$

$$q = \left(0.405 + \frac{0.003}{h(m)} \right) \left[1 + 0.55 \left(\frac{h}{h+w} \right)^2 \right] \sqrt{2g} h^{3/2} \quad (4)$$

the dimensional term $0.003/h$ being introduced to compensate for low-head effects now attributed to surface tension and viscosity. In a series of investigations extending over the next ten years, Bazin also went deeply into such varied aspects of weir flow as the distribution of velocity and pressure through the nappe, and the effects of incomplete ventilation, submergence, weir inclination, and geometry of the crest; his nappe-profile measurements are still used as the basis of spillway design.

Bazin's formulation of the discharge coefficient soon led others to attempt further improvements by slight changes in the type of algebraic expression

used. From 1911 to 1928 Rehbock⁽⁶⁾ proposed a number of variants, the most pertinent of which was

$$q = \left(0.605 + 0.08 \frac{h}{w} + \frac{1}{305 h(\text{ft})} \right) \frac{2}{3} \sqrt{2g} h^{3/2} \quad (5)$$

Comparison of Eq. (5) with Eq. (4) will show that the primary distinction lies in the use of the ratio h/w in place of $h/(h+w)$ as the geometric parameter. The remaining term of Eq. (5)—which, like the corresponding one of Bazin, is not dimensionally homogeneous with the others—again reflects capillary and viscous effects at low heads. If the latter factors are ignored, and if the basic weir equation is written in terms of a discharge coefficient C_d ,

$$q = \frac{2}{3} C_d \sqrt{2g} h^{3/2} \quad (6)$$

it will be seen that the essential aspects of the Bazin and Rehbock formulas may be reduced for comparison to

$$C_d = 0.608 + 0.334 \left(\frac{h}{h+w} \right)^2 \quad (7)$$

and

$$C_d = 0.605 + 0.08 \frac{h}{w} \quad (8)$$

which are plotted against $h/(h+w)$ in Fig. 1. The two curves evidently differ by little more than 1% for heads as great as twice the height of weir.

When Mises,⁽⁷⁾ in 1917, determined the coefficient of contraction analytically for various two-dimensional forms of conduit outlet, he noted that the values for a symmetrical slot in a normal plate at the end of a conduit would—in combination with Eq. (2)—duplicate the trend of the Rehbock formula very closely over a considerable range if the ratio of slot dimension b to conduit dimension B were used to represent the ratio $h/(h+w)$. His curves for C_C and C_d are also shown in Fig. 1. To be noted in particular is the limiting theoretical value $\pi/(\pi+2) = 0.611$ in comparison with the empirical values 0.608 and 0.605 chosen by Bazin and Rehbock. One of Mises' students, Lauck,⁽⁸⁾ nearly a decade later approximated not only the discharge coefficient but also the entire nappe profile for the weir of infinite relative height, by means of the Cauchy integral theorem.

Inspection of the Bazin and the Rehbock formulas will indicate that the latter must approach the limit $C_d = \infty$ as the relative height of the weir approaches the limit zero (i.e., the free overfall), a trend that is necessarily shared by the orifice function of Mises, whereas the Bazin function has the finite limit $C_d = 0.942$. Now it is obvious that discharge over the free overfall is finite rather than infinite, since the effective head is the critical depth. However, it was noted by Boss⁽⁹⁾ that the critical stage of flow is already established upstream from terminal sills well before they attain zero height, which would yield a trend contrary to that of Eq. (6). That is, following the procedure of Rouse,⁽¹⁰⁾ the discharge coefficient for such conditions can be

determined by introducing into Eq. (6) the critical-depth relationship

$$q = \sqrt{g y_c^3} = \sqrt{g(h+w)^3} \quad (9)$$

Thus,

$$C_d = 1.06 \left(1 + \frac{w}{h}\right)^{3/2} \quad (10)$$

which is plotted at the upper right of Fig. 1. Evidently, the discharge characteristics of terminal sills follow quite a different functional relationship from that of even moderately low weirs, with an intermediate maximum value of the discharge coefficient. Now the coefficient of contraction C_c can be determined from simultaneous solution of Eqs. (10), (6), and (2) and plotted as at the lower right of Fig. 1. If, after Rouse, this coefficient is assumed to approximate the relative thickness of the nappe at its highest point, then this plot indicates that the flow profile will also attain a maximum stage at the borderline between weirs and sills.

In order to investigate these aspects of the problem, the second author undertook in 1931-33 in the River Hydraulic Laboratory of the Department of Civil and Sanitary Engineering at M.I.T. a systematic series of profile (as well as velocity and pressure) measurements on the nappe of a weir that was successively reduced in height until the overfall limit was reached. The results of the profile tests were reflected in a subsequent book,(11) but they were found to cover the transition range inadequately and hence were never published in their entirety. Similar measurements over a less extensive range of the parameter $h/(h+w)$ were undertaken later by the Bureau of Reclamation and published(12) for purposes of spillway design. Because it was believed that certain characteristics of the weir-sill range were nevertheless of technical interest, generalized plots of the M.I.T. data showing a parallel between the discharge-coefficient and nappe-profile functions were included in the Proceedings of the Fourth Hydraulics Conference(13) of the Iowa Institute of Hydraulic Research.

Continued efforts have since been made at the Iowa Institute to complete both the analytical and the experimental phases of the weir and sill problem. The relaxation method has already been applied to the improvement of Lauck's approximation of the nappe profile for the infinitely high weir(14) and at the time of writing the study is being extended to other values of $h/(h+w)$. However, since numerical integration is not as readily applicable to low weirs and sills as to high, the gaps left in the M.I.T. study were in 1956 filled in experimentally by the first author(15) under the direction of the second, to the end of providing a basis for both design and further theoretical analysis. It is to the presentation of the composite results that this paper is devoted.

Experimental Procedure

The M.I.T. experiments were conducted in a 50-cm glass-walled flume, the rate of flow through which was measured with a ventilated sharp-crested weir 40 cm high in accordance with Eq. (5). The experimental weir was

initially of identical characteristics, but its effective height was changed by the addition of successive false floors on the upstream side. These were constructed of troweled cement mortar over sand, and each consisted of a 6-ft. level section preceded by a very gradual rise from the original floor of the flume. Three weir heights—40, 20, and 10 cm—were produced in this way. The 40-cm weir was then removed, and still another false floor was added at a height of 37.5 cm above the flume floor, with a brass-angle end to simulate the free overfall. A supplementary weir crest could be attached to the end with wingscrews to produce additional weir heights of 5, 2 1/2, and 1 1/4 cm. Full ventilation was provided below the nappe in all instances.

Profile measurements were made at 1-cm sections upstream and downstream from the crest with point and hook gages reading by vernier to 0.1 mm. For each of the seven weir heights the same nine rates of discharge were investigated; these corresponded to heads on the measuring weir ranging by 2-cm increments from 2 to 18 cm. Supplementary measurements of pressure distribution along the floor, up the weir plate, and through the nappe, as well as checks upon the constancy of the total head at various points, were also made, but neither the experimental techniques nor the results are pertinent to the present discussion.

The tests conducted at the Iowa Institute employed the same type of free-overfall structure as the one finally constructed at M.I.T., except that it was built of brass plate and angles and mounted in a 1-ft. flume. The level portion was 4 ft. in length, its height above the floor of the flume was 1 ft., and the approach curve had the form of a quarter ellipse with an axis ratio of 3.5:1. The adjustable weir plate was machined to a sharp upstream edge, the top surface having a width of about 1/32 in. To minimize capillary distortion of the lower surface of the nappe at small weir heights, the crest surfaces were rubbed with paraffine. For the very smallest height (0.005 ft.) the crest was remachined to a knife edge. The test procedure was essentially the same as that at M.I.T., although the range of head was limited to $0.1 \text{ ft.} < h < 0.5 \text{ ft.}$ and the range of weir height to $0.005 \text{ ft.} < w < 0.05 \text{ ft.}$ Discharge measurement was effected by means of a 90° elbow meter in the 6-in. supply line that had been previously calibrated against a 12-in. sharp-crested weir mounted in the flume itself, the Rehbock formula being used as reference just as in the M.I.T. experiments.

Discussion of Results

As has long been realized, the head on a weir must be measured a considerable distance upstream from the crest, where the effect of the curvilinearity of flow upon the surface elevation is still negligible. A distance equal to three or four times the head is generally considered to suffice. Unfortunately, with relatively low weirs the effect of channel resistance becomes appreciable, so that the nappe profile is asymptotic to a sloping rather than a horizontal line. In other words, the head measurement then is subject to two types of error, the one increasing with proximity to the crest and the other with distance from it.

In order to determine that section at which the net error would be a minimum, so that the heads for different weir heights could be evaluated consistently, a composite dimensionless plot was made of all profile measurements upstream from the crest for the most extreme case—the free overfall—

as shown in Fig. 2. Since the computed critical depth was used as the reference length, and since the critical section has been shown to be the last at which hydrostatic distribution of pressure (i.e., absence of curvilinearity) can be assumed to prevail,(10) the abscissa of the desired section should be that having an ordinate value of unity, or $x/h = 4$. Inasmuch as this value for the free overfall agrees with that commonly used for weirs of great relative height, it was adopted for all subsequent evaluations in the intermediate range as well.

From the experimental determinations of discharge and surface profile for the various heights of weir and sill, the coefficient of discharge was evaluated according to Eq. (5) and plotted as in Fig. 3. Herein the Rehbock parameter h/w is used as abscissa in the weir range, because of the linearity of the resulting function. Its reciprocal w/h then logically serves as the abscissa in the sill range, the relative scales of the two being so chosen as to yield approximate agreement in the intermediate range. All of the Iowa data are shown, together with a comparable number from M.I.T. (i.e., all at the higher heads). Inspection of the diagram will indicate that Eq. (8) for weirs applies with good approximation over the range $0 < h/w < 6$, and Eq. (9) for sills over the range $0 < w/h < 0.06$. Although some discrepancy between the two sets in the zone of overlap is apparent, a smooth transition between the two functions can readily be drawn.

In Fig. 4 are superposed a systematic series of nappe profiles extending through the weir range to the case of maximum coefficient, $h/w = 10$. Figure 5 shows the corresponding family of profiles for sills. Like the coefficient plot of Fig. 3, the profiles (except for the lower surface of the weir nappe) are seen to be characterized by similar trends, the case $h/w = 10$ or $w/h = 0.1$ evidently representing a maximum for both the discharge coefficient and the nappe deflection.

As had previously been noted by the second author and used as the basis of the generalized profile diagrams already mentioned,(13) plots of z/h as functions of h/w and w/h with x/h as parameter bear a striking resemblance to the coefficient function shown in Fig. 3. Revised in accordance with the sill data now at hand, these diagrams are presented as Figs. 6 and 7, together with measured points for two representative values of x/h . The confocal rectilinear portions of the curves below $h/w = 5$ are identical with those previously published, but the remainder will be found to differ appreciably. Similarity with the coefficient curve is maintained well into the sill range, however, except in the very neighborhood of the overfall limit.

Although the foregoing experimental data were obtained with heads of relatively small magnitude and hence can be expected to apply only approximately to conditions at larger scale, it is believed that the degree of approximation will not be appreciably lower than the experimental precision evident in the figures. The Rehbock equation, for example, indicates that capillary and viscous effects change the discharge by about 1% at a head of 0.3 ft. Since this is representative of the heads that were investigated, there is no reason to expect scale effects of a higher order to be present in the results.

CONCLUSIONS

Through the combination of experimental measurements made at considerably different times and places, information is now at hand for the coefficient

of discharge and the form of the nappe profile as the relative height of a ventilated, sharp-crested weir at the end of a channel varies over its complete range from infinity to zero. In the range $0 < h/w < 6$ the coefficient of weir discharge is given approximately by the formula

$$C_d = 0.61 + 0.08 \frac{h}{w}$$

In the range $0 < w/h < 0.06$, the coefficient of discharge is given approximately by

$$C_d = 1.06 \left(1 + \frac{w}{h}\right)^{3/2}$$

In the intermediate zone there is a continuous transition between the two functions with a maximum at approximately $h/w = 10$; the latter might hence be regarded as the borderline between weir flow and sill flow. This value of h/w also marks the condition of maximum nappe deflection, the nappe for both weirs and sills gradually rising and thickening as this common value is approached. Nappe profiles for design purposes may be determined either by interpolation of the profile curves or by direct reading of the generalized profile coordinates presented in the paper.

REFERENCES

1. Poleni, G., De Motu Aquae Mixto, Padua, 1717.
2. Du Buat, P.L.G., Principes d'Hydraulique, Paris, 1779.
3. Bidone, G., "Expériences sur la dépense des reversoirs," Memorie della Reale Accademia delle Scienze di Torino, Vol. 28, 1824.
4. Weisbach, J., Lehrbuch der Ingenieur- und Maschinen-Mechanik, Brunswick, 1845.
5. Bazin, H. E., Expériences nouvelles sur l'écoulement en déversoir, Paris, 1898.
6. Rehbock, T., discussion of E. W. Schoder and K. B. Turner's "Precise Weir Measurements," Transactions A.S.C.E., Vol. 93, 1929.
7. Mises, R. von, "Berechnung von Ausfluss- und Ueberfallzahlen," Zeitschrift des V.D.I., 1917.
8. Lauck, A., "Ueberfall über ein Wehr," Zeitschrift für angewandte Mathematik und Mechanik, Vol. 5, 1925.
9. Boss, P., "Berechnung der Abflussmengen und der Wasserspiegelage bei Abstürzen und Schwellen unter besonderer Berücksichtigung der dabei auftretenden Zusatzspannungen," Wasserkraft und Wasserwirtschaft, No. 2-3, 1929.
10. Rouse, H., "Discharge Characteristics of the Free Overfall," Civil Engineering, Vol. 6, No. 4, 1936.

1345-8

HY 4

August, 1957

11. Rouse, H., Fluid Mechanics for Hydraulic Engineers, New York, 1938.
12. "Studies of Crests for Overfall Dams," Bulletin 3, Part IV, Boulder Canyon Project Final Reports, Bureau of Reclamation, 1948.
13. Ippen, A. T., "Channel Transitions and Controls," Engineering Hydraulics, New York, 1950.
14. McNown, J. S., Hsu, E. Y., and Yih, C. S., "Applications of the Relaxation Technique in Fluid Mechanics," Transactions A.S.C.E., Vol. 120, 1955.
15. Kandaswamy, P. K., "Discharge Characteristics of Low Weirs and Sills," M. S. Thesis, State University of Iowa, 1957.

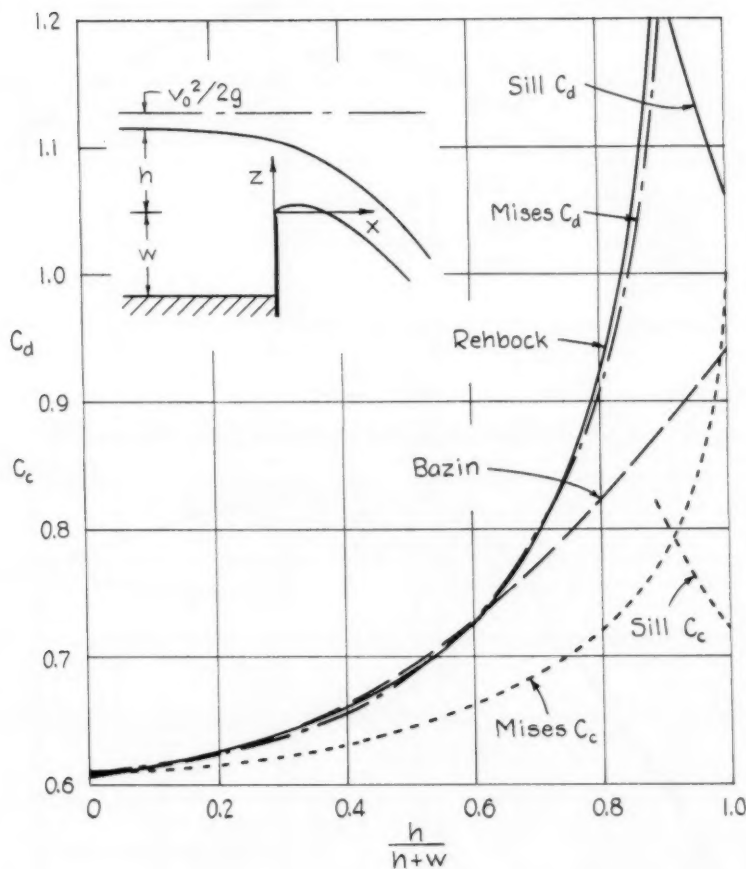


Fig. 1. Comparison of Discharge Functions for Weirs and Sills.

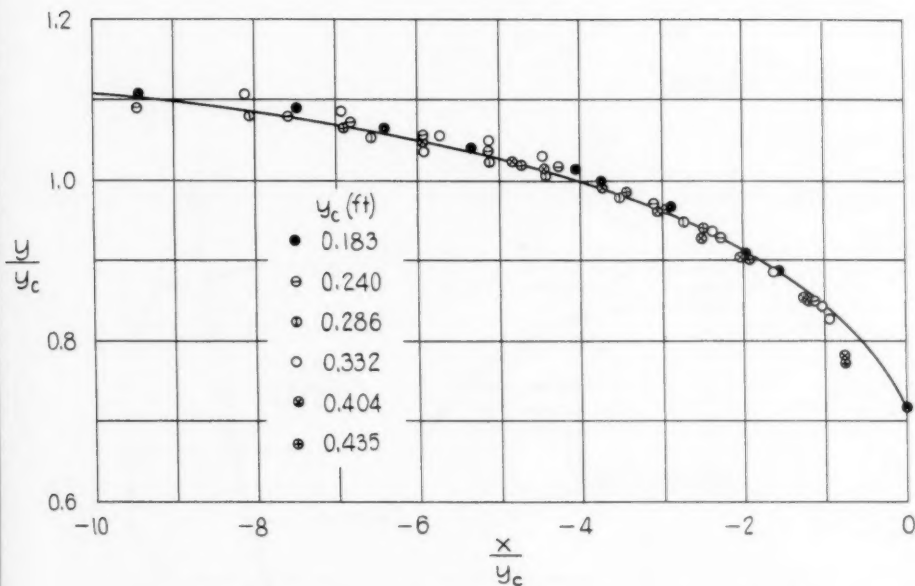


Fig. 2. Location of Critical Section Upstream from Free Overfall.

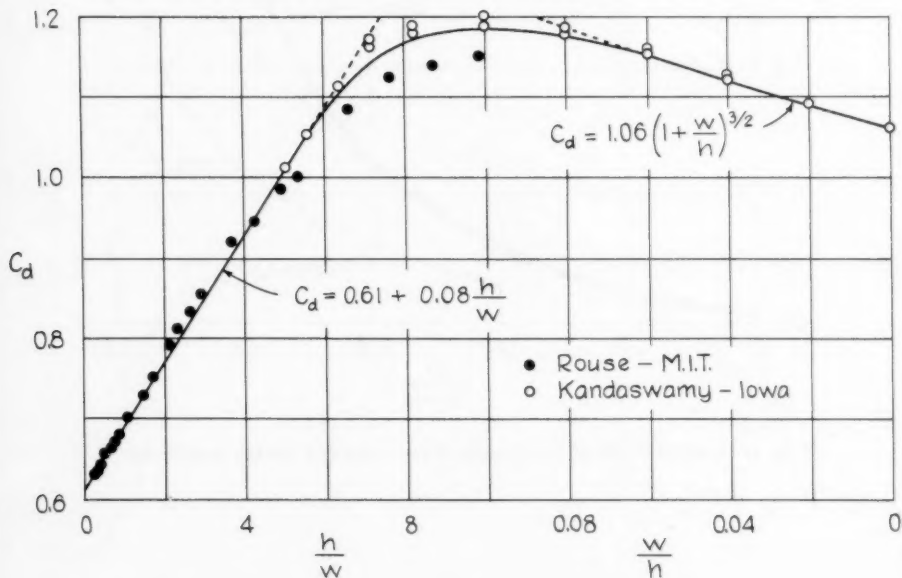


Fig. 3. Experimental Evaluation of Discharge Coefficient for Entire Weir-Sill Range.

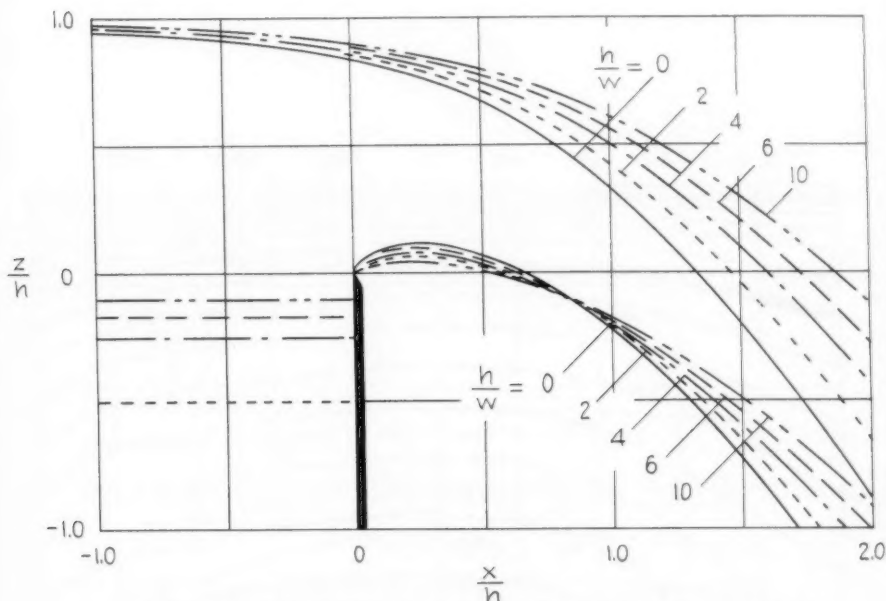


Fig. 4. Variation of Nappe Profile with Relative Height of Weir.

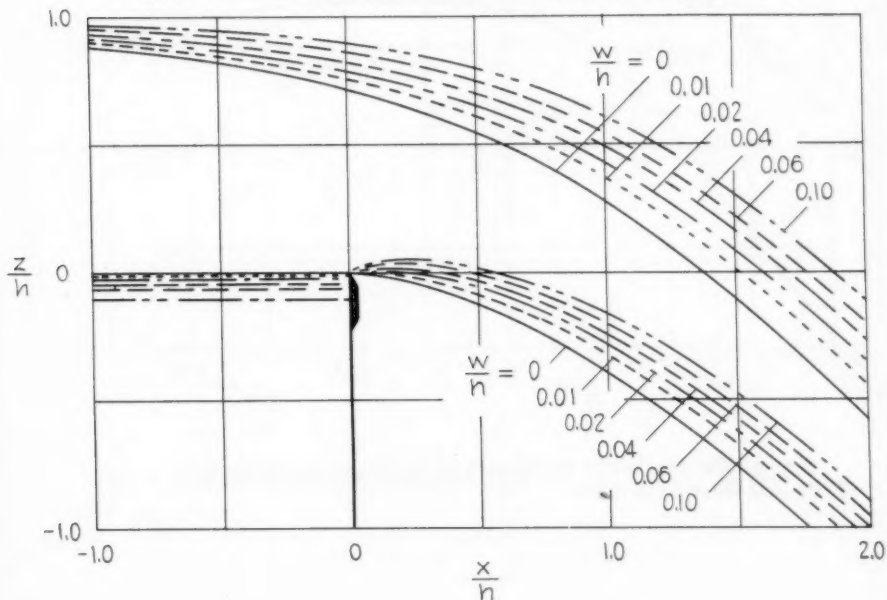


Fig. 5. Variation of Nappe Profile with Relative Height of Sill.

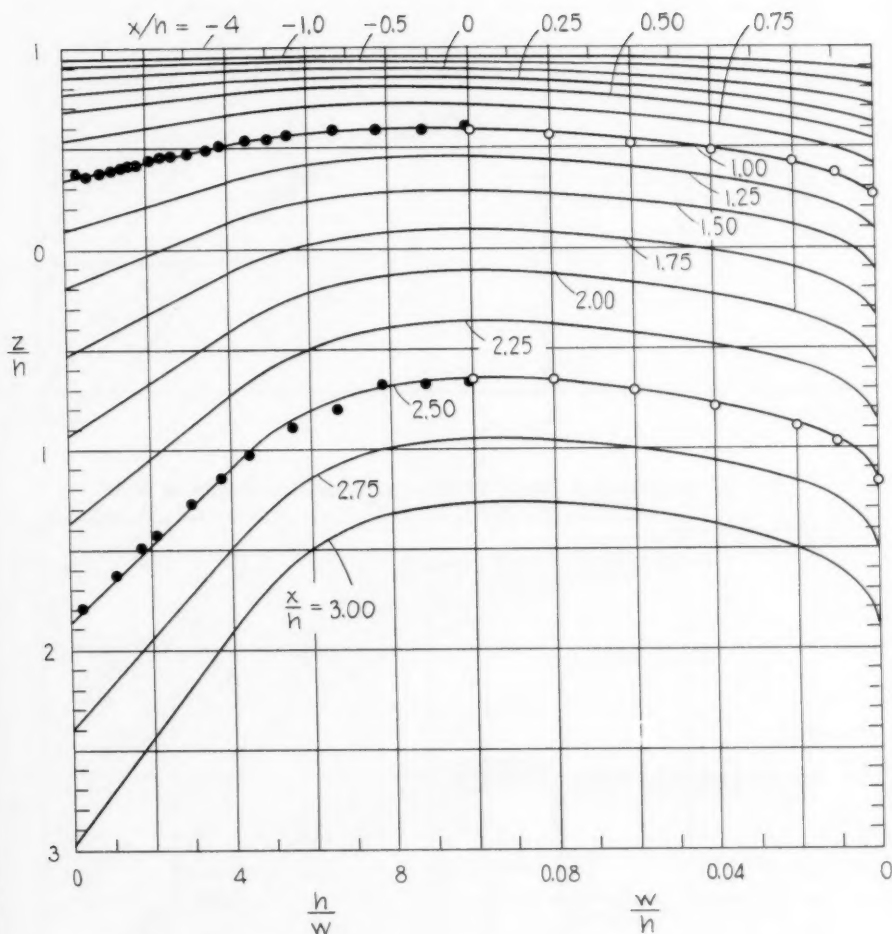


Fig. 6. Generalized Coordinates of Upper Nappe Surface for Terminal Weirs and Sills.

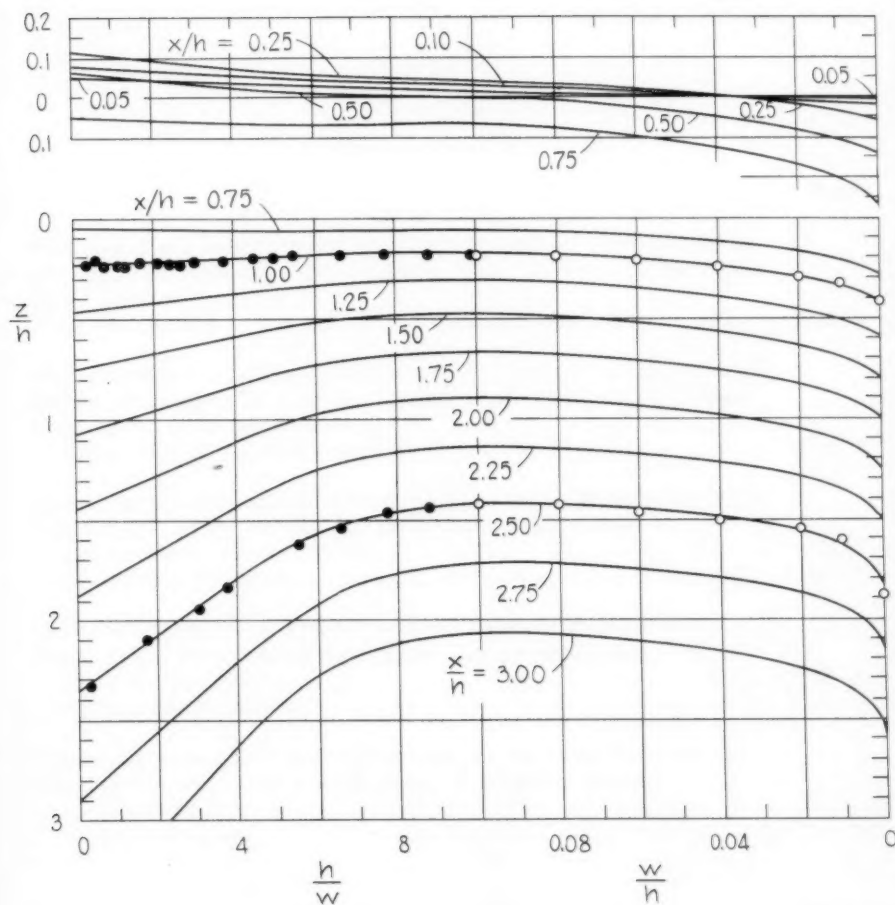
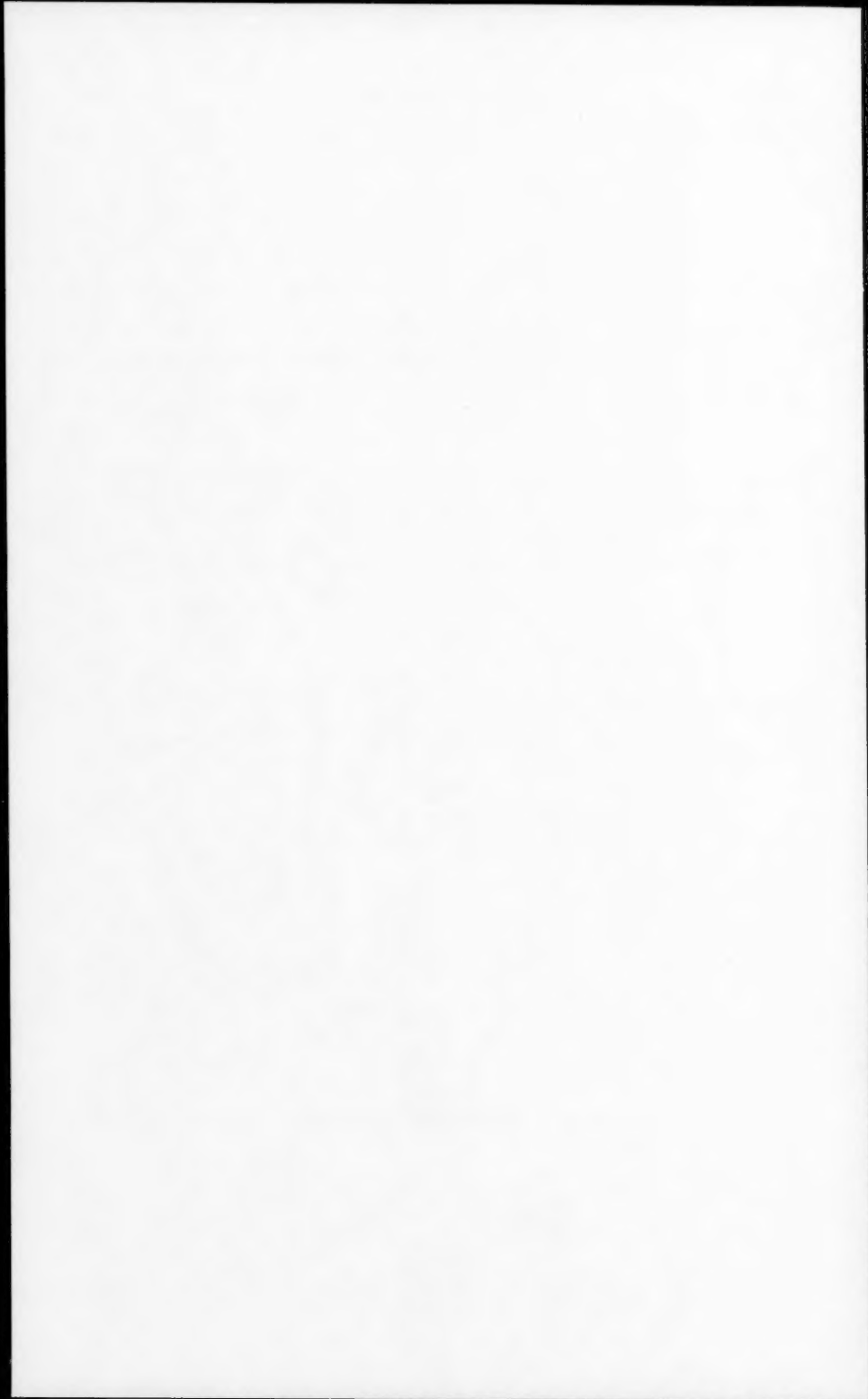


Fig. 7. Generalized Coordinates of Upper Nappe Surface for Terminal Weirs and Sills.



Journal of the
HYDRAULICS DIVISION
Proceedings of the American Society of Civil Engineers

CONTENTS

DISCUSSION

(Proc. Paper 1348)

	Page
Free Outlet and Self-Priming Action of Culverts, by Wen-Hsiung Li and Calvin C. Patterson. (Proc. Paper 1009. Prior discussion: 1131, 1177. Discussion closed.) by Wen-Hsiung Li and Calvin C. Patterson (closure)	1348-3
The Application of Sediment-Transport Mechanics to Stable-Channel Design, by Emmett M. Laursen. (Proc. Paper 1034. Prior discussion: 1177. Discussion closed.) by Emmett M. Laursen (closure)	1348-7
Measuring Streamflow under Ice Conditions, by A. M. Moore. (Proc. Paper 1162. Prior discussion: none. Discussion closed.) by Charles E. Behlke by Steponas Kolupaila	1348-9 1348-10
Technical Problems of Flood Insurance, by H. A. Foster. (Proc. Paper 1165. Prior discussion: none. Discussion closed.) by G. N. Alexander by Steponas Kolupaila	1348-15 1348-18
Frequency Analysis of Streamflow Data, by David K. Todd. (Proc. Paper 1166. Prior discussion: none. Discussion closed.) Corrections by M. A. Benson	1348-21 1348-21

(over)

Note: Paper 1348 is part of the copyrighted Journal of the Hydraulics Division of the American Society of Civil Engineers, Vol. 83, HY 4, August, 1957.

Butterfly Valve Flow Characteristics, by M. B. McPherson, H. S. Strausser, and J. C. Williams, Jr. (Proc. Paper 1167. Prior discussion: none. Discussion closed.)

by Turgut Sarpkaya	1348-31
by G. Dugan Johnson	1348-47
by Henry Voltmann	1348-48
by Ronald E. Nece	1348-49

A Study of Bucket-Type Energy Dissipator Characteristics, by M. B. McPherson and M. L. Karr. (Proc. Paper 1266.)

Corrections	1348-57
-----------------------	---------

Discussion of
"FREE OUTLET AND SELF-PRIMING ACTION OF CULVERTS"

by Wen-Hsiung Li and Calvin C. Patterson
(Proc. Paper 1009)

WEN-HSIUNG LI,¹ A.M. ASCE, and CALVIN C. PATTERSON,² J.M. ASCE—The writers are glad to receive discussion from investigators of three hydraulic laboratories. As their comments overlap to a certain extent, the authors would like to answer them together.

The writers use mD for the mean piezometric head at the outlet in Eq. (1) and then define an effective mD by Eq. (4). As can be seen from the accompanying sketch, and from Eq. (3) and (4),

$$\text{Effective } mD = \text{Actual } mD + (\Delta_1 - \Delta_2) + (\alpha_1 - \alpha_2) \frac{v^2}{2g}$$

Note that the location of the projected hydraulic grade line corresponds to the effective mD , not the actual mD . Thus the values of effective mD presented in the paper are theoretically the same as those obtained by projecting the hydraulic grade line to the outlet section. This can also be seen from

Eq. (21) in Mr. French's discussion by putting $\frac{1}{Q} \int (\frac{p_1}{\rho g} + z) dQ = \text{actual } mD$, $\alpha'_1 = \alpha_2$, and $h_e + f \frac{L}{D} \frac{v^2}{2g} = \Delta_2$. The small differences between Δ_1 and Δ_2 and between α_1 and α_2 are of no great importance in practice. Since Δ_1 and α_1 are unknown and will most likely be approximated in practice by Δ_2 and α_2 respectively, the quantity effective mD is even more useful than the actual mD :

$$H + sL = \text{effective } mD + \Delta_2 + \alpha_2 \frac{v^2}{2g}$$

In presenting the data of effective mD , the writers call the quantity v/\sqrt{gD} a Froude Number. Mr. Blaisdell thinks that this quantity is not a Froude number "as ordinarily conceived" relating to free-surface flow. This is a matter of definition. It seems that the generally accepted definition of a Froude number is a dimensionless quantity in the form of v/\sqrt{gD} (or its variations). It is an indication of the relative magnitudes of the inertia and gravitational forces(1) in a flow system, e.g. the flow from a closed container through an orifice.(2) In a particular problem, the Froude number may sometimes be interpreted in a particular way, such as the ratio of a characteristic velocity to the speed of propagation of an infinitesimal surface-wave, or as a measure of the ratio of the velocity head to the depth of flow or to the depth of

1. Associate Prof. of Civ. Eng., The Johns Hopkins Univ., Baltimore, Md.
2. Engr., Anderson and Nichols, Consulting Engrs., Baltimore, Md.

the conduit. Such interpretation may be helpful in particular cases but, it seems to the writers, should not be considered as a definition. The Froude number is significant in determining the value of mD because the pressure distribution at the outlet section depends on the relative magnitudes of inertia and gravitational forces acting on the jet. The writers use v/\sqrt{gD} instead of one of its variations to take advantage of the fact that, at the same v/\sqrt{gD} , the values of m for unsupported jets are about the same for square and circular pipes.

Considering the nature of the measurements, the differences between Mr. Flack's data and the writers' data of m for horizontal culverts with no outlet-apron are not unexpected. It is believed that the data presented for various culvert slopes and outlet conditions are consistent enough for practical purposes.

The writers appreciate the comments on the self-priming action of culverts. The work of Mr. French in this respect is particularly interesting to the writers. They are glad that Mr. French adds Type A to the three types of priming mentioned by the writers who, in writing the paper, considered Type A as the limiting case of Type 1. It seems that Mr. French's Type B of priming is the transient phenomenon of what the writers call Type 2 priming. In the paper, the writers suggest a way of presenting the data on priming for practical use. As there is no exact knowledge about turbulent non-uniform flow, air entrainment and vortex formation (as of 1957), there is no exact way of transferring model data to a prototype. A practicable, though approximate, method has to be used. It should be recalled that, in using any empirical information, it is a sound engineering practice to allow a margin of safety. The data presented in the paper, being experimental results, should be used in the same spirit. Friction is a major influence in Type 1 and Type 2 priming. In Type 3 priming where air entrainment is most important and friction only

plays a secondary part, the action depends mainly on D/H . The use of $\frac{sD}{n^2}^{1/3}$ is not incorrect though not absolutely necessary.

REFERENCES

1. Engineering Hydraulics, edited by Rouse, Wiley & Sons, N.Y., 1950, p. 140.
2. Rouse, H. "Fluid Mechanics for Hydraulic Engineers," McGraw-Hill Co., N.Y., 1938, p. 19.

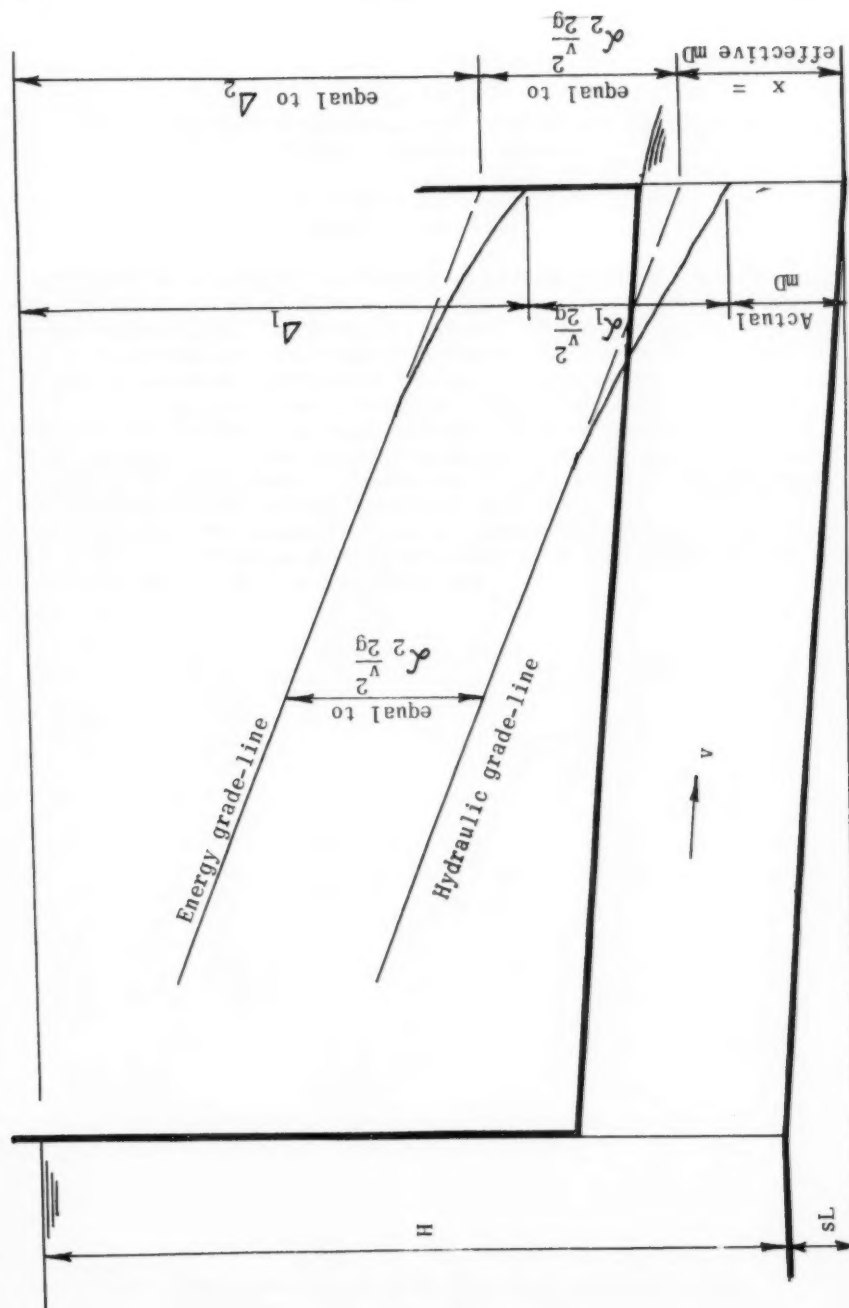
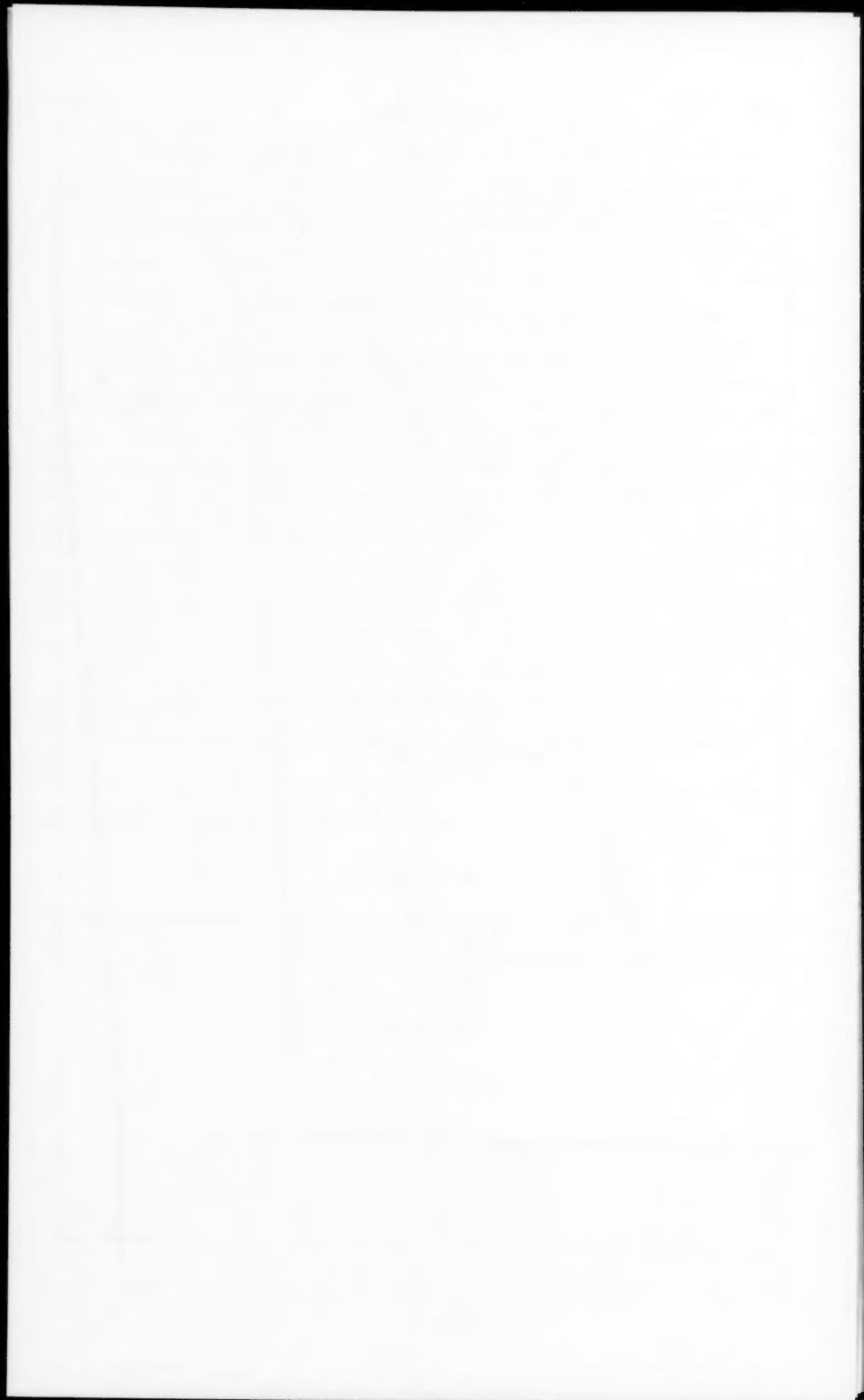


Fig. 1.



Discussion of
"THE APPLICATION OF SEDIMENT-TRANSPORT MECHANICS
TO STABLE-CHANNEL DESIGN

by Emmett M. Laursen
(Proc. Paper 1034)

EMMETT M. LAURSEN.¹—A discussion such as that of Mr. Shulits can only gladden the heart of a writer, for it amplifies and reinforces the original contentions set forth. The "formula dilemma," as Mr. Shulits puts it, is such that at the present time the design of stable channels cannot proceed with any substantial degree of confidence on the basis of sediment-transport mechanics alone—experience is absolutely essential. Sediment-transport mechanics can serve as a guide and the many formulas can serve as scaling relationships, however, and in that way supplement experience. When the formulas are used to compare different channels the gross quantitative disagreements largely disappear and the similarities are emphasized.

In a personal communication Mr. J. W. Delleur has pointed out that power of n in the Brown-Einstein equation is incorrect. In Table I the power should be 3 and in Table II the power should be 6/5.

1. Research Engr., Iowa Inst. of Hydr., Research, Iowa City, Iowa.



Discussion of
"MEASURING STREAMFLOW UNDER ICE CONDITIONS"

by A. M. Moore
(Proc. Paper 1162)

CHARLES E. BEHLKE,* A.M. ASCE.—As more and more of the cheaper water power sites in the United States are developed, the day approaches when American industry must look to the great power potential of northern Canada and the Territory of Alaska. In these areas of great water power potential the winters may last as long as eight or nine months each year. It is in the North that the methods of evaluating ice-affected records of stream flow, so well described by Mr. Moore, have greatly magnified significance.

It is quite common in Arctic and subarctic regions for the winter streamflow to constitute a relatively minor amount of the total annual flow. However, since stream beds may drop quite rapidly, the winter flow can be quite important to a hydro development because of the frequent lack of potential reservoir volume. It is therefore quite important that streamflow records be obtained for the winter months. With a very few exceptions, the methods which Mr. Moore has so adequately described of evaluating streamflow from stage records would be quite applicable to these northern areas.

Discharge measurements by themselves are quite tedious and difficult to make in cold weather especially if the thickness of the ice cover on the stream is very great. It is quite common for ice thicknesses on northern streams to range from zero to six feet. This presents a considerable problem before the current meter can be placed in the stream. The efficiency of a man gets quite low as the temperature drops, so a man taking a discharge measurement in the very cold weather of the winter may take several days to obtain a measurement which would take him only a few hours in the warmer weather. To add to the difficulty, the daylight hours are much shorter in these northern areas than they are further south, so a single discharge measurement may take two men two or three days to complete if the weather is not too cold or otherwise inclement. If the weather becomes colder than about minus 40°, very little is lost by simply stopping work and waiting for warmer weather. This means that men must wait at a location sometimes for long periods of time before they are able to make the discharge measurement. It is not uncommon in Alaska and northern Canada for the temperature to drop to as low as minus 60°, and colder, which means that during a normal winter there is a good deal of time during which the weather is too cold to work outside efficiently.

Since discharge measurements during the winter in northern climates are quite expensive, streams may be gaged only a few times during these months. The discharge is then known only at the time of the measurement and must be estimated for other times. A record of the stage, even though it is effected by ice cover, anchor ice, or ice jams, would be quite valuable for a determination of the discharge during winter months as has been shown by

* Associate Prof., Dept. of Civ. Eng., Oregon State College, Corvallis, Ore.

Mr. Moore's paper. The obtaining of such a record in a cold climate is, at present, practically impossible because of the limitations of the methods used for obtaining these records. The standard type of gage well as well as the intake pipes leading from the river to the well freeze quite early in the fall and remain frozen quite late in the spring and even into the summer. The writer has had the experience of being a member of a party which thawed the intake pipes to a gage house on the Tanana River, one of Alaska's major rivers, after the first of July. This freezing can affect spring and summer records which are very important. In Alaska, since the frost has usually penetrated deepest into the ground sometime in May, intake pipes thawed after the spring runoff begins may refreeze again very quickly. This points up the very serious fact that considerable changes must be made in the matter of obtaining stage relationships for these northern streams before good records can be obtained.

The writer would warn the inexperienced engineer against attempting to correlate stream discharges with air temperatures at low temperatures. Mr. Moore has pointed out that this can be done at moderate temperatures below freezing. The writer has seen engineers very carefully adjust their estimates of stream discharge with changes in temperature where the temperature ranges were in the order of from minus 20° to minus 65° with the cover on the ground perhaps averaging 3 feet of very light, well insulating snow. Since winter stream flow in northern climates is derived entirely from groundwater, it is quite improbable that the particular day's discharge from a stream could be affected by the temperature for that day, but it would be more a function of a mean temperature extending over a much longer period of time as well as the depth and density of snowcover on the basin.

Some engineers make a practice of installing thermograph thermocouples in the gage well instead of in the stream. This can make a considerable difference in the temperature which would be recorded for the stream at a particular time. The writer has measured differences between gage well and stream temperatures of upwards from fifteen degrees F. in the summer. In the winter after the gage freezes, the temperature for the stream would erroneously be recorded as below freezing by perhaps a considerable amount. This is obviously not a true record of stream temperatures, and the use of such records should be reviewed critically by the engineer having recourse to them.

STEPONAS KOLUPAILA.*—This paper by Mr. Moore is a valuable contribution to the complicated problem of determination of streamflow under ice conditions. The phenomenon of siphon action is of particular interest. The writer had occasions to observe similar strange effects in a cross section jammed with frazil ice: the water flow, partly in the form of a slurry, was concentrated in a few separate channels under extremely different hydraulic conditions. There is no substitute for intelligence and experience in computations of winter flow, more so than in any other field.

The writer was very interested in the method of adjustment of daily discharges applied by the author. Obviously, the author uses the Stout method: he corrects the water stages to the "effective heights," as this is explained, e.g., in the "Stream Flow" by Grover and Harrington, p. 285. Another method of correction of discharges seems to be of greater flexibility and accuracy:

* Prof. of Civ. Eng., Univ. of Notre Dame, Notre Dame, Ind.

the ratio is determined between the actually measured water discharge Q' and that read on the discharge curve (available for open channel conditions) Q . This ratio $k = Q'/Q$ varies through the winter period due to the changes in thickness of ice cover, presence or disappearance of frazil ice, depth of water and, particularly, the smoothing of subsurface roughness by flowing water. The obtained ratio is to be interpolated between actual measurements, adjusted at the beginning and the end of ice cover, when direct measurements are too dangerous or impossible; meteorological data can be useful in tracing the diagram of k . Daily discharges are to be computed multiplying the value read from discharge curve and the ratio k from diagram. Fig. 1 illustrates this method.

This "discharge correction method" in contrast to the "gage correction method" was initiated by the writer in 1928 and since that time has been in use in many European countries. Several detailed procedures were recommended for deficient data, especially for previous years without any direct winter measurements. Thus, the writer was able to compute the runoff of the Nemunas River in Lithuania for 1812 - 1943, for complete 132 years, one of the longest series of existing reliable runoff data. Further developments of this method might be mentioned. Mr. A. Ogievskii derived a "hydrometeorological method" for corrections k : air temperature is used; accumulation of the sub-freezing temperatures aids in construction and detailization of the diagram. Recently, Mr. H. A. Klein obtained an approximate empirical formula for the variation of the k ratio in Elbe River: $k = 0.308 + 0.02 T$, where T is the number of days since ice cover was established.

This method was presented by the writer at several international conferences: Leningrad 1928, Tallinn 1928, Seville 1929, Barcelona 1929, Helsingfors 1936, Edinburgh 1936, Lübeck 1938. In this country Mr. N. C. Grover, chief engineer in the Water Resources Division, U. S. Geological Survey, tried in 1936 to introduce this, as he called it, "Lithuanian method" into practice of his Division. Several valuable reports were submitted on this subject, as by M. C. Boyer and B. J. Peterson, G. E. Harbeck, C. C. McDonald and others. Unfortunately, these interesting reports were not published in the Water-Supply Papers. The writer is indebted to Mr. McDonald for a copy of his dissertation "Determination of stream flow for periods of ice effect," 1943, which is of very great value and still retains its importance.

The writer disagrees with the statement of Mr. Moore that engineering literature contains few references concerning the effect of ice on stream flow measurements. Starting with the pioneer work, done by eminent American hydrologists H. K. Barrows, R. E. Horton, and W. G. Hoyt, there are many papers in many languages. Some of the most interesting are presented in the subsequent reference list.

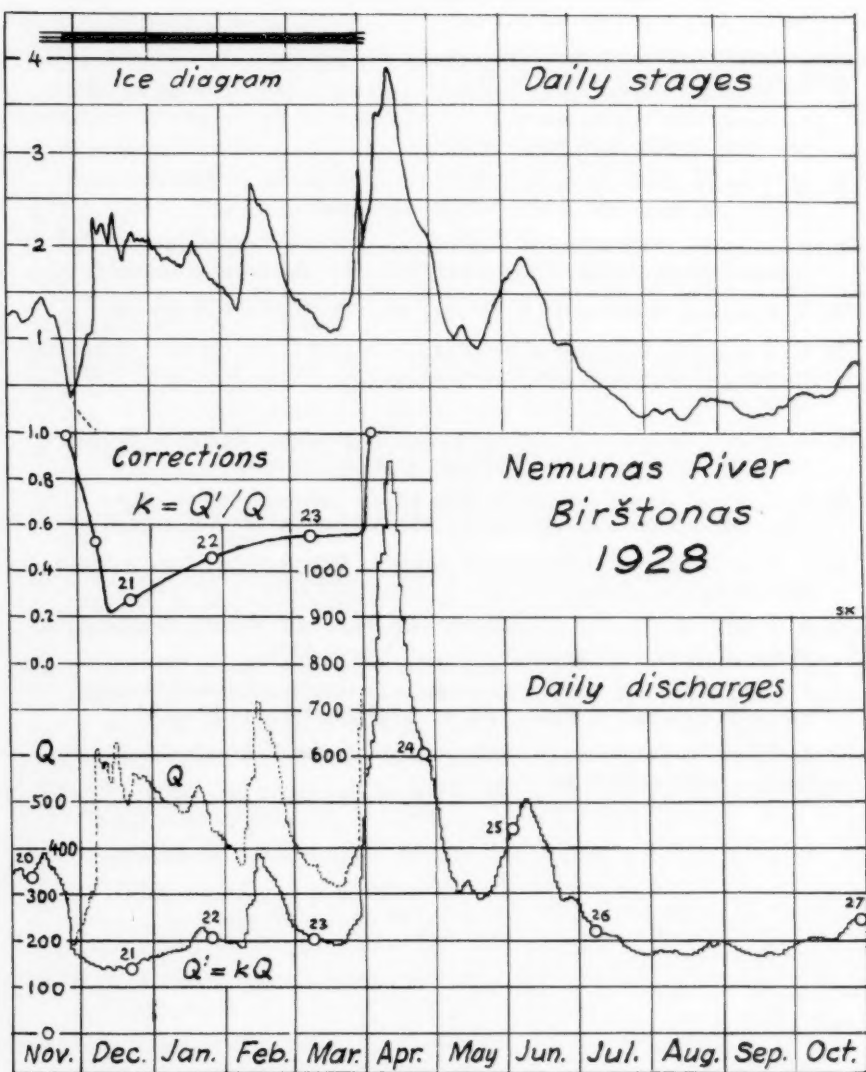
The opinion of the author concerning the accuracy of winter records is completely true. His suggestion to reexamine all previous winter flow computations before 1950 and to improve the annual runoff data is of great significance and should be materialized. The publication of reports on winter flow would contribute much to the progress of establishment of the runoff balance.

REFERENCES

1. H. K. Barrows and R. E. Horton, Determination of stream flow during the frozen season. Water-Supply and Irrigation Paper No. 187. Washington 1907.

2. S. Kolupaila, Determination of the winter flow. Kaunas 1928 (in Lithuanian), Tallinn 1928 (in German), Madrid 1931 (in French), Madrid 1931 (in German).
3. S. Kolupaila, The river flow beneath the ice. Transactions of the International Commissions of Snow and of Glaciers, Edinburgh 1936. Riga 1938. (in English).
4. F. I. Bydin, Method of computation of the winter flow using series of curves. Vestnik Irrigatsii, No. 6. Tashkent 1929 (in Russian).
5. F. I. Bydin, A diagram for computation of winter discharges. Vestnik Irrigatsii, No. 4. Tashkent 1930 (in Russian).
6. S. Kolupaila, On the determination of the winter flow at conditions of variable bottom. III Hydrologische Konferenz der Baltischen Staaten, Warsaw 1930 (in German).
7. A Dębski, Contribution to the method of determination the winter flow during winter. IV Hydrologische Konferenz der Baltischen Staaten, No. 34. Leningrad 1933 (in German and in Russian).
8. A Dębski, Water flow under ice cover conditions. III Hydrologische Konferenz der Baltischen Staaten, Warsaw 1930 (in German).
9. A. B. Ogievskii, Regime of runoff of the upper and middle Dnieper River. Kiev 1932 (in Russian).
10. S. Kolupaila, Determination of the runoff of the Nemunas River, 1812 - 1932. IV Hydrologische Konferenz der Baltischen Staaten, No. 25 Leningrad 1933 (in German and in Russian).
11. F. I. Bydin, Winter Regime of rivers and methods of its investigation. Issledovaniia rek SSSR, No. 5. Leningrad 1933 (in Russian).
12. F. Fedorov, Computation of river flow when covered by ice. Gidrotehnicheskoe Stroitelstvo, No. 7. Moscow 1933 (in Russian).
13. W. Lászlóffy, Ice conditions in rivers, particularly in Danube in Hungary. Vizügyi Közlemények, No. 3. Budapest 1934 (in Hungarian).
14. F. Schaffernak, Hydrography. Vienna 1935, Springer (in German).
15. D. L. Sokolovskii and V. K. Stabrikov, Methods of winter flow computations of the Volga River. Materialy po gidrologii, hidrografii i vodnym silam SSSR, No. 25. Leningrad 1935 (in Russian).
16. R. A. Flerova, Basic methods of winter flow computation. Issledovaniia rek SSSR, No. 7. Leningrad 1935 (in Russian).
17. S. Kolupaila, Our experience in the computation of winter flow. V Hydrologische Konferenz der Baltischen Staaten, No. 7C. Helsingfors 1936 (in German).
18. A. Koval, Some methods of winter flow determination. Meteorologija i Gidrologija, No. 1. Moscow 1937 (in Russian).
19. I. I. Tsarev, Computation of the winter flow in rivers with frazil. Meteorologija i Gidrologija, No. 7. Moscow 1937 (in Russian).

20. A. V. Ogievskii, Hydrometeorological method of the determination of the winter flow. Association Internationale d'Hydrologie Scientifique, Bulletin No. 23. Riga 1939 (in German).
21. J. Wallner, Flood forecasting. Berlin 1938, Springer (in German).
22. W. Sperling, Evaluation of discharge measurements, particularly under ice conditions and aquatic growth. VI Baltische Hydrologische Konferenz, No. 17A. Berlin 1938 (in German).
23. M. Wegner, Observations of winter flow. VI Baltische Hydrologische Konferenz, No. 17C. Berlin 1938 (in German).
24. S. Kolupaila, Difficulties in construction and use of discharge curves. VI Baltische Hydrologische Konferenz, No. 17D. Berlin 1938 (in German).
25. S. Kolupaila, Hydrometry, I volume. Kaunas 1939 (in Lithuanian).
26. G. Trossbach, Influence of freezing on the flow in the streams of Eastern Europe. Wasserkraft und Wasserwirtschaft, No. 3. Munich 1943 (in German).
27. A. Hahn, The flow in frozen and grown up streams. Deutsche Wasserwirtschaft, No. 9. Munich-Stuttgart 1942 (in German).
28. H. A. Klein, "Winter flow of the Elbe River. Mitteilungen der Bundesanstalt für Gewässerkunde, No. 79. Koblenz 1956 (in German).
29. L. G. Shuliakovskii, Computation of winter flow in rivers free of frazil. Meteorologija i Gidrologija, No. 2. Leningrad 1954 (in Russian).
30. H. F. Hill, Jr., Winter stream flow computations. Thesis, University of Maine, College of Technology. Orono, Maine, 1928.
31. S. Kolupaila and M. Pardé, The regime of rivers in Eastern Europe. Revue de Géographie Alpine, No. 4. Grenoble 1933 (in French).
32. S. Kolupaila, Nemunas, hydrologic study. Revue de Géographie Alpine, No. 2. Grenoble 1937 (in French).



„Lithuanian method“ of winter flow determination

Fig. 1.

Discussion of
"TECHNICAL PROBLEMS OF FLOOD INSURANCE"

by H. A. Foster
(Proc. Paper 1165)

G. N. ALEXANDER,* A.M. ASCE.—Mr. Foster's latest paper concerning the application of statistics to flood estimation entitled "Technical Problems on Flood Insurance" is, as he states, based largely on his preceding paper on "Flood Insurance." (1) His first article on statistics for engineers, published by the ASCE some thirty years ago (2) still remains a classic in this field. As the later papers give insufficient technical background to the author's findings concerning flood probabilities it is not possible in this discussion to enter into the technical detail that characterised his first article.

The two basic questions concerning flood probabilities are:

Question (A) What is the "best estimate" of the probability or return period of a flood greater than a specified magnitude?
To answer this question decisions are required on—
(1) The type of distribution
(2) The method of parameter estimation.

Question (B) What is the "precision" or reliability of this estimate?

The earlier papers, such as those of Foster (2) and Goodrich (3) dealt only with the first step of Question A, viz. Distribution Type. There is little discussion as yet on the second step in engineering journals, but it is treated in statistical text books.

The importance of Question B was recognised some thirty years ago by the actuary Arne Fisher, in his discussion on Goodrich's paper (3) when he stated—

"the paper deals only with a subject of graduation, and leaves almost untouched the far more subtle and difficult aspects of the probable or presumptive values of future observations."

As statistics is applied to flood data primarily to enable inferences to be made concerning the magnitude of future floods, this problem is paramount. This question of precision is closely related to that of sampling errors, which as the author states is now being recognised by the engineering hydrologist, although as yet no particular procedures are generally accepted.

Given sufficient data and using recognised statistical techniques, Questions A & B above can be answered for recurrence intervals not greatly exceeding the length of record; the difficulties arise when extrapolation is necessary. For an assumed distribution, the precision of an estimate decreases approximately as the logarithm of the recurrence interval and increases as the square root of the length of record. Consequently extrapolation of short records can give quite misleading results, but with long records

* Engr.-in-Charge of Water Resources Section, State Rivers and Water Supply Comm., Melbourne, Australia.

some extrapolation is possible without undue loss of accuracy.

Failure to recognise the magnitude of the sampling errors invariably associated with short records was largely responsible for discrediting the use of probability methods in relation to floods. The writer believes that statistical techniques properly applied must ultimately form the basis of estimating flood probabilities which in turn are essential to actuarial estimates of premiums for flood insurance.

We next examine more closely, but still very generally, the means of reducing the arbitrariness in current procedures in seeking to answer Questions A and B.

Question (A) Methods of Curve-Fitting

As the author states "the various proposed methods of curve-fitting generally produce reasonably good results with a given flood record when used to express probabilities or recurrence intervals within the length of record."

Step (1) Type of Distribution:

Attempts have been made by some authors to justify certain types of distribution for flood estimation on "a priori" grounds. Thus, floods are regarded by Gumbel(4) and others as "extreme values" and hence they favour the Fisher-Tippett type of distribution. Others contend that the log-normal distribution is basically more appropriate, as floods may be regarded as the product of a number of independent causes. Arguments of this sort carry little weight, as they are seldom backed by study of causes of floods and their hydrographs; also the conventional use of the Chi-squared test for "goodness of fit" is of doubtful utility.

Chow has shown(5) that for a specific value of the variance, the asymptotic extreme value distribution and log-normal distribution when standardized are practically identical. From unpublished analyses carried out in the writer's office, it appears that the log-normal can also be used in lieu of the finite extreme value distribution based on a normal parent by selection of the appropriate parent size. This suggests that the log-normal distribution is sufficiently "flexible" for most cases. The statistical characteristics of the log-normal are becoming better known and its conservatism in extrapolation renders it particularly suitable for estimating design floods for spillways.

Step (2) Estimation of Parameters:

As long as there are insufficient grounds for differentiating between particular distributions and methods of parameter estimation, there is some justification for the time-saving process of fitting curves "by eye." However, if extrapolated values are quoted, it is desirable to specify the type of distribution used and the method of fitting, for the different procedures give at times very different answers.

Having selected the distribution, a decision is now required on the most appropriate method of estimating parameters. Two methods are commonly used by statisticians viz. the "method of moments" and method of "maximum likelihood." For certain theoretical reasons the maximum likelihood method is preferred by most statisticians, at least for fitting within the range of observations. However, if curves have to be extrapolated the method of moments automatically weights the extreme values, and there may on this account be some justification for its use—but this is a contentious technical problem outside the scope of this discussion. Even when fitting a log-normal

distribution, estimates from extrapolated curves will differ significantly depending on whether the fit is to the original observations, or—as appears more desirable—to their logarithms.

Question (B) Precision of Estimates

The author refers to the question of the reliability or precision of estimates towards the end of the paper stating "the question of the reliability of probability estimates of future floods is of much greater significance in a programme of flood insurance than in justifying a flood protection project." Any estimates are of much greater value if some indication is given of their reliability and this is particularly true of flood estimates.

This question of the precision of estimates as a function of sample size is a basic problem of statistical inference. It may be said to date from "Student's" work on the t-test published nearly 50 years ago. However, there is still controversy concerning the more technical problems of statistical inference such as the relation between the Neyman-Pearson concept of "confidence limits" and Fisher's "fiducial limits?"⁽⁶⁾ In addition to these two methodological developments, "tolerance limits" may also be obtained over the range of observations. Hydrologists seeking to apply these procedures concerning probability limits naturally have some doubts in trying to decide between them—apart from any mathematical difficulties that may arise.

Although the practical differences in the results using alternative methods may be small within the range of observations, the validity of inferences over the extrapolated estimates is questionable, particularly when the fitted curve depends on the distribution type assumed. For example, when the log-normal distribution and the Pearson Type III were both fitted to 50 years of annual maxima of monthly discharges of the River Murray at Jingellic, it was found that the log-normal estimate for 100 year return period was very close to the upper 2 1/2% risk curve (95% confidence limits) for the Pearson Type III. Such differences, although disturbing to those unfamiliar with the characteristics of statistical methods, are believed to be no greater than differences associated with other more popular methods of floods estimation for long recurrence intervals such as the "maximum possible precipitation" technique.

The rather misleading title to this technique implies that no particular probability is associated with the estimate obtained, nor is its precision indicated. The method does show how, given certain meteorological conditions, floods can occur whose recurrence intervals are so great that probability methods which ignore the effect of sampling errors need re-interpretation. It is believed that this meteorological method and that of statistical inference from flood data will be reconciled when the probabilities associated with such steps as storm maximization and transposition can be ascertained.

CONCLUSION

It is clear that there is still much to be done both statistically and hydrologically before the estimation of future floods by statistical inference is placed on a firm foundation. With the recent enactment of flood insurance legislation in U.S.A. and the consequent need for actuarial determination of premiums, it may be expected that studies of this sort will be accelerated. Mr. Foster has made notable contributions in this field, and it is hoped that this paper will stimulate others to publish their findings.

REFERENCES

1. H. A. Foster (1954), "Flood Insurance," Proc. ASCE, Sep. No. 483.
2. H. A. Foster (1924), "Theoretical Frequency Curves and their Application to Engineering Problems," Tr. ASCE, Vol. 87 p. 142.
3. R. D. Goodrich (1927), "Straight Line Plotting of Skew Frequency Data," Tr. ASCE Vol. 90 p. 1.
4. E. J. Gumbel (1954), "Statistical Theory of Extreme Values and Some Practical Applications," Nat. Bureau of Standards, App. Maths. Series No. 33.
5. V. T. Chow (1954), "The Log-Probability law and its Engineering applications," Proc. ASCE, Sep. No. 536.
6. R. A. Fisher (1956), "Statistical Methods and Scientific Inference."

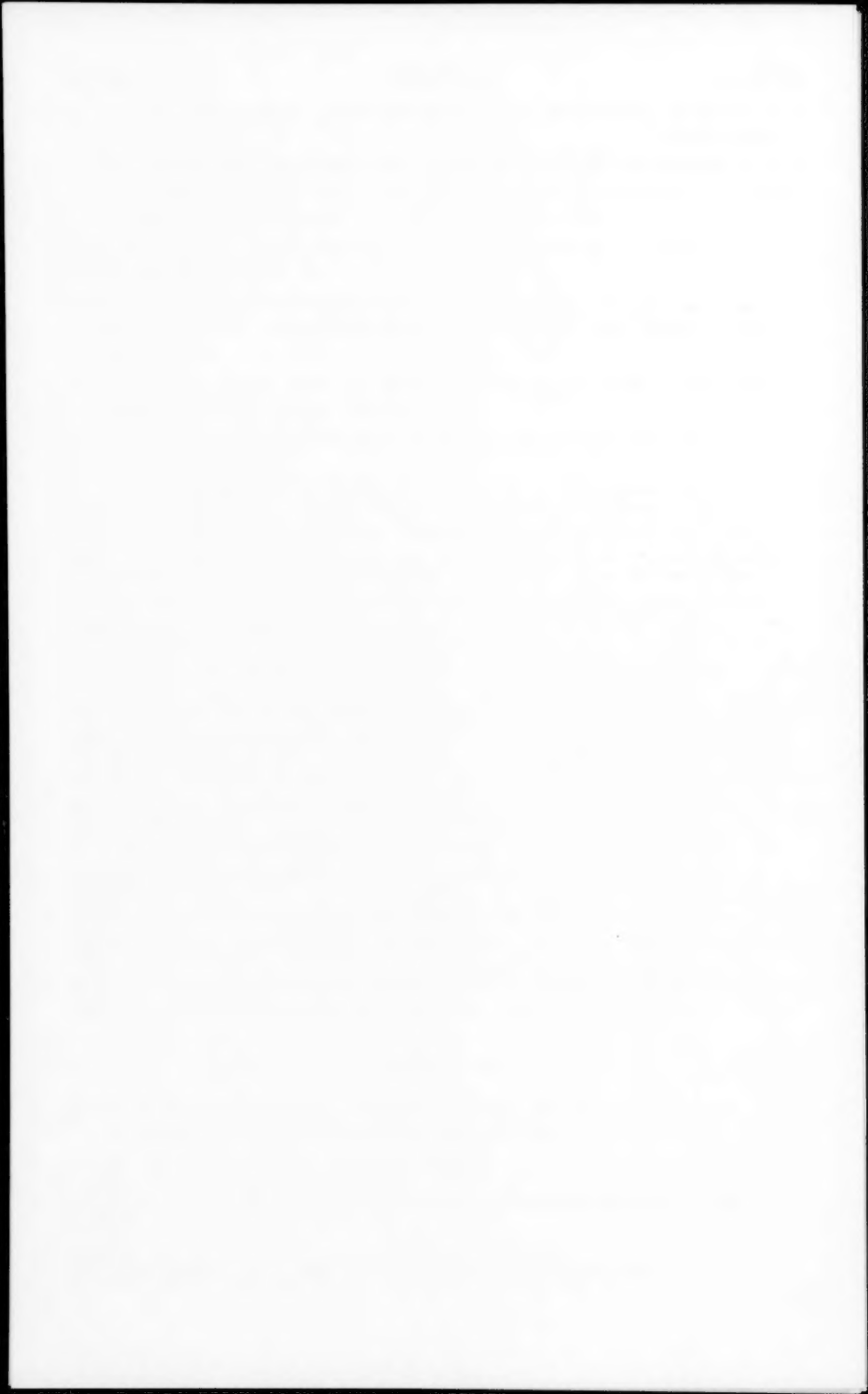
STEPONAS KOLUPAILA.*—In his discussion of the determination of flood probability, the author states: "After studying and comparing various methods of curve-fitting that have been proposed for hydrological studies, the author has not been able to reach any definite conclusions regarding which one is the best for use in flood-insurance studies." As it is known, Mr. Foster offered his method in 1924 and prepared his tables, based on two characteristic values—coefficient of variation and coefficient of skew. Foster's method was quite popular and widely used here and overseas. After some unfortunate failures occurred in extrapolation of probability curve this method was almost entirely eliminated. The writer feels that the cause of such a failure was the improper application and lack of experience. The coefficient of variation can be easily established and checked, although it may be based on short period of available data. The coefficient of skew is more intricate: the usual period of 20 to 30 years is definitely not sufficient for establishment of any reasonable value. Sometimes the addition of just one year causes a great change of this coefficient. Therefore it is more sound to presume a value by analogy with some more reliable long range data. The adjustment suggested by A. Hazen for inadequate length of records is not satisfactory. Different rules were offered for improvement of the coefficient of skew. Russian hydrologists made some significant progress: they introduced different empirical relationships and an additional "guarantee-factor." The results obtained with these corrections are more satisfactory. The writer has a successful experience with Foster's method and therefore hopes that this excellent American method will be restored at home in near future.

REFERENCES

1. H. A. Foster, Theoretical frequency curves and their application to engineering problems. Transactions, ASCE, 87 (1924).
2. A. Hazen, Flood flows. 1930, J. Wiley.
3. D. Johnstone and W. P. Cross, Elements of applied hydrology. 1949, Ronald Press.

* Prof. of Civ. Eng., Univ. of Notre Dame, Notre Dame, Ind.

4. S. Kolupaila, Probability of maximum discharge. Kaunas 1937 (in Lithuanian).
5. A. A. Luchsheva, Practical hydrology. Leningrad 1950 (in Russian).



Discussion of
"FREQUENCY ANALYSIS OF STREAMFLOW DATA"

by David K. Todd
(Proc. Paper 1166)

CORRECTIONS—Through an oversight, Figs. 10 through 16 were not published with this paper when it was published in February, 1957. These figures, therefore, are reproduced herewith.

M. A. BENSON.¹—The author is to be commended for attempting to bring before engineers a summary of information on the application of statistical analysis to streamflow data. The subject is not entirely new to engineers. For a comprehensive discussion of flood-frequency practices and a complete bibliography on the subject the writer would like to call attention to the recent article of Chow² on this subject.

Mr. Todd refers to available data in the annual Water-Supply Papers of the U. S. Geological Survey. Mention should also be made of the compilations of records of surface waters of the United States through September 1950, now being published in a series of volumes, each of which covers a major drainage basin of the United States. Volumes already published are in Water-Supply Papers 1301, 1311, 1313, 1316, and 1317 respectively. These include listings, in readily available form, of annual peak discharges.

The author states that, "For temporary or small structures where designs are based upon flood frequencies about 10 years or less, the basic flood method (partial-duration series) should be used;---." The author repeats here the recommendation of the Sub-committee of the A.S.C.E. Joint Division Committee on Floods. However, experience has shown that it is preferable in most cases to use the annual-flood method, even for small design frequencies. The annual-flood method is simpler, the problem of the independence of floods is not then involved, and it is always possible to convert from the annual-flood to the partial-duration series (see Langbein, reference (22) in original article).

The author says "Most extrapolation by eye of frequencies is arbitrary, hence it does not provide a sound basis for estimating frequencies of high floods. To overcome this difficulty analytical techniques have been developed for fitting a cumulative frequency curve to specified types of frequency distributions." He says further that "With the aid of statistical parameters determined from the streamflow data and special plotting papers, it is possible to estimate say the 10,000-year flood from a record of 20 years duration. That such practices are dangerous has been well emphasized by the ASCE Subcommittee on Review of Flood Frequency Methods."

1. Hydraulic Engr., U. S. G. S., U. S. Dept. of the Interior, Washington 25, D. C.
2. Ven Te Chow, Hydrologic Studies of Floods in the United States, Symposia Darcy, Dijon 1956-Tome III, Union Geodesique et Geophysique Internationale, p. 134-170.

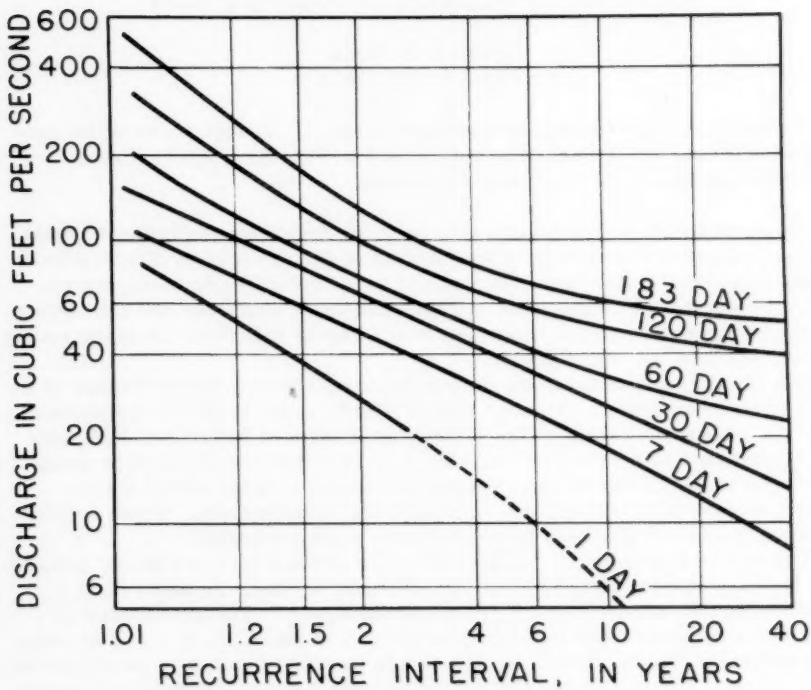


FIG. 10 DROUGHT FREQUENCY CURVES FOR
VARIOUS DURATIONS, MILWAUKEE
RIVER AT MILWAUKEE, (AFTER 13)

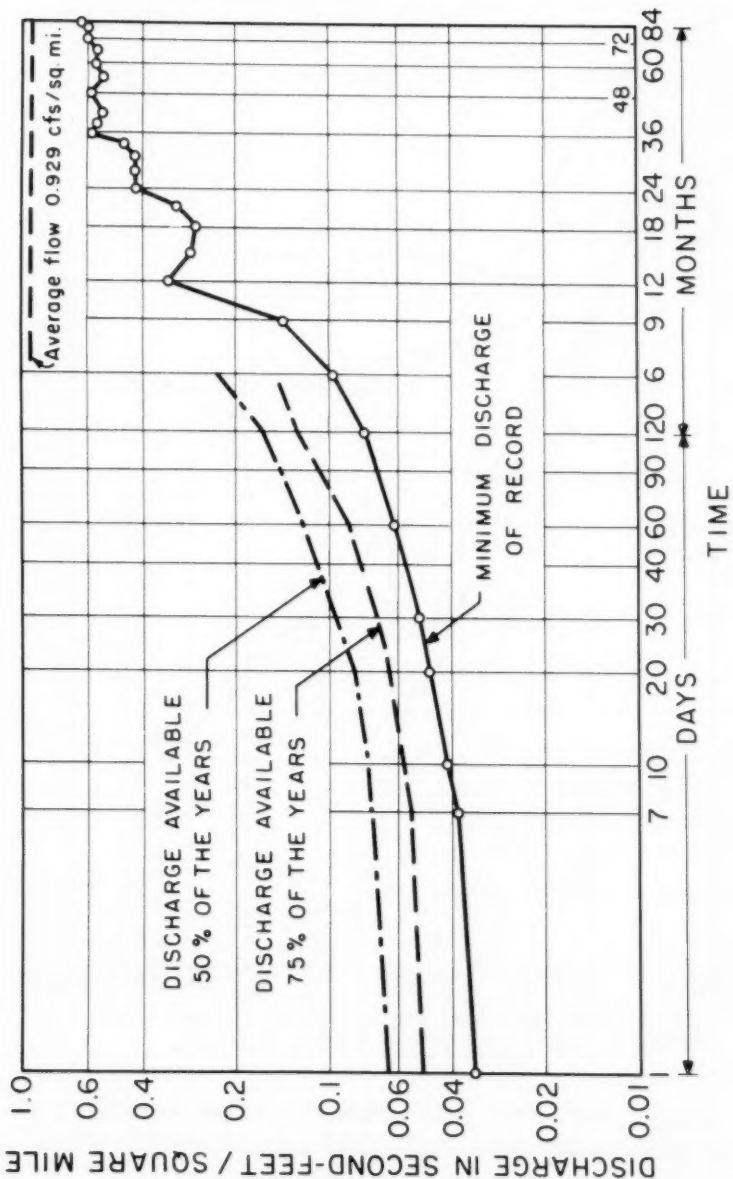


FIG. II DROUGHT FREQUENCY CURVES, WEST BRANCH MAHONING RIVER NEAR NEWTON FALLS, OHIO. (AFTER II)

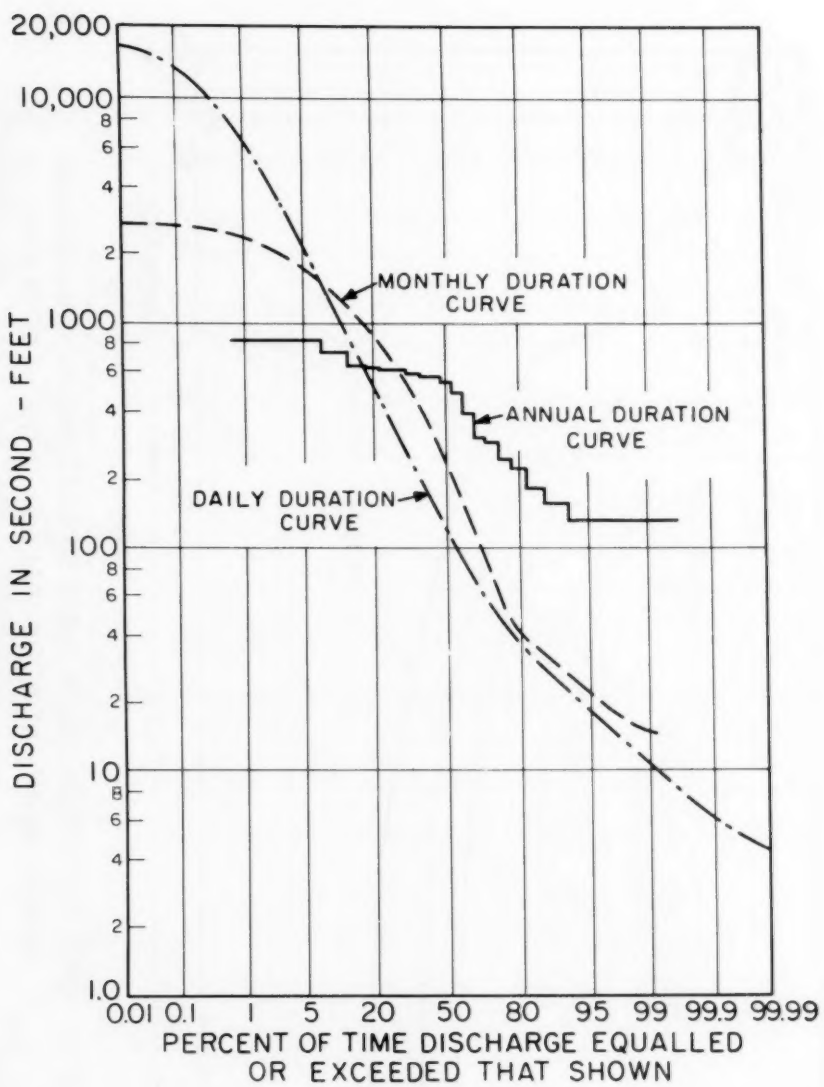


FIG. 12 DAILY, WEEKLY AND ANNUAL-FLOW DURATION CURVES, BIG WALNUT CREEK AT REES, OHIO.
(AFTER 10)

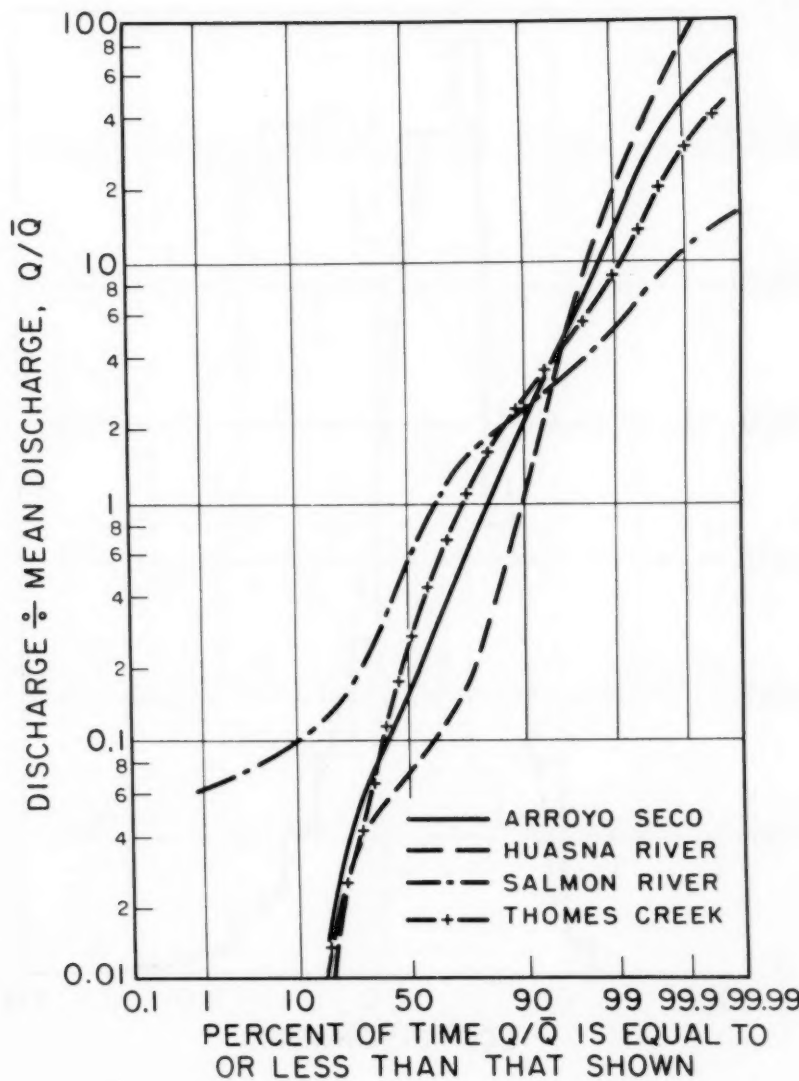


FIG. 13 FLOW-DURATION CURVES FOR FOUR CALIFORNIA STREAMS (AFTER 27)

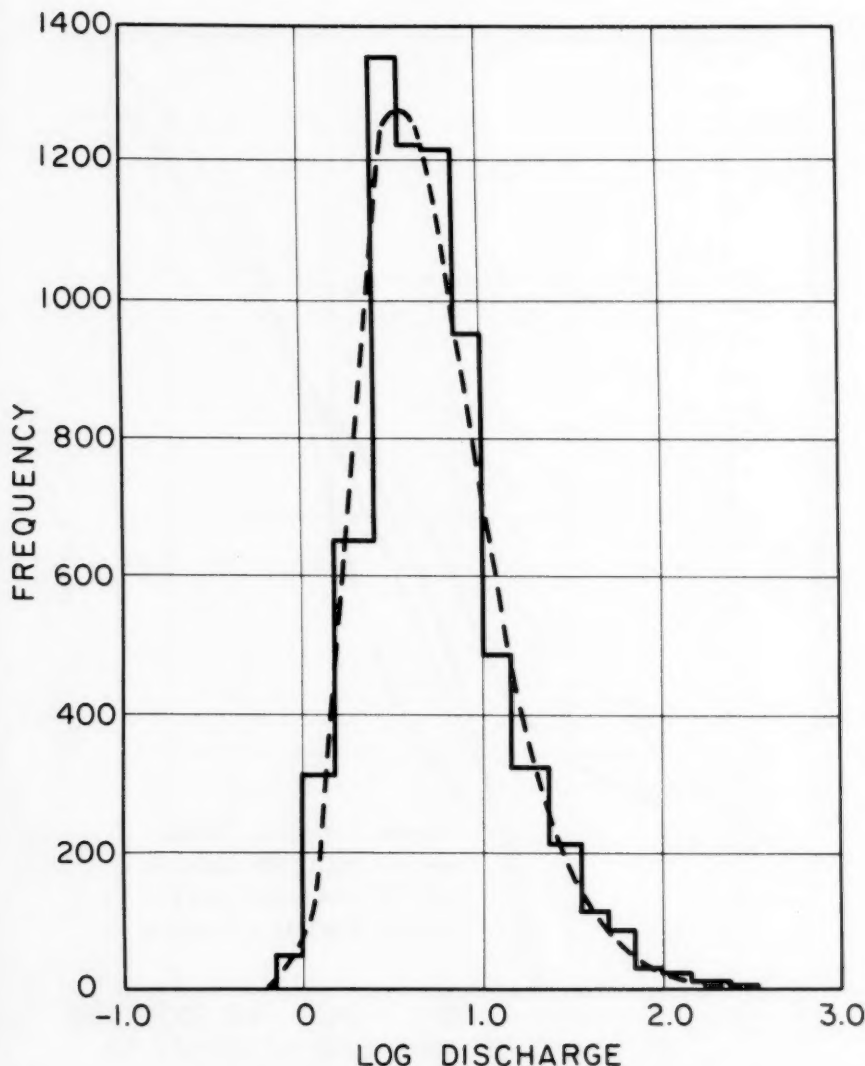


FIG. 14 OBSERVED AND FITTED FREQUENCY DISTRIBUTIONS OF MEAN DAILY FLOWS,
CUCAMONGA CREEK AT UPLAND, CALIF.
(AFTER 27)

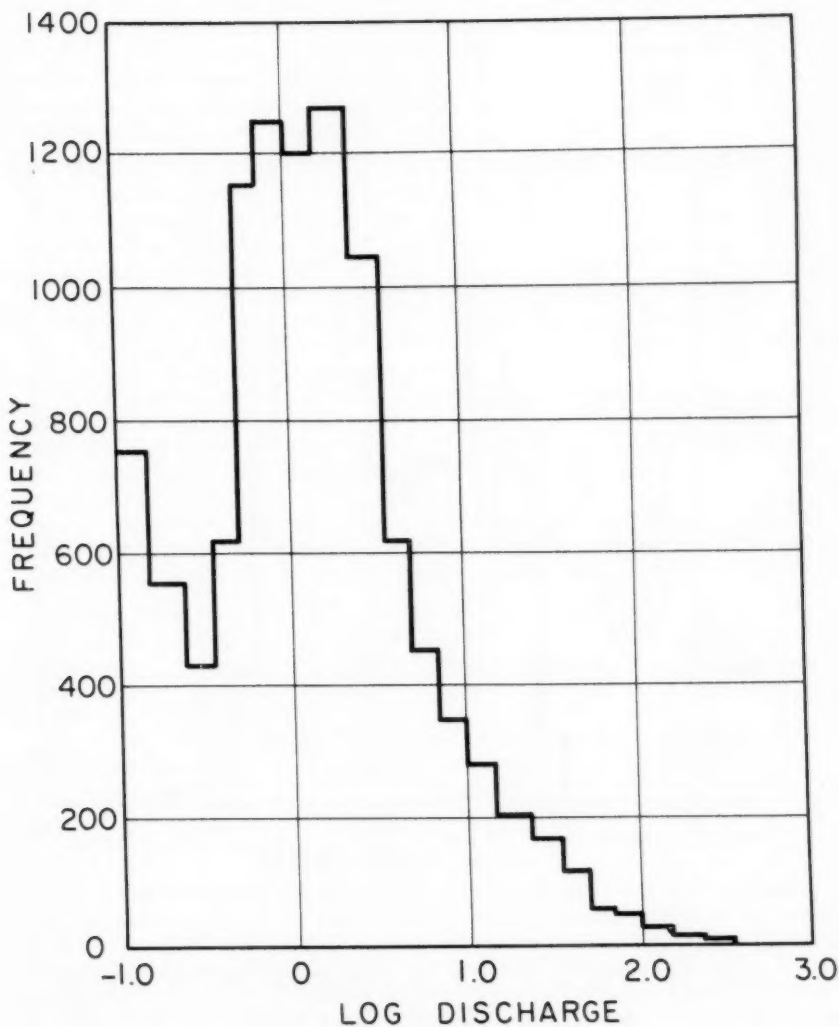


FIG. 15 FREQUENCY DISTRIBUTION OF MEAN DAILY FLOWS, FISH CREEK NEAR DUARTE, CALIFORNIA. (AFTER 27)

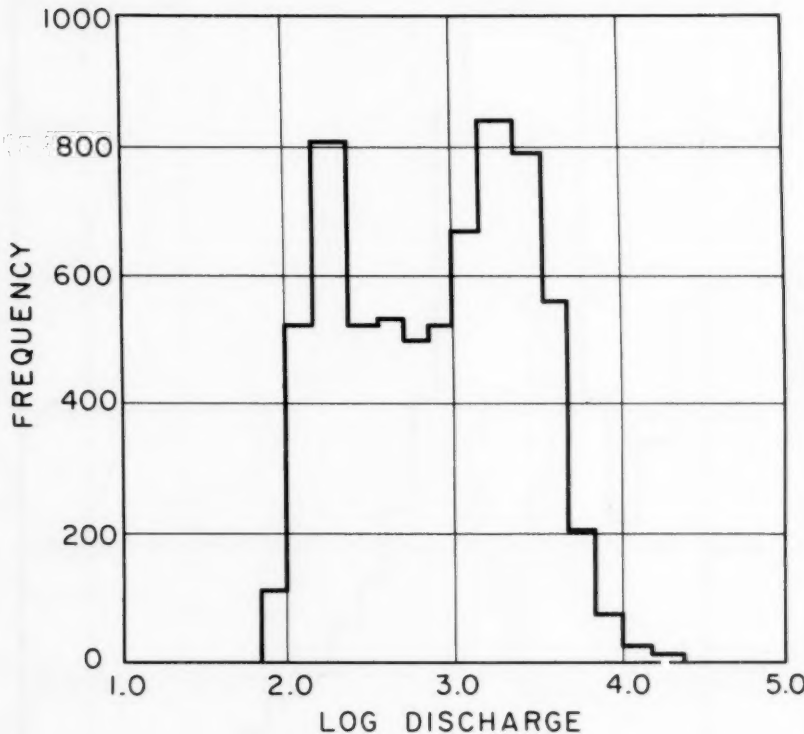


FIG. 16 FREQUENCY DISTRIBUTION OF MEAN DAILY FLOWS, SALMON RIVER AT SOMESBAR, CALIFORNIA. (AFTER 27)

The writer questions the implied superiority of fitted mathematical distributions over graphical techniques. It has not yet been possible to demonstrate *a priori* that flood peaks should conform to any mathematical or statistical distribution. Hence, it is not only dangerous but meaningless to estimate a 10,000-year flood from a 20-year record by means of a fitted curve. Pertinent statements on the general subject of graphical versus mathematically-fitted curves have been made by Ezekiel:³

"When there is some logical basis for the selection of a particular equation, the equation and the corresponding curve may provide a definite logical measurement of the nature of the relationship. When no such logical basis can be developed, a curve fitted by a definite equation yields only an empirical statement of the relationship and may fail to show the true relation. In such cases a curve fitted freehand by graphic methods, and conforming to logical limitations on its shape, may be even more valuable as a description of the facts of the relationship than a definite equation and corresponding curve selected empirically."

"In any event, estimates of the probable value of the dependent variable cannot be made with any degree of accuracy for values of the independent variable beyond the limits of the cases observed; and can be made most accurately only within the range where a considerable number of observations is available. It may be possible to extrapolate the curve if its equation is based on a logical analysis of the relation as well as on the cases observed; but in that case the logical analysis, and not the statistical examination, must bear the responsibility for the validity of the procedure."

See also Thomas,⁴ who says, "Indeed insofar as extrapolation made beyond the range of the recorded floods is concerned, the most elaborate analytical procedure of curve-fitting gives results that are no more reliable than those obtained by a simple estimation by eye of the flood frequency curve on any kind of probability paper."

The author refers briefly to the method of regional flood-frequency analysis which can be employed to estimate flood frequencies in ungaged areas. His figure 6 illustrates such methods, developed for the Atlanta, Ga. area, but he omits mention of the many statewide regional-frequency studies in which such methods have been described and developed for a large part of the country.

The author discusses the fact that in some regions floods may be caused by either rain or snow melt and, because "two different populations are intermingled----it follows, therefore, that not one but two straight lines of differing slope should be used to fit such flood frequency curves." Because the populations are in truth intermingled, the use of two straight lines does not follow as a solution. There is in general no particular flood magnitude below which all floods are caused by one factor and above which they are caused by another. In most parts of the country floods have multiple causes which are not distinct but combine or merge one into the other. The situation has been well analyzed by Hazen,⁵ who many years ago analyzed the effect on

3. Mordecai Ezekiel, *Methods of Correlation Analysis*, 2nd Edition, 1941, John Wiley & Sons, N. Y., p. 127.
4. Harold A. Thomas, Jr., *Frequency of Minor Floods*, Journal, Boston Society of Civil Engineers, October 1948, p. 428.
5. Allen Hazen, *Flood Flows*, John Wiley & Sons, N. Y., 1930, p. 102.

1348-30

HY 4

August, 1957

frequency curves of the multiple causes of floods, but said, "It is true of course that these causes grade into each other and that no lines of demarcation can be drawn."

The discussions of the frequency analysis of low flows and of all flows could be expanded considerably, if a survey of these subjects is to be at all complete.

Discussion of
"BUTTERFLY VALVE FLOW CHARACTERISTICS"

M. B. McPherson, H. S. Strausser and J. C. Williams, Jr.
(Proc. Paper 1167)

TURGUT SARPKAYA,¹ J.M. ASCE.—Valuable information adding to the gradually increasing knowledge of the performance of butterfly valves is contributed by the authors. The paper constitutes a well-arranged review of previous studies in addition to the newly presented basic analytical relationships, their interpretations and sensible applications to actual flow conditions. However, the authors have not dealt with the following features of the problem: (a) Variation of contraction coefficient at each end of the valve plate with the angle of valve opening and with the angle of complete closure; (b) Stability of flow for various valve openings; and (c) An explanation for the large scatter of experimental data for small values of α ($\alpha < 20^\circ$) or for near-full-open positions of valve plate.

For some time, this writer has been interested in the application of mathematical methods to practical problems of fluid flow, and has contended that many existing semi-empirical relationships would find wider application if all parts of the relationships were, wherever possible, freed from empirical values and experimental coefficients. Having once obtained the pure mathematical results, engineers can then compare them with the experimental results. Since the writer feels that the results obtained by the authors are significant, it seems worthwhile to apply the methods of hydrodynamics to butterfly valve flow in order to have a better understanding of the variations of various parameters involved in the phenomenon. From this viewpoint, the omission of any discussion of the rather surprising analogy which permits the use of hydrodynamic theory for certain problems of viscous motion is deemed to be regrettable. Having this object in mind the theoretical solution of the present problem is given in this discussion. Then the experimental results are compared with the theoretical ones and answers provided for the points stated above.

It is well known that many plane irrotational flow patterns which include the formation or deflection of free jets can be analyzed completely by the method known as the Helmholtz(1)-Kirchhoff(2) theory of free streamlines. The results obtained may be significant not only for the corresponding two-dimensional flows of real incompressible fluids but, in some instances, for their three-dimensional counterparts as well. The analyses consists of the definition of successive conformal transformations involving a hodograph, or velocity plane, and the application of Schwartz(3)-Christoffel(4) transformation. The writer would like to emphasize the fact that from the mathematical viewpoint, the direct calculation of free-streamline flows is restricted to two-dimensional irrotational flows of incompressible fluids which are free from gravitational effects and for which the solid boundaries are straight. As flows of real fluids seldom satisfy fully these stringent restrictions, the practical value of the results is open to question. The significance of the various

1. Nazilli, Turkey.

restrictions can be shown only by comparing the calculated results with those obtained from observations of real flows. For the present problem since the shear is not a primary factor, (the effect of shear will be discussed later) for the flow accelerates rapidly, the differences between comparable ideal and real flows are small. The importance of gravitational effects for the coefficient of contraction is already known to be definitely secondary. Being fully aware of the restrictions and limitations of the applicability of this method, the solution of butterfly valve problem proceeds as follows: If the coefficients of contraction at points B and H are C_{c1} and C_{c2} respectively as is shown in the physical plane (Fig. 1), then the main objective of the present investigation becomes the determination of the relationships:

$$\frac{C_{c1}}{C_{c2}} = f_{1-2}(\alpha, \beta) \quad (1)$$

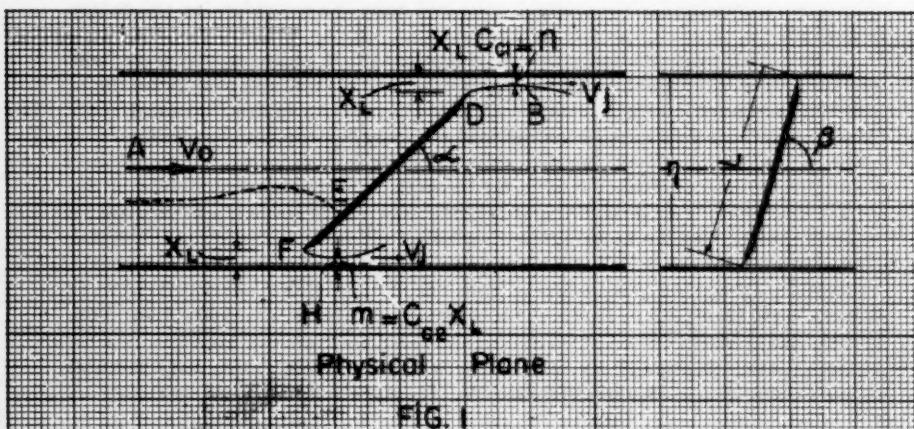
The existing relationships are:

$$n = C_{c1} \frac{\eta}{2} \left(1 - \frac{\sin \alpha}{\sin \beta}\right) \quad (2)$$

$$m = C_{c2} \frac{\eta}{2} \left(1 - \frac{\sin \alpha}{\sin \beta}\right) \quad (3)$$

$$\beta = \sin^{-1} \frac{\eta}{L} \quad , \quad \frac{n}{m} = \frac{C_{c1}}{C_{c2}} \quad (4a), (4b)$$

$$\frac{V_0}{V_j} \frac{2}{1 - \frac{\sin \alpha}{\sin \beta}} = C_{c1} + C_{c2} \quad (5)$$



in which n -and m -represent the thickness of the jets at B-and H-respectively; η is the width of channel; β the angle of closure; α the variable angle; and L the length of valve plate. The velocities of both jets are equal to V_j and the velocity far upstream from the valve plate is V_0 .

If z -and w -are used for the complex variable and the complex potential, then the variable ζ defined as (dw/dz) is given by

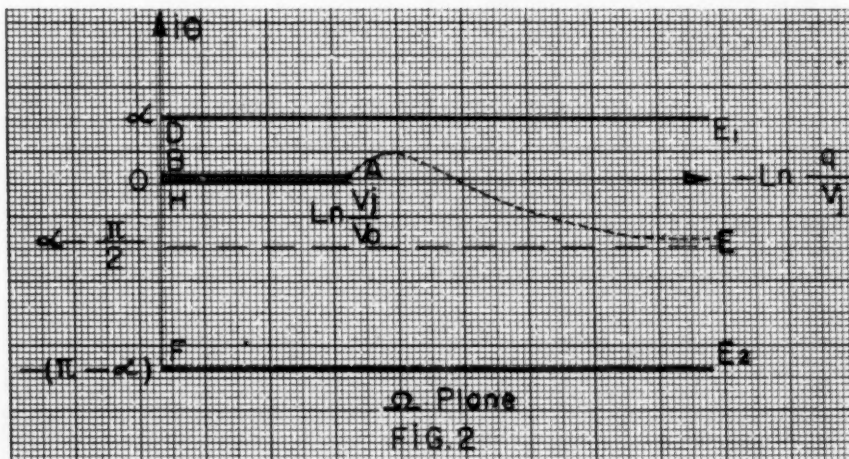
$$\zeta = -u + iv = -q e^{-i\theta} \quad (6)$$

in which u -and v -are the velocity components in the x -and y -directions, q is the magnitude of the velocity vector, and θ is the angle of its inclination.

If the variable Ω ,

$$\Omega = \ln\left(-\frac{V_j}{\zeta}\right) = -\ln\frac{q}{V_j} + i\theta \quad (7)$$

is introduced, the flow region in the physical plane (Fig. 1) can be mapped onto a corresponding region in the Ω -plane, as indicated in Fig. 2. Either ζ -or



Ω -must be related to w by means of known methods through still another complex variable designated as t . This relationship completes the rather complicated functional analysis because, as has already been seen, either ζ -or Ω -can be expressed in terms of (dw/dz) .

Any polygonal boundary in one complex plane can be transformed into the entire real axis of another through application of the Schwartz-Christoffel theorem, the interior of the polygon being transformed into either the upper or the lower half of the second plane. Thus, the outline in the Ω -plane is directly transformable into the real axis of the t -plane. Therefore, if we open out the Ω -plane and lay it along the real axis of the t -plane as shown in Fig. 3, the interior of the Ω -plane transforms into the lower half of the t -plane. The transforming function can be written as follows:

$$\Omega = M \int \frac{dt}{(t-t_1)^{\gamma_1/\pi} (t-t_2)^{\gamma_2/\pi} \dots} + N \quad (8)$$



t-Plane

FIG. 3

As many factors $(t - t_n)$ are introduced into the transformation as there are vertices of the polygonal boundary in the Ω -plane. The value t_n is the locus of the transformed point on the real axis in the t -plane, and γ_n is the exterior angle of the polygon at that point in the t -plane. Three of the t_n values can be assigned arbitrarily but with due regard to the geometrical characteristics of the Ω -plane, and the remainder must be given parametric values to be evaluated in terms of given quantities, along with M -and N , from the integrated function.

The desired mapping function between Ω -and t -becomes:

$$\Omega = M \int \frac{(t+a) dt}{\sqrt{(t+f)(t+l)(t-l)(t-d)}} + N \quad (9)$$

The transformation equation between the w -plane and the t -plane is obtained directly from the complex potentials for sources and sinks, point A being considered as a source of strength $(2\eta V_0)$ and points B and H as sinks of strengths $(2nV_j)$ and $(2mV_j)$ respectively:

$$w = \frac{V_j}{\pi} \left\{ n \ln(t-l) + m \ln(t+l) - \eta \frac{V_0}{V_j} \ln(t+a) \right\} \quad (10)$$

or

$$w = \frac{\eta V_j}{2\pi} \left\{ 1 - \frac{\sin \alpha}{\sin \beta} \right\} \left[C_{c_1} \ln(t-l) + C_{c_2} \ln(t+l) - (C_{c_1} + C_{c_2}) \ln(t+a) \right] \quad (10a)$$

and w -is connected to z by the relation,

$$z = -\frac{1}{V_j} \int e^{\Omega} dw \quad (11)$$

The evaluation of this and the other foregoing integrals are shown in the appendix of this discussion paper in order not to lose sight of the practical nature of the problem under consideration.

The results or the functional relationships obtained from these equations

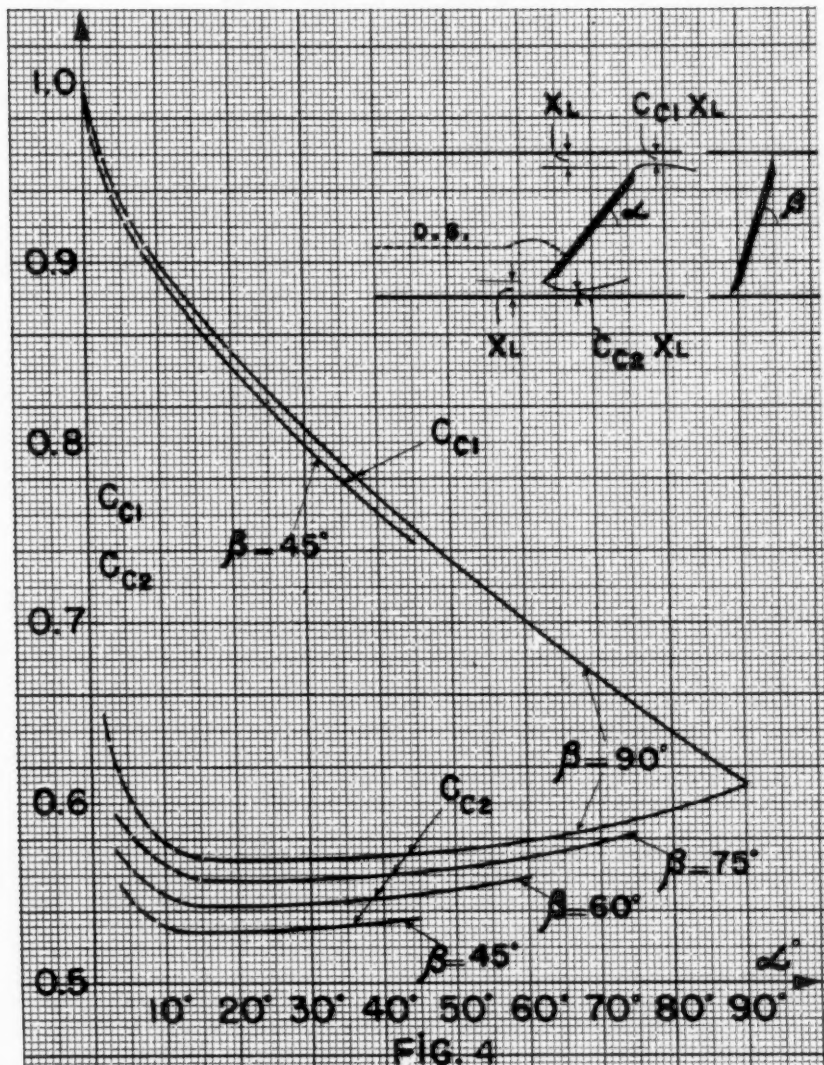


FIG. 4

are shown in Fig. 4. The significance of this figure is obvious. The contraction coefficient C_{C1} varies greatly with α , but very little with the angle of closure β , whereas the contraction coefficient C_{C2} varies appreciably with β , but very little with α , for the values of α greater than approximately 150° . But for small values of α , C_{C2} varies extremely fast and approaches unity. The values of the corresponding angles (corresponding to $\alpha < 100^\circ$) used in evaluating the elliptic functions (see appendix) approach their limit so closely that difficulties are encountered because of limitations in the tables available to the writer. (5,6,7,8,9,10) For those portions of the curves which could not

be computed readily the trend is indicated by broken lines.

In accordance with the authors' equations (1) and (7a), the discharge coefficient C_Q for free discharge can be written as follows:

$$C_Q = \frac{\pi}{4\sqrt{2}} (C_{c1} + C_{c2}) \left\{ 1 - \frac{\sin \alpha}{\sin \beta} \right\} \quad (12)$$

C_Q values computed from Eq. (12) for $\beta = 75^\circ$ using the contraction coefficients obtained in Fig. 4, are plotted in Fig. 5, and the solid-line is obtained. In the same figure the experimental data obtained by the authors for 4"CDC valve and 6"CDC valve are also plotted. Though, the complete closure angle of the latter valve differs 2.5° from the former, another theoretical curve has not been drawn for $\beta = 77.5^\circ$ in order not to make the figure illegible. The agreement between the theoretical and experimental results is fairly good, the theoretical discharge coefficient being somewhat smaller.

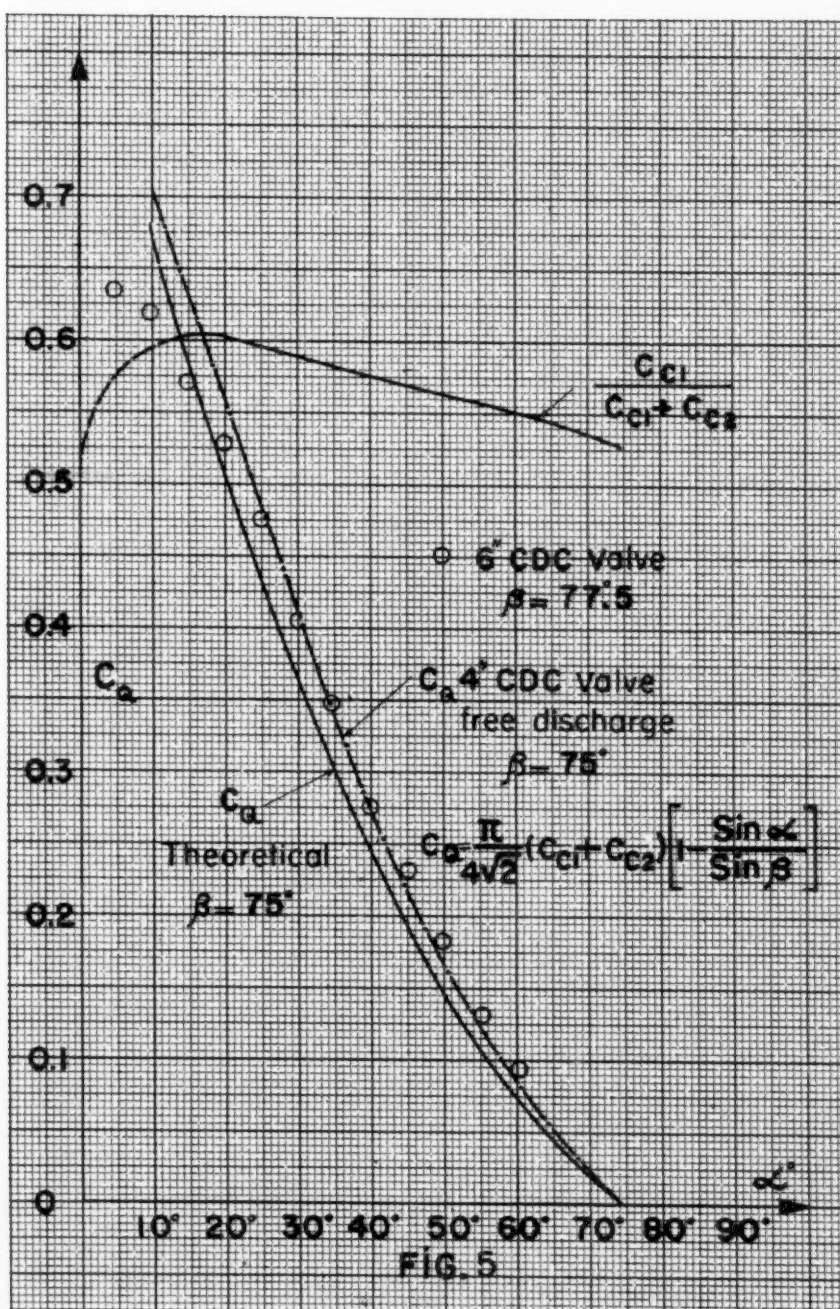
A similar computation has been made for $\beta = 90^\circ$, and the resultant theoretical curve with the experimental points (Genissiat and Dow data, as reported by the authors) are shown in Fig. 6. The agreement between the theoretical and experimental results is excellent.

So far we have discussed the effects of geometric variables on each coefficient of contraction and on the discharge coefficient. It is seen that the coefficients of contraction are functions of α -and β -only. Under the heading, "General Analysis for Enclosed Flow," authors state that: "In these tests, the magnitude of y (see authors' Fig. 1) was not noticeably changed by varying the discharge." Authors are perfectly correct in their observations, because, theoretically the value of y (n -and m -in Fig. 1 of this discussion paper) does not depend on the magnitude of discharge.

The second point we have proposed to discuss was the stability of flow for various valve openings and in connection with this the explanation for large scatter of experimental data for very small values of α -or for near-full-open positions of valve plate. The stability of flow depends on the stability of the stagnation point on the valve plate. As α -becomes smaller, the stagnation point or rather specifically speaking the stagnation line approaches the lower edge of the valve plate and theoretically it reaches the edge when α -is zero. But, practically the stagnation point or line reaches the sharp end of the plate when α - becomes about 15° . To illustrate this, a curve has been drawn computing the location of the stagnation line for $\beta = 90^\circ$ and for various values of α , as shown in Fig. 7. The dimensionless parameter λ -becomes practically zero for $\alpha = 20^\circ$.

In the case of axially symmetrical flow, the locus of stagnation points is curvilinear. Therefore, the stagnation points in the vicinity of valve axis are very close to the edge of valve plate, whereas the stagnation points in the vicinity of the diameter perpendicular to the valve axis are relatively far from the edge. The writer believes that in the case of axially symmetrical flow for a critical value of α -the stagnation points relatively near the plate edge jump abruptly to the edge of the plate changing the discharge coefficient. In the two-dimensional case the entire stagnation line jumps abruptly to the edge of the plate for small values of α . For a critical value of α , however, the stagnation line is unstable and jump to the edge and then back alternately resulting in unstable flow.

It would be very interesting to compare the discharge and contraction



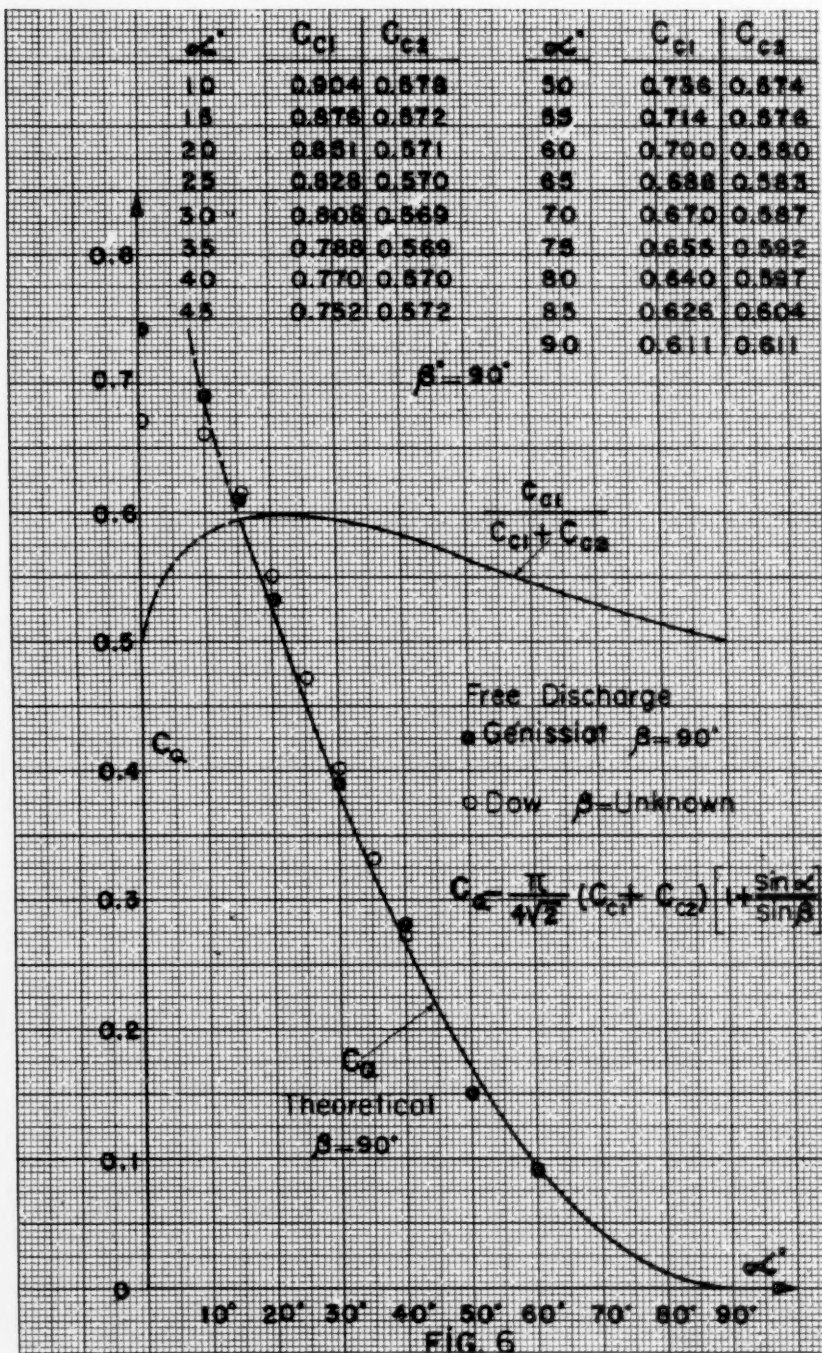
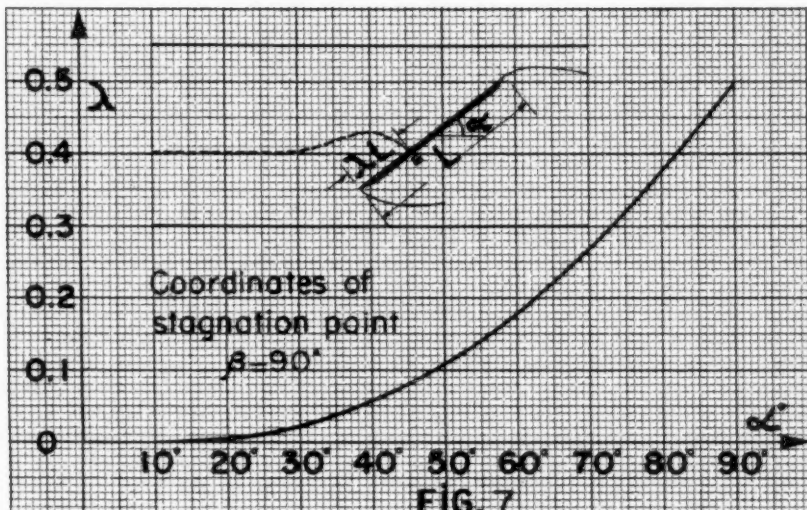


FIG. 6



coefficients obtained from two separate tests as follows: (a) First setting $\alpha = 25^\circ$ and decreasing it a few degrees each time, (b) First setting $\alpha = 5^\circ$ and increasing it a few degrees each time. Each test might well result in a separate curve in the range of critical values of α . The results obtained from such an experiment should prove useful in obtaining a better understanding of the stability of flow.

It seems to be evident from the foregoing explanation that the scatter of the experimental data for small values of α is largely due to the rapid and abrupt variations in the location of stagnation line in that region. Moreover, the geometry of valve plate also has an important effect on the variations of aforementioned coefficients. Theoretically, the plate is a thicknessless or one dimensional surface, but practically it has a thickness. Therefore, as noted by the authors under the heading: "Comparison of Actual and Analytical Flow Coefficients," "For a blade with a relatively wide tip, the point of separation will be at one or the other edge, depending upon the relative blade angle. The sudden, slight shift of C_Q trends for some valves is due to this transfer of the separation point."

The writer would like finally to comment on the discharge and on the contraction coefficients for submerged flows. It is evident from the experimental data given by the authors that the discharge coefficients for submerged flows are larger than the ones for free discharge as amply explained by the authors. They have observed that as stated under the heading: "Free discharge and submerged flow characteristics," "The free-discharge and submerged characteristics appear to be related, but are distinctly different at near-open positions. In submerged flow, the fluid fills or nearly fills the void between the two jets up to the blade, resulting in an expansion of the given fluid within the same fluid. In free-discharge of a liquid, the void is normally filled with air. For this reason, it would be logical to assume that the flow characteristics might not be identical even though the installations are quite similar."

The authors, therefore, assume that the action of turbulent shear in

causing the submerged jets to expand has some influence upon the pressure field that controls the rate of efflux. This writer was inclined to accept this explanation if it were not due to another contradictory observation and statement made by Mr. Curtis⁽¹¹⁾ and his associates on the "Coefficient of contraction for a submerged jet." Mr. Curtis states that "The minimum dimension of the submerged-jet profile is somewhat larger than that of free-jet, the coefficient of contraction being correspondingly higher—i.e., $C_c = (0.79^2) = 0.63$." At this point one would think that since the discharge coefficient depends upon the sum of contraction coefficients, the discharge coefficient also would be larger substantiating the experimental data given by Mr. McPherson and his associates for submerged discharge case. But Mr. Curtis continues to say that "Since the discharge coefficients of the two jets have already been seen to be essentially the same, (experimentally), one is forced to conclude that the rate of flow through the orifice is essentially independent of the tangential forces exerted upon the jet by the fluid into which it emerges." This writer is forced to conclude that the departures of the characteristics of submerged flow case from free-discharge case requires further study and a better explanation. Unfortunately, the authors' explanations can not be advocated as a panacea.

REFERENCES

1. Helmholtz, H., "Über discontinuirliche Flüssigkeitsbewegungen," *Monatsberichte Akad. d. Wiss. Berlin*, 1868, pp. 215-228.
2. Kirchhoff, G., "Zur Theorie freier Flüssigkeitsstrahlen," *Crelle*, Vol. 70, 1869, pp. 289-298.
3. Schwarz, H. A., "Notizia sulla rappresentazione conforme di un'area ellittica sopra un'area circolare," *Ann. di Mat.*, 2da Ser., Vol. III, 1869, p. 166.
4. Christoffel, E. B., "Sul Problema delle Temperature Stazionarie e la rappresentazione di una Data Superficie," *Ann. di Mat.*, 2da Ser., Vol. I, 1867, pp. 95-103.
5. Milne-Thomson, L. M., "Jacobian Elliptic Function Tables," Dover, New York, 1950.
6. Jahnke, E., and Emde, F., "Tables of Functions," Dover, New York, 1945.
7. Legendre, A. M., "Tafeln der elliptische Integrale," Wittwer, Nachdruck, Stuttgart 1931.
8. Adams, E. P., "Smithsonian math. formulae," Washington, 1922. pp. 260-309.
9. Nagaoka, H., and Sakurai, S., "Table No. 1," *Inst. of phys. and chem.*, Tokyo 1922.
10. Hayashi, K., "Tafeln der Besselschen, Theta-, Kugel-, und anderer Funktionen," Springer, Berlin, 1930.
11. Curtis, D. D., Martinez, J. E., and Vazquez, V., "Coefficient of Contraction for a Submerged Jet" *ASCE Proc. Paper No. 1038*, pp. 17-20, Aug. 1956, Vol. 82.

12. Legendre, A. M., "Fonctions Elliptiques" Deuxième Supplément, 1828, §IX. p. 146 et seq.
13. Jacobi, "Fundamenta Nova," §§ 62, 63; Ges. Werke, 1881, Bd. 11. pp. 229-231; see also, Cayley, "Elliptic Functions," second Edition (1895), Chap. VI.
14. Neville, E. H., "Jacobian Elliptic Functions," Clarendon, Oxford, 2nd Ed., 1951.
15. King, L. V., "On the Direct Numerical Calculation of Elliptic Functions and Integrals," Cam. Univ. Press., 1924.

APPENDIX

The integral given by equation (9) can be decomposed into two component integrals:

$$\Omega = M \int \frac{t \, dt}{\sqrt{(t^2-1)(t-d)(t+f)}} + M \int \frac{a \, dt}{\sqrt{(t^2-1)(t-d)(t+f)}} + N \quad (13)$$

Let us consider the transformation of Legendre: (12)

$$t = \frac{a_0 \sin^2 \phi + b_0}{c_0 \sin^2 \phi + d_0} \quad (14)$$

a_0, b_0, c_0 and d_0 can be so chosen that the above integrals simplify and reduce to known integrals. It should be noted that these integrals, depending on the values of t , require separate treatment for each interval under consideration.

I-In the intervals DE_1 and FE_2 , i.e., for $t \geq d$ and $t \leq -f$, one has

$$t = \frac{(d+f) \sin^2 \phi_1 - d(1+f)}{(d+f) \sin^2 \phi_1 - (1+f)} \quad (15)$$

$$\phi_1 = \sin^{-1} \sqrt{\frac{(t-d)(1+f)}{(t-1)(d+f)}}, \quad 0 < \phi_1 < \pi/2, \quad (16)$$

and

$$dt = \frac{2(d-1)(d+f)(1+f) \sin \phi_1 \cos \phi_1}{[(d+f) \sin^2 \phi_1 - (1+f)]^2} \quad (17)$$

If Eqs. (15) and (17) are replaced in Eq. (13), one obtains

$$\begin{aligned}
 S_2 = & \int \frac{2M}{\sqrt{(1+f)(1+d)}} \frac{(d+f)\sin^2\phi_1 - d(1+f)}{(d+f)\sin^2\phi_1 - (1+f)} \frac{d\phi_1}{\sqrt{1-k_1^2\sin^2\phi_1}} + \\
 & + \int \frac{2M a}{\sqrt{(1+f)(1+d)}} \frac{d\phi_1}{\sqrt{1-k_1^2\sin^2\phi_1}} + N
 \end{aligned} \quad (18)$$

Integral (18) can be separated into a first and third kind elliptic integral:

$$\Omega = \frac{2M}{\sqrt{(1+f)(1+d)}} \left\{ (1+a) F(\phi_1, k_1) + (d-1) \Pi_L(\phi_1, -\frac{d+f}{1+f}, k_1) \right\} + N \quad (19)$$

$\Pi_L(\phi, n, k)$, is the third kind elliptic integral of Legendre, and may be written as

$$\Pi_L(\phi_1, n, k) = \int \frac{d\phi}{(1+n\sin^2\phi)\sqrt{1-k^2\sin^2\phi}} \quad (20)$$

The parameter n is taken as real, and may take any value, positive or negative. For the intervals under consideration,

$$n_1 = -\frac{d+f}{1+f} \quad -\infty < n_1 < 1$$

Legendre's integral is connected with Jacobi's by the relation,

$$\Pi_L(\phi_1, n_1, k_1) = u_1 - \frac{\text{sn}(\epsilon_1, k_1)}{\text{cn}(\epsilon_1, k_1) \text{dn}(\epsilon_1, k_1)} \Pi_j(u_1, \epsilon_1 + iK') \quad (21)$$

in which u_1 is written for $F(\phi_1, k_1)$. sn , cn , dn , are elliptic functions and K' is the complete elliptic integral of the first kind for the complementary modulus. ϵ_1 is given by the relation

$$n_1 = -\frac{d+f}{1+f} = -k_1^2 \text{sn}^2(\epsilon_1 + iK', k_1) = -\frac{1}{\text{sn}^2(\epsilon_1, k_1)}$$

and

$$\text{sn}^2\epsilon_1 = \frac{1+f}{d+f}, \quad \text{cn}^2\epsilon_1 = \frac{d-1}{d+f}, \quad \text{dn}^2\epsilon_1 = \frac{d-1}{d+1}$$

In order to make the notations simpler, $\text{sn}(\epsilon_1, k_1)$, $\text{cn}(\epsilon_1, k_1)$, and $\text{dn}(\epsilon_1, k_1)$ will be denoted by $\text{sn} \epsilon_1$, $\text{cn} \epsilon_1$, and $\text{dn} \epsilon_1$, respectively.

The solution of Jacobi's integral is given by

$$\Pi_j(u_1, \epsilon_1 + ik) = u_1 Z(\epsilon_1, k_1) + \frac{u_1 \operatorname{cn} \epsilon_1 \operatorname{dn} \epsilon_1}{\operatorname{sn} \epsilon_1} + \frac{1}{2} \operatorname{Im} \frac{H(\epsilon_1 - u_1)}{H(\epsilon_1 + u_1)} \quad (22)$$

in which $H(\epsilon_1 \pm u_1)$ is Jacobi's Theta-function, (13) and

$$k_1^2 = \frac{2(f+d)}{(1+f)(1+d)}$$

Hence Legendre's integral becomes:

$$\Pi_L(\phi_1, n_1, k_1) = - \frac{\operatorname{sn} \epsilon_1}{\operatorname{cn} \epsilon_1 \cdot \operatorname{dn} \epsilon_1} \left\{ u_1 Z(\epsilon_1, k_1) + \frac{1}{2} \operatorname{Im} \frac{H(\epsilon_1 - u_1)}{H(\epsilon_1 + u_1)} \right\} \quad (23)$$

From Eqs. (19) and (23), we have

$$\Omega = \frac{2M}{\sqrt{(1+f)(1+d)}} \left\{ (1+a)u_1 - (d-1) \frac{\operatorname{sn} \epsilon_1}{\operatorname{cn} \epsilon_1 \cdot \operatorname{dn} \epsilon_1} \left[u_1 Z(\epsilon_1) + \frac{1}{2} \operatorname{Im} \frac{H(\epsilon_1 - u_1)}{H(\epsilon_1 + u_1)} \right] \right\} + N \quad (24)$$

which is the solution sought for the intervals under consideration. The constants M and N are determined from the comparison of Ω -and t -planes for the corresponding values and were found to be one and $i\alpha$ respectively.

II—For the interval HB, i.e., $|t| < 1$,
If t is taken as

$$t = \frac{-2f \sin^2 \phi_2 + (1+f)}{2 \sin^2 \phi_2 - (1+f)} \quad (25)$$

and the foregoing manipulations repeated, one obtains

$$\Omega = \frac{2M}{\sqrt{(1+d)(1+f)}} \left\{ (a-f)F(\phi_2, k_2) + (f-1)\Pi_L(\phi_2, -\frac{2}{1+f}, k_2) \right\} \quad (26)$$

in which

$$n_2 = -\frac{2}{1+f} \text{ which varies between zero and } -k_2^2$$

Writing $u_2 = F(\phi_2, k_2)$ and $n_2 = -k_2^2 \operatorname{sn}^2(\epsilon_2, k_2) = -\frac{2}{1+f}$
one has

$$\Pi_L = u_2 + \frac{\operatorname{sn} \epsilon_2}{\operatorname{cn} \epsilon_2 \cdot \operatorname{dn} \epsilon_2} \left\{ u_2 Z(\epsilon_2, k_2) + \frac{1}{2} \operatorname{Im} \frac{\theta(\epsilon_2 - u_2)}{\theta(\epsilon_2 + u_2)} \right\} \quad (27)$$

and therefore,

$$\Omega = \frac{2}{\sqrt{(1+d)(1+f)}} \left\{ (a-1) \frac{u_2 + (f-1)}{cn \epsilon_2 \cdot dn \epsilon_2} \left[u_2 z(\epsilon_2) + \frac{1}{2} \operatorname{Im} \frac{\theta(\epsilon_2 - u_2)}{\theta(\epsilon_2 + u_2)} \right] \right\} \quad (28)$$

in which

$$\phi_2 = \sin^{-1} \sqrt{\frac{(1+f)(1+t)}{2(t+f)}}$$

$$k_2 = k_1 = \sqrt{\frac{2(f+d)}{(1+f)(1+d)}} \quad \text{and} \quad k'_2 = k'_1 = \sqrt{\frac{(d-1)(f-1)}{(d+1)(f+1)}}$$

$$sn \epsilon_2 = \sqrt{\frac{1+d}{f+d}}, \quad cn \epsilon_2 = \sqrt{\frac{f-1}{f+d}}, \quad dn \epsilon_2 = \sqrt{\frac{f-1}{f+1}}$$

$\theta(\epsilon^+ u)$ also is Jacobi's Theta-function and connected to $H(\epsilon^+ u)$ by the relation

$$\theta(z + iK') = iB\theta(z)$$

where

$$\operatorname{Ln} B = \frac{\pi K'}{4K} - \frac{\pi i z}{2K}$$

K and K' are complete elliptic integrals of the first kind connected by the following relationships:

$$K = \operatorname{sn}^{-1}(1, k) \quad , \quad K' = \operatorname{sn}^{-1}(1, k') = \operatorname{sn}^{-1}(1, \sqrt{1-k'^2})$$

III—For the interval BD, i.e., $1 < t \leq d$,
If t is taken as

$$t = - \frac{(d-1) \sin^2 \phi_3 + (1+d)}{(d-1) \sin^2 \phi_3 - (1+d)} \quad (29)$$

one obtains

$$\Omega = \frac{2M}{\sqrt{(1+f)(1+d)}} \left\{ (a-1) u_3 + 2 \prod \left(\phi_3, -\frac{d-1}{d+1} k_3 \right) \right\} + N \quad (30)$$

Repeating the intermediate manipulations, one has

$$\Omega = \frac{2M}{\sqrt{(1+f)(1+d)}} \left\{ (a+1)u_3 + 2 \frac{\operatorname{sn} \varepsilon_3}{\operatorname{cn} \varepsilon_3 \cdot \operatorname{dn} \varepsilon_3} \left[u_3 z(\varepsilon_3) + \frac{1}{2} \operatorname{ln} \frac{\theta(\varepsilon_3 - u_3)}{\theta(\varepsilon_3 + u_3)} \right] \right\} + N \quad (31)$$

in which

$$k_3^2 = \frac{(d-1)(t-1)}{(d+1)(t+1)} = k_2^2 \quad , \quad k_3^2 = k_1^2 = k_2^2 = \frac{2(d+t)}{(1+t)(1+d)}$$

and

$$n_3 = -k_3^2 \operatorname{sn}^2(\varepsilon_3, k_3) = -\frac{d-1}{d+1} \quad , \quad -k_3^2 < n_3 < 0$$

$$\operatorname{sn} \varepsilon_3 = \sqrt{\frac{t+1}{t-1}} \quad , \quad \operatorname{cn} \varepsilon_3 = \sqrt{\frac{2}{t-1}} \quad , \quad \operatorname{dn} \varepsilon_3 = \sqrt{\frac{2}{d+1}}$$

and

$$\phi_3 = \sin^{-1} \sqrt{\frac{(d+1)(t-1)}{(d-1)(t+1)}}$$

IV—For the interval FH, i.e., $-1 \geq t \geq -f$
If t is taken as

$$t = \frac{d(t-1) \sin^2 \phi_4 - f(d+1)}{(t-1) \sin^2 \phi_4 + (d+1)} \quad (32)$$

one obtains

$$\Omega = \frac{2M}{\sqrt{(1+f)(1+d)}} \left\{ (d+a)u_4 - (d+f) \Pi_4(\phi_4, \frac{t-1}{d+1}, k_4) \right\} \quad (33)$$

in which

$$n_4 = \frac{f-1}{d+1} > 0 \quad , \quad n_4 = -k_4^2 \operatorname{sn}^2(\varepsilon_4, k_4) = k_4^2 \operatorname{sn}^2(\varepsilon_4, k'_4) / \operatorname{cn}^2(\varepsilon_4, k'_4)$$

$$n_4 = k_4^2 \tan^2 \theta \quad , \quad \sin \theta = \operatorname{sn}(\varepsilon_4, k'_4)$$

Thus,

$$\Pi = u_4 + \frac{\operatorname{sn}(\varepsilon_4, k'_4) \cdot \operatorname{cn}(\varepsilon_4, k'_4)}{\operatorname{dn}(\varepsilon_4, k'_4)} \left\{ i u_4 z(i \varepsilon_4) - i \frac{1}{2} \operatorname{ln} \frac{\theta(u_4 - i \varepsilon_4)}{\theta(u_4 + i \varepsilon_4)} \right\} \quad (34)$$

From Eqs. (33) and (34), one has

$$\Omega = \frac{2M}{\sqrt{(1+d)(1+f)}} \left\{ (a-f)u_4 - (d+f) \frac{\operatorname{sn}(\varepsilon_4, k'_4) \cdot \operatorname{cn}(\varepsilon_4, k'_4)}{\operatorname{dn}(\varepsilon_4, k'_4)} \right. \\ \left. \left[i u_4 z(i \varepsilon_4) + i \frac{1}{2} \operatorname{ln} \frac{\theta(u_4 - i \varepsilon_4)}{\theta(u_4 + i \varepsilon_4)} \right] \right\} \quad (35)$$

in which

$$u_4 = F(\varphi_4, k_4) \quad , \quad k_3^2 = k_4^2 = \frac{2(d+f)}{(1+f)(1+d)} \quad ,$$

$$k_4^2 = \frac{(d-1)(f-1)}{(d+1)(f+1)} \quad , \quad \operatorname{sn}(\varepsilon_4, k'_4) = \frac{\sqrt{f+1}}{\sqrt{f+d}} \quad ,$$

$$\operatorname{cn}(\varepsilon_4, k'_4) = \sqrt{\frac{d-1}{f+d}} \quad , \quad \operatorname{dn}(\varepsilon_4, k'_4) = \sqrt{\frac{d-1}{d+1}}$$

and

$$\varepsilon_4 = \operatorname{sn}^{-1} \left\{ \sin \left(\tan^{-1} \sqrt{\frac{f+1}{d-1}} \right) \right\}$$

Intermediate steps in the solutions of the above integrals have been omitted for the sake of brevity. However, the reader will find an excellent account of the theory of Jacobian elliptic functions in reference (14), and in the other references stated previously.

In order to obtain z from Eq. (11), dw should be written as,

$$dw = \frac{q V_1}{2 \pi} \left(1 - \frac{\sin \alpha}{\sin \beta} \right) \left(\frac{c_{c1}}{t-1} + \frac{c_{c2}}{t+1} - \frac{c_{c1} + c_{c2}}{t+a} \right) dt \quad (36)$$

The rest of the integration could only be performed by numerical methods. The best and well-known method for this purpose is King's(15) A.G.M. scale method.

If, for a fixed value of β , numerical values are assigned to a , f , and d satisfying the boundary conditions in the transformed planes, corresponding simultaneous values may be obtained for C_{c1} and C_{c2} and α . It should be

noted that this process was a tedious trial-and-error solution. For this reason, the plot in Fig. (4) was prepared to make possible the intermediate determination of an approximate result through the practical range of values. For large values of α , say greater than 15° , and for a given β , C_{c2} values are very nearly equal. Thus only three values of C_{c2} for a given β were computed and a curve drawn through them. Similarly for a fixed α and for a wide range of values of β , C_{c1} values are very nearly equal. Therefore only four values of C_{c1} were sufficient to draw the appropriate curve.

The writer believes that a more accurate numerical computation could be carried out. However, this has been precluded by the limited time available for the discussion. Besides, the above results are deemed to be sufficiently accurate for practical purposes.

G. DUGAN JOHNSON,¹ M. ASCE.—The authors do not concern themselves with the characteristics of, or problems associated with, butterfly valves for "wide open or fully closed" service in penstocks and at hydraulic turbine inlets, but limit their discussion "to the flow of water through control-type valves for near-closed to near-open positions." They say that "for most applications flow characteristics are a function of geometry only" and attempt to demonstrate "the effects of geometric variables and present a basis for the analytical determination of flow coefficients" from which they indicate a method for predicting the inception of cavitation under regulating conditions.

The authors state that "flow coefficients for the near-open positions are influenced by the relative blade thickness and the blade shape," "viscous effects are noted with $\alpha_0 = 0^\circ$ to 20° " and "attainment of a high degree of test accuracy within this range is difficult because of the relatively large discharge rates and small head losses involved." They also note that discrepancies in various published data for the near-closed positions "can be explained by the difference in closure angle."

For the intermediate valve disc positions, they developed a two-dimensional plastic flow section (8" wide by 1" thick) to observe and measure the shapes of the two separate jets issuing from the orifices formed between the side walls and the centerline profiles of the discs modeled. They reasoned that "since the jet area is a function of the variable (y), measurements of the jet thickness in a two-dimensional flow model, representing a narrow section of the center part of the blade, should provide a basis to understand and predict prototype performance." The writer agrees that such studies should be of qualitative assistance in understanding the characteristics of flow patterns at the centerline, but cannot accept the quantitative results as being even approximately applicable to prototype performance.

It is a well-known fact that the discharge and contraction coefficients of an orifice of any shape are critically affected by the edge condition, which must be accurately reproduced in the model in order to predict prototype performance. The authors recognized this when they added the dotted line to the right hand orifice in Figure 1, but they minimized it unduly when they assumed that centerline flow patterns were even remotely similar to flow lines around any circular disc nearer its trunnions.

Consequently, the writer feels that any attempt to predict prototype discharge performance for valves in pipelines on the basis of such two-dimensional model tests would only be adequate where extremely rough

1. Chf. Hydr. Engr., S. Morgan Smith Co., York, Pa.

approximations were acceptable, and that prediction of cavitation inception which depends upon the maximum (rather than the average) velocity squared on the basis of such tests would be meaningless.

HENRY VOLTMANN.¹—The authors are to be commended for the very interesting, complete and valuable paper they have presented. Definite knowledge of butterfly valve performance becomes of vastly increasing importance in the hydraulic field and while many reports have been available of past tests, the data, as referred to by the authors, have not always been specific as to the test conditions.

It may be interesting to add to the data presented the following information concerning a 6" butterfly valve.

Independent water flow tests were run on this butterfly valve in a "continuous pipe" installation by Mr. J. J. Colleville under the direction of Mr. M. B. McPherson at Lehigh University in 1953. The data from these tests agree very favorably with the data in Figure 7 and Table IV of the authors' paper (nomenclature is identical):

α_0	C_Q	Range of N_R	No. of Test Runs
10°	1.48	$3.3 - 5.9 \times 10^5$	5
20°	1.00	$2.5 - 5.9 \times 10^5$	6
30°	0.613	$2.6 - 5.6 \times 10^5$	6
40°	0.38	$2.5 - 5.6 \times 10^5$	6
45°	0.31	$2.1 - 4.7 \times 10^5$	5
50°	0.23	$0.5 - 4.0 \times 10^5$	11
60°	0.13	$1.3 - 2.7 \times 10^5$	7
70°	0.040	$0.5 - 1.0 \times 10^5$	5
80° (Closure)		---	-

The valve was lens-shaped with a t_{max}/D of 0.188. There was no indication of any variation in the flow coefficient due to viscous effects. The C_Q values obtained for individual test runs varied a maximum of 5% from the average values given in the above table, except at 70° , where only small rates of flow were attainable and the errors were consequently higher.

The following piezometer station-distances were employed in the tests (four taps/station):

Distance, in pipe diameters, from valve body	
Upstream	2D, 4D, 10D, 20D and 30D
Downstream	1D, 2D, 3D, 4D, 5D, 7D, 9D, 11D, 13D and 15D.

A straight piezometric head line was obtained for all tests with the upstream stations, to and including the 2D station. The piezometric head line was straight in the downstream pipe, starting at the 5D station for blade angles of 10° to 40°, and starting at the 4D station for 45° to 70°. The valve loss, ΔH , was obtained by graphically extending the upstream and downstream piezometric head lines to the valve and measuring the difference. As with the authors' test data, the downstream pipe was filled with water in all test runs.

ACKNOWLEDGMENTS

The 6" butterfly valve mentioned herein was manufactured by the W. S. Rockwell Co. of Fairfield, Conn.

RONALD E. NECE.¹ J.M. ASCE.—The authors have presented the results of an interesting and comprehensive series of tests performed upon butterfly valves, and the information presented adds to the knowledge of this type of valve. The authors have also performed a service in presenting the results of some other investigators in a systematic form. Other data were undoubtedly considered, but not presented, in this paper. Historically, the results of Weisbach, originally given in 1845 and tabulated in (D-1),² were the earliest given for butterfly valves.

Of the many types of valves used to regulate flows for different applications in continuous pipelines, the butterfly seems to lend itself most readily to a theoretical analysis which will predict, with reasonable accuracy, the non-recoverable head loss through the valve. This discussion shall be confined to this one area of the investigations presented by the authors.

The head loss caused by the presence of a constriction in a continuous pipe which causes a contraction of the flow, followed in turn by the rapid expansion of the stream to the full conduit area downstream from the valve, may be analyzed by the combination of energy and momentum considerations. This head loss may be expressed, using the authors' notation,

$$\Delta h = \frac{(v_2 - v_3)^2}{2 g} \quad (1)$$

which is the familiar expression for the Borda-Carnot loss, where only the flow expansion downstream from the constriction is considered as being a source of loss.

This expression may be rewritten as

$$\Delta h = \left(\frac{A}{C_C a} - 1 \right)^2 \frac{v^2}{2 g} \quad (2)$$

1. Asst. Prof. of Hydraulics, Dept. of Civ. and San. Eng., Massachusetts Inst. of Technology, Cambridge, Mass.
2. Numerals in parentheses refer to corresponding items in the list of References in this discussion.

where: C_c = coefficient of contraction
 a = transverse projection of the restricted area of the valve.
 A = cross-sectional area of the valve body downstream from the constriction, in many cases identical with the area of the pipe.
 V = average flow velocity in the pipe.

Equation (2) may be written in the common form

$$\Delta h = K_L \frac{V^2}{2g} \quad (3)$$

where K_L = dimensionless head loss coefficient. For discharges generally associated with butterfly valves the Reynolds numbers are sufficiently high so that the flow geometry is essentially constant with varying discharges for a given valve configuration, with the result that K_L is also a constant. Any theoretical expression for K_L thus depends upon the value of C_c associated with the area ratio, a/A .

The following simple "model," shown in Fig. 1, may be considered as one method of use in predicting head loss characteristics. The valve is considered to be in a two-dimensional duct of height B ; the disk, which is pivoted at the duct center line, is of zero thickness, has the same width as the duct, and affects full closure of the valve at an angle α of 90° . The flow past the disk is then divided into two jets of widths C_c , b and $C_c 2b$.

For various angles α and slot height ratios $2b/B$ von Mises has calculated the values of C_c for irrotational flow. These are listed in (D-2). From these calculated results the average value of C_c for the valve geometry may be obtained by interpolation for the assumed condition of equal pressures, and velocities, at the vena contracta of each jet. The distribution of the flow past the two ends of the disk is also determined as a part of this calculation. Thus, for the "model," K_L may be expressed as a function of α alone.

Limitations to the validity of the "model" are immediately obvious. The disks of actual valves possess a finite thickness of both blade and hub; thus, when the valve is fully open, there is still a reduction in flow area through the valve, with the consequent head loss. Actual disks are usually tapered toward the tips, and the tips sometimes additionally rounded; both of these conditions have the effect of tending to decrease the contraction of the streams on either side of the disk. For circular pipes and disks, the area "a" becomes a crescent-shaped opening, and the flow conditions are no longer two-dimensional. Also, the disk angle at closure may be less than 90° ; the 4" and 6" CDC valves reported by the authors had closure angles of 75° and 77.5° , respectively. The "model" also assumes no stops, recesses, or projections on the walls, and assumes that the tips of the disk, when at the full closure position, contact but are not recessed into, the valve walls. In addition, the two-dimensional measurements listed in the authors' Table I indicate an unequal distribution of discharges around the two tips of the disk.

Head losses predicted from the "model" would thus not be expected to furnish very good agreement with actual data at either extreme of disk angle. When the valve is fully open, the thickness of the disk and/or disk hub become predominate in the formation of the flow geometry; at, or near, full closure the calculated area ratio will obviously depart from the actual for valves having maximum α values of less than 90° .

In Table I are given the calculated values of K_L for the "model" over the range of disk angles of 0° - 90° . Also given in the table are the values of K_L obtained by the authors for the 4" and 6" CDC valves, values based upon test data by Dickey and Coplen and by Netsch and Schulz (authors' references (10) and (9), respectively), as well as the older values given by Weisbach. The values of the discharge coefficient, C_Q , as given by the authors, may be converted to those for K_L by equating comparable expressions for the head loss. This yields the relationship,

$$K_L = \frac{1.24}{C_Q^2} \quad (4)$$

The values of K_L for the authors' references (9) and (10) were recalculated from the original papers. The values given are not precise, as they were determined from small-scale test data curves.

As one of the series of check and control valves designed for specialized applications tested recently at the Hydrodynamics Laboratory of the Massachusetts Institute of Technology, some characteristics of the butterfly swing check valve "H" shown in Fig. 2 were determined. This valve differed from the others considered in this discussion in that there was a smooth transition from an 8" diameter pipe upstream from the valve to an 8" square flow passage within the valve proper, followed again by a smooth transition to the circular pipe. The rectangular disk, allowed to rotate freely, was eccentrically hinged as shown. For steady flows through the valve in the normal, or forward, direction, the angles α assumed by the disk over the range of discharges of 1200 to 2000 GPM were 15° and $15^\circ 30'$ for two slightly different shaped disks; the average values of K_L were 0.82 and 0.66, respectively. For discharges between 500 and 1200 GPM, the average value of K_L for the two disks were 0.65 and 0.72, respectively, indicating changes in the internal flow geometry with Reynolds number, these changes in this case possibly being caused more by the transition section effects upon the flow than by flow changes due to the valve disk. A description of the test facilities and results obtained for some of the other types of valves investigated are obtained in (D-3).

Some of the data listed in Table I are plotted on Fig. 3. The solid line is designated as the "simple model theory." The test points for swing check valve "H" are also plotted. It might be mentioned that data for some commercial valves of 10" and 24" diameter with circular disks also fall within the spread of the curves plotted. As expected, the differences between the "model" values and the test data are greatest for the largest and smallest values of α .

The known physical size and shape of the valve and its disk for a particular valve could be used to determine more precisely the actual flow area ratios and to give better flow deflection angles in choosing values of C_Q . It is likely that by these more refined calculations the actual K_L values for valves having a relatively simple interior could be estimated more precisely, dependent primarily, of course, upon satisfactory values of C_Q . The simple "model" presented here is not to be considered a rigorous approach to the problem, and undoubtedly compensating factors in some cases cause its agreement with test data to be fortuitous. The complete characteristics of a given valve could

be determined only by a model test. However, the results clearly indicate that the butterfly valve is one type of control device where the application of the simple energy-momentum relationships will lead to a decent approximation of head loss characteristics. The same approach may be used with a varying degree of success with other more common types of valves; i.e., gate, plug, etc. In smaller gate valves especially the head loss coefficient is found to vary with the size of the valve because of the relatively greater significance of the boundary configuration, gate recesses, and relatively thicker gate disk. Comparisons of various valves, using the area ratio a/A as the basis of comparison, are given in (D-3).

LIST OF REFERENCES

1. Forcheimer, Phillip, Hydraulik, Teubner, Leipzig and Berlin, 1930.
2. Rouse, Hunter, Engineering Hydraulics, John Wiley and Sons, New York, 1950.
3. Nece, Ronald E. and DuBois, Richard E., "Hydraulic Performance of Check and Control Valves," Journal of the Boston Society of Civil Engineers, Vol. 42, July, 1955.

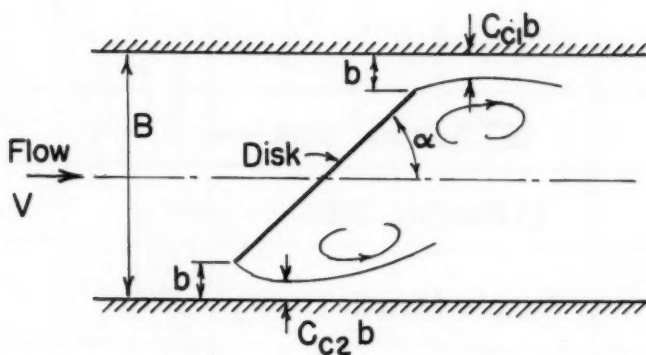


FIG. 1

'MODEL' VALVE FOR PREDICTION
OF HEAD LOSS CHARACTERISTICS

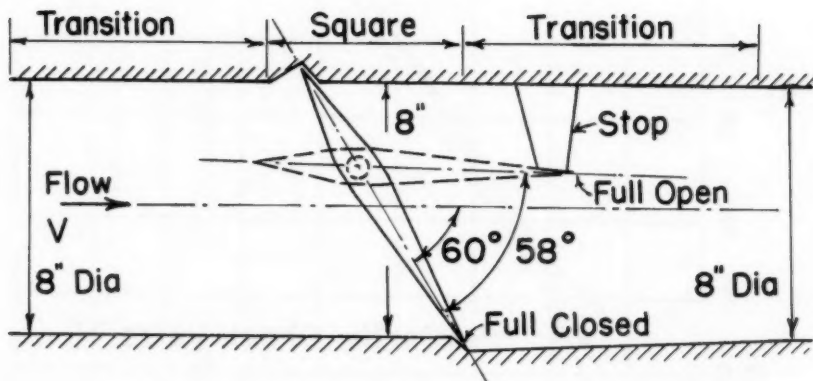


FIG. 2

SCHEMATIC DETAIL,
BUTTERFLY CHECK VALVE 'H'

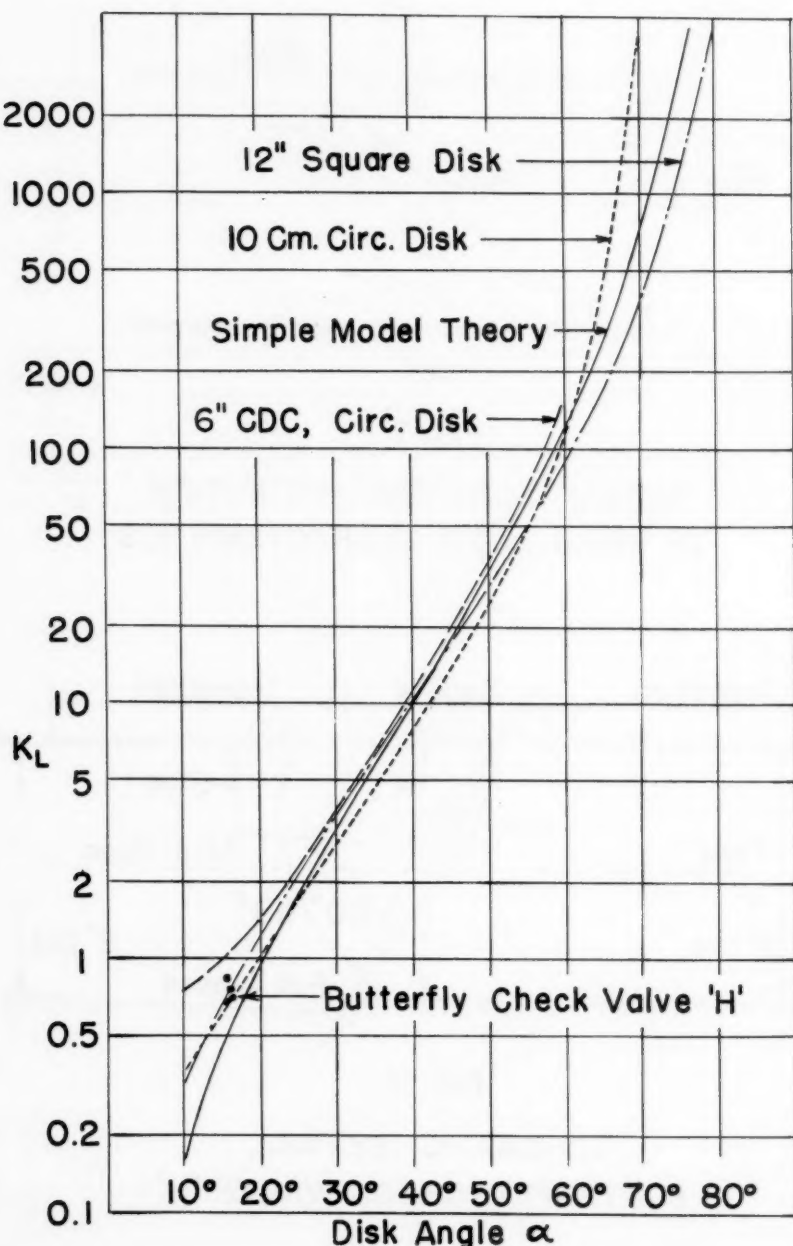
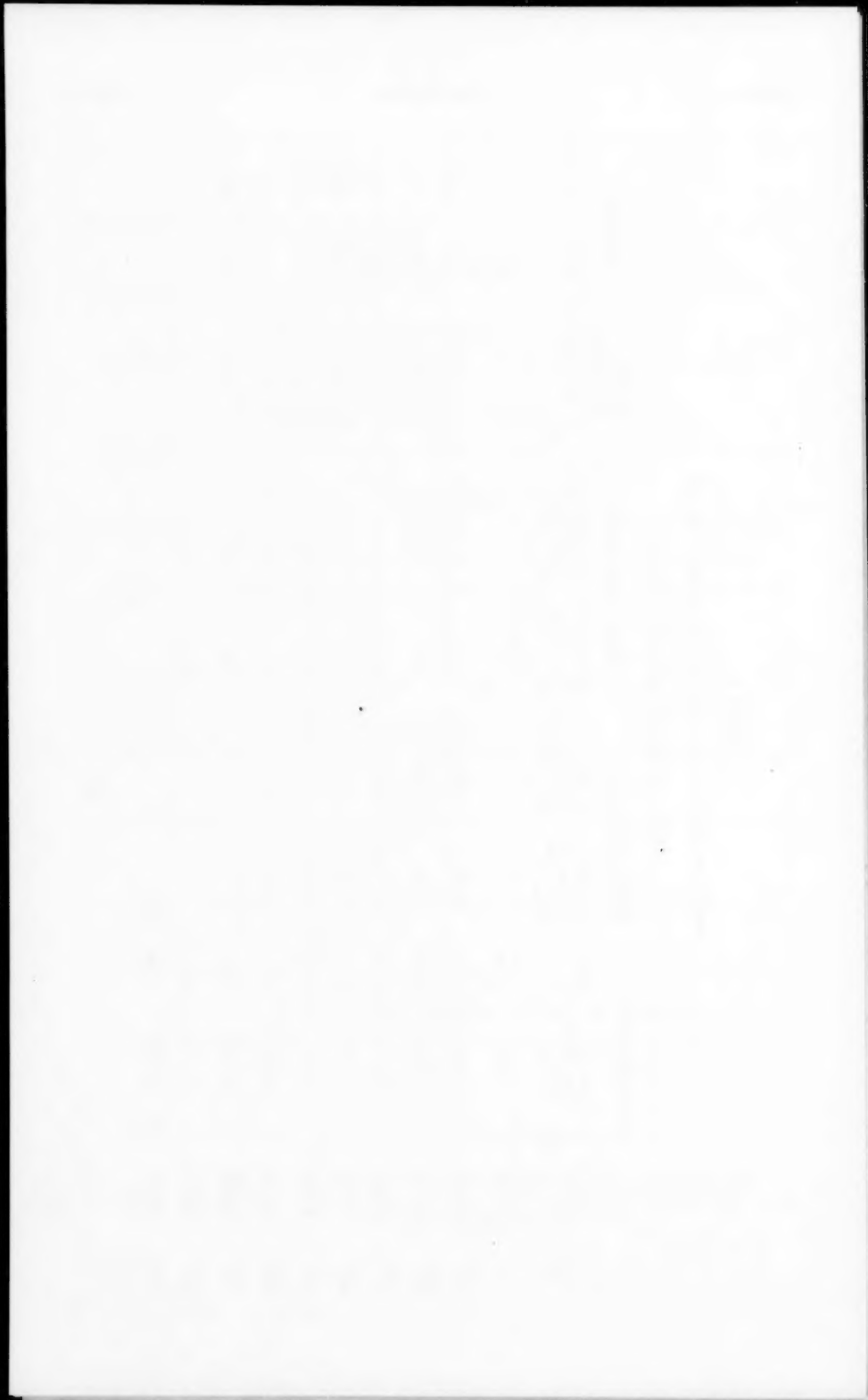


FIG. 3

TABLE I
Head Loss Coefficient, K_L vs. Valve Angle α for



Discussion of
"A STUDY OF BUCKET-TYPE ENERGY DISSIPATOR CHARACTERISTICS"

by M. B. McPherson and M. L. Karr
(Proc. Paper 1266)

CORRECTIONS—As the result of a printer's error, the illustrations that accompanied Proc. Paper 1266 were the illustrations that were used in Proc. Paper 1167. The illustrations for Proc. Paper 1266 are reproduced herewith:

DEFINITION SKETCH

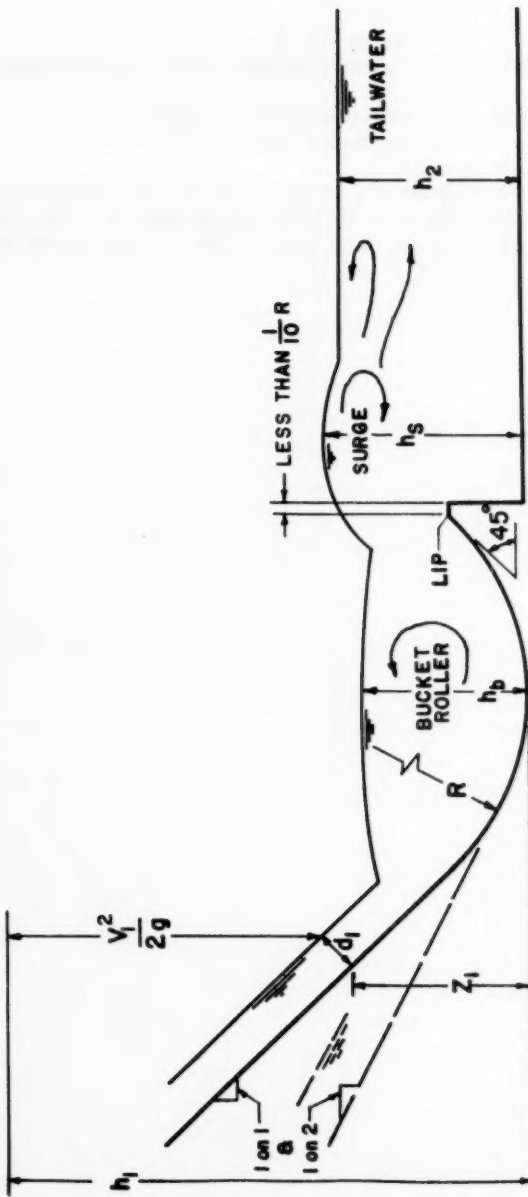


FIGURE 1

BASIS FOR USING BUCKET INVERT AS DATUM FOR h_2 & h_s
WITH (a) AND (e) CONSTANT, (b), (c) & (d) DID NOT CHANGE
WITH THE VARIOUS FLOOR CONFIGURATIONS SHOWN.

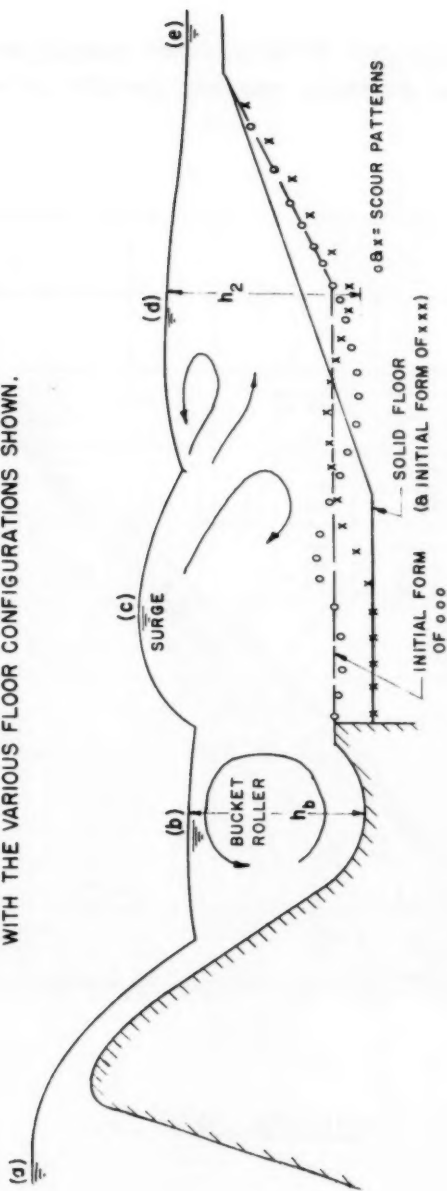


FIGURE 2

**CHARACTERISTICS OF BUCKET-TYPE ENERGY DISSIPATORS
WITH ENTRANCE AND EXIT ANGLES OF 45°**

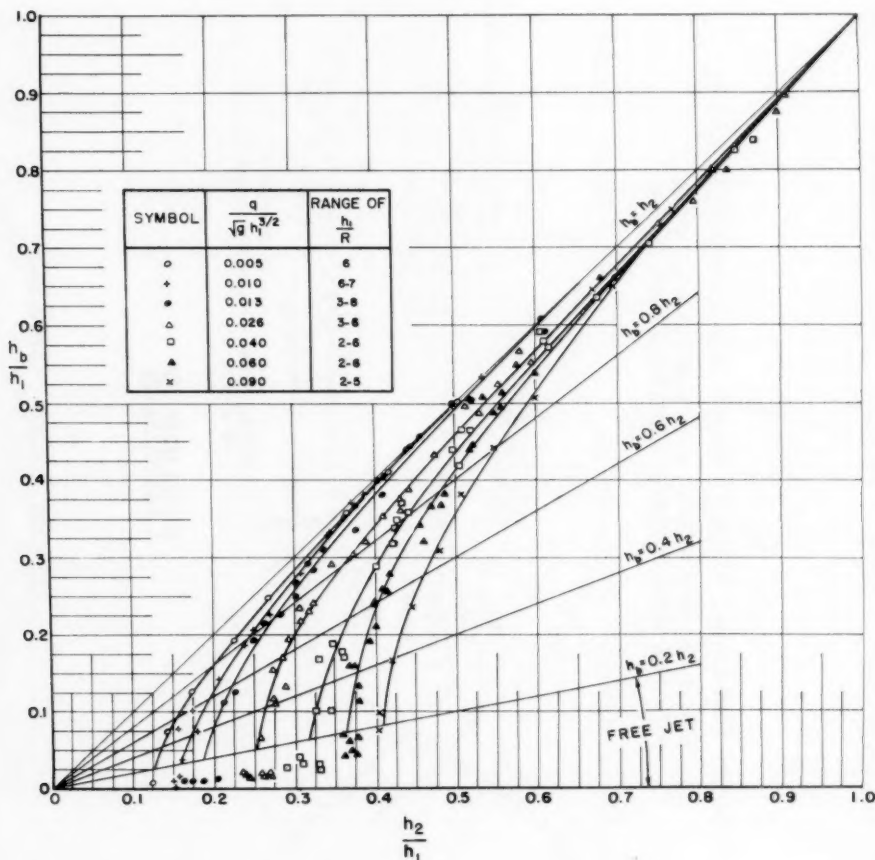


FIGURE 3

SURGE HEIGHTS FOR BUCKET-TYPE ENERGY DISSIPATORS
WITH ENTRANCE AND EXIT ANGLES OF 45°

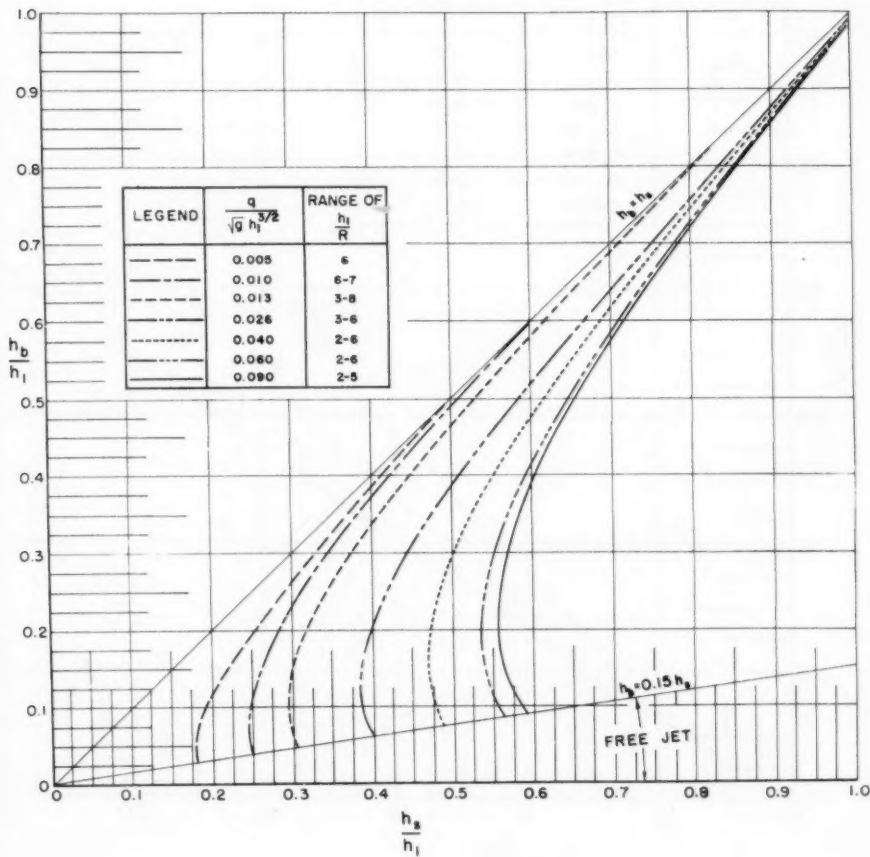


FIGURE 4

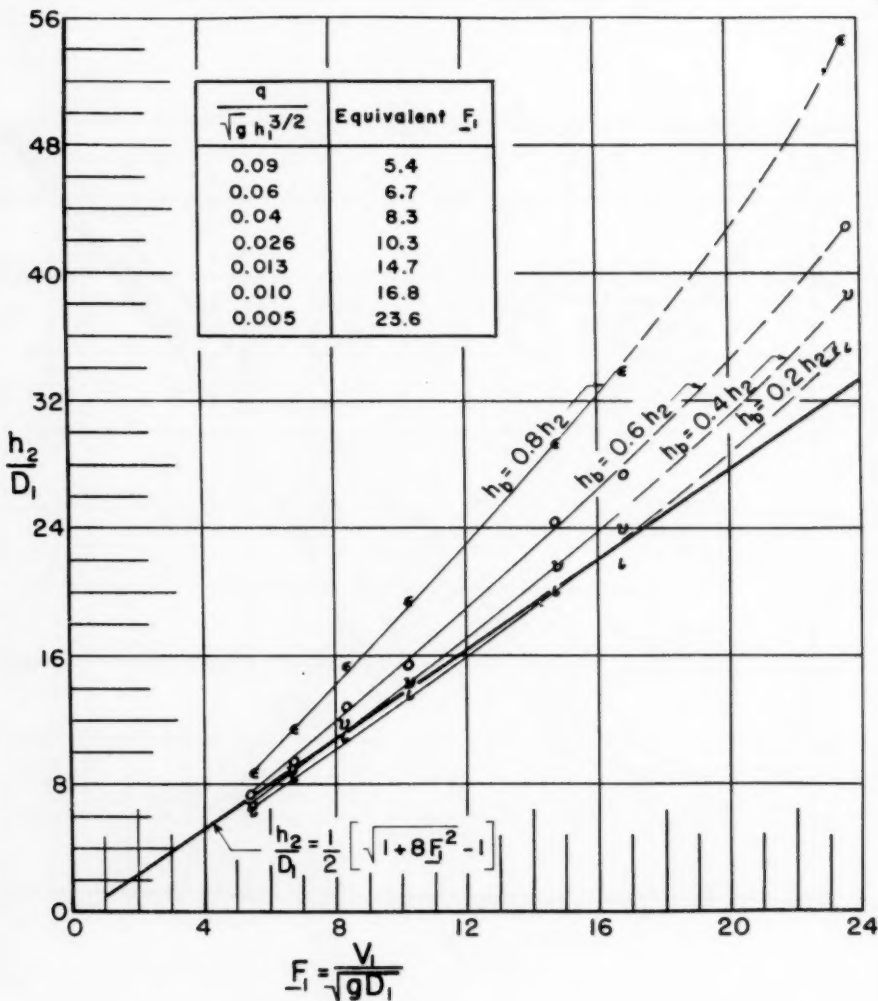
(TAILWATER/ EQUIVALENT D_1) vs F_1
FOR 45° EXIT ANGLE

FIGURE 5

CHARACTERISTICS OF BUCKET-TYPE ENERGY DISSIPATORS
WITH EXIT ANGLE OF 45° AND ENTRANCE
SLOPE OF 1 ON 2

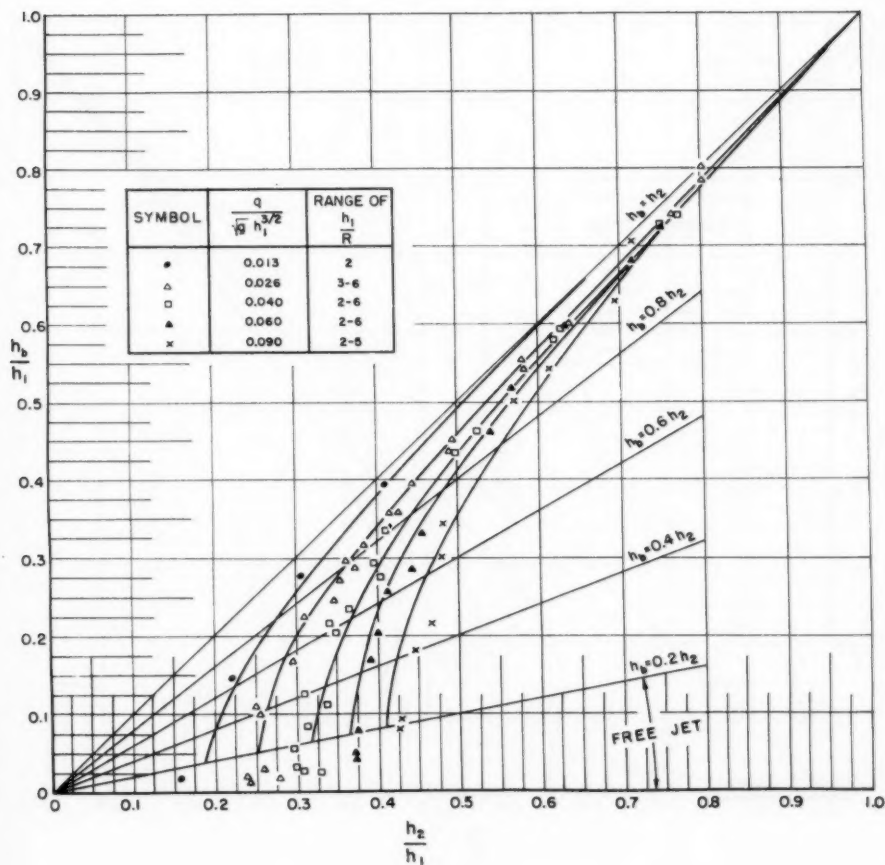


FIGURE 6

SURGE HEIGHTS FOR BUCKET-TYPE ENERGY DISSIPATORS
WITH EXIT ANGLE OF 45° AND ENTRANCE
SLOPE OF 1 ON 2

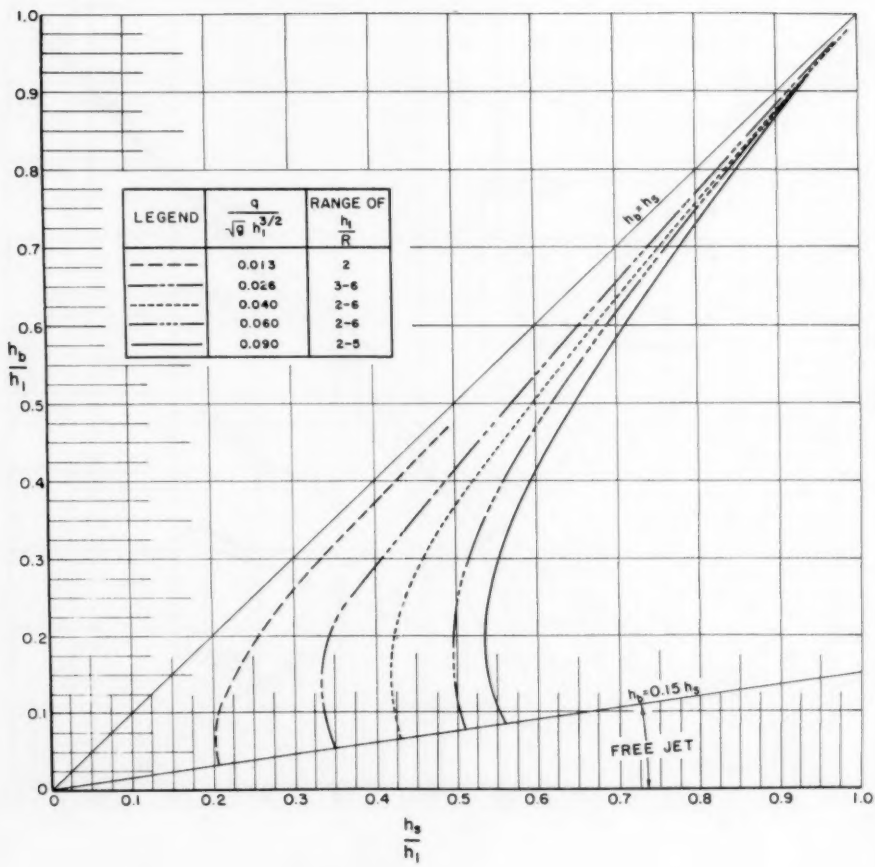


FIGURE 7

1. *U. S. Fish Commission, 1881*, p. 100.

PROCEEDINGS PAPERS

The technical papers published in the past year are identified by number below. Technical-division sponsorship is indicated by an abbreviation at the end of each Paper Number, the symbols referring to: Air Transport (AT), City Planning (CP), Construction (CO), Engineering Mechanics (EM), Highway (HW), Hydraulics (HY), Irrigation and Drainage (IR), Pipeline (PL), Power (PO), Sanitary Engineering (SA), Soil Mechanics and Foundations (SM), Structural (ST), Surveying and Mapping (SU), and Waterways and Harbors (WW), divisions. Papers sponsored by the Board of Direction are identified by the symbols (BD). For titles and order coupons, refer to the appropriate issue of "Civil Engineering." Beginning with Volume 82 (January 1956) papers were published in Journals of the various Technical Divisions. To locate papers in the Journals, the symbols after the paper numbers are followed by a numeral designating the issue of a particular Journal in which the paper appeared. For example, Paper 1013 is identified as 1013 (HY6) which indicates that the paper is contained in the sixth issue of the Journal of the Hydraulics Division during 1956.

VOLUME 82 (1956)

AUGUST: 1034(HY4), 1035(HY4), 1036(HY4), 1037(HY4), 1038(HY4), 1039(HY4), 1040(HY4), 1041(HY4)^c, 1042(PO4), 1043(PO4), 1044(PO4), 1045(PO4), 1046(PO4)^c, 1047(SA4), 1048(SA4)^c, 1049(SA4), 1050(SA4), 1051(SA4), 1052(HY4), 1053(SA4).

SEPTEMBER: 1054(ST5), 1055(ST5), 1056(ST5), 1057(ST5), 1058(ST5), 1059(WW4), 1060(WW4), 1061(WW4), 1062(WW4), 1063(WW4), 1064(SU2), 1065(SU2), 1066(SU2)^c, 1067(ST5)^c, 1068(WW4)^c, 1069(WW4).

OCTOBER: 1070(EM4), 1071(EM4), 1072(EM4), 1073(EM4), 1074(HW3), 1075(HW3), 1076(HW3), 1077(HY5), 1078(SA5), 1079(SM4), 1080(SM4), 1081(SM4), 1082(HY5), 1083(SA5), 1084(SA5), 1085(SA5), 1086(PO4), 1087(SA5), 1088(SA5), 1089(SA5), 1090(HW3), 1091(HM4)^c, 1092(HY5)^c, 1093(HW3)^c, 1094(PO4), 1095(SM4).

NOVEMBER: 1096(ST6), 1097(ST6), 1098(ST6), 1099(ST6), 1100(ST6), 1101(ST6), 1102(IR3), 1103(IR3), 1104(IR3), 1105(IR3), 1106(ST6), 1107(ST6), 1108(ST6), 1109(AT3), 1110(AT3)^c, 1111(IR3)^c, 1112(ST6)^c.

DECEMBER: 1113(HY6), 1114(HY6), 1115(SA6), 1116(SA6), 1117(SU3), 1118(SU3), 1119(WW5), 1120(WW5), 1121(WW5), 1122(WW5), 1123(WW5), 1124(WW5)^c, 1125(BD1)^c, 1126(SA5), 1127(SA5), 1128(WW5), 1129(SA5)^c, 1130(PO4)^c, 1131(HY6)^c, 1132(PO6), 1133(PO6), 1134(PO6), 1135(BD1).

VOLUME 83 (1957)

JANUARY: 1136(CP1), 1137(CP1), 1138(EM1), 1139(EM1), 1140(EM1), 1141(EM1), 1142(SM1), 1143(SM1), 1144(SM1), 1145(SM1), 1146(ST1), 1147(ST1), 1148(ST1), 1149(ST1), 1150(ST1), 1151(ST1), 1152(CM4)^c, 1153(HW1), 1154(EM1)^c, 1155(SM1)^c, 1156(ST1)^c, 1157(EM1), 1158(EM1), 1159(SM1), 1160(SM1), 1161(SM1).

FEBRUARY: 1162(HY1), 1163(HY1), 1164(HY1), 1165(HY1), 1166(HY1), 1167(HY1), 1168(HA1), 1169(SA1), 1170(SA1), 1171(SA1), 1172(SA1), 1173(SA1), 1174(SA1), 1175(SA1), 1176(SA1), 1177(HY1)^c, 1178(SA1), 1179(SA1), 1180(SA1), 1181(SA1), 1182(PO1), 1183(PO1), 1184(PO1), 1185(PO1)^c.

MARCH: 1186(ST2), 1187(ST2), 1188(ST2), 1189(ST2), 1190(ST2), 1191(ST2), 1192(ST2)^c, 1193(PL1), 1194(PL1), 1195(PL1).

APRIL: 1196(EM2), 1197(HY2), 1198(HY2), 1199(HY2), 1200(HY2), 1201(HY2), 1202(HY2), 1203(SA2), 1204(SM2), 1205(SM2), 1206(SM2), 1207(BD2), 1208(WW1), 1209(WW1), 1210(WW1), 1211(WW1), 1212(WM2), 1213(EM2), 1214(EM2), 1215(PO2), 1216(PO2), 1217(PO2), 1218(SA2), 1219(SA2), 1220(SA2), 1221(SA2), 1222(SA2), 1223(SA2), 1224(SA2), 1225(PO1), 1226(WW1)^c, 1227(SA2), 1228(SM2), 1229(EM4)^c, 1230(HY2)^c.

MAY: 1231(ST3), 1232(ST3), 1233(ST3), 1234(ST3), 1235(IR1), 1236(IR1), 1237(WW2), 1238(WW2), 1239(WW2), 1240(WW2), 1241(WW2), 1242(WW2), 1243(WW2), 1244(HW2), 1245(HW2), 1246(HW2), 1247(HW2), 1248(WW3), 1249(HW2), 1250(WW2), 1251(WW2), 1252(WW2), 1253(IR1), 1254(ST3), 1255(WW3), 1256(HW2), 1257(IR1)^c, 1258(HW2)^c, 1259(ST3)^c.

JUNE: 1260(HY3), 1261(HY3), 1262(HY3), 1263(HY3), 1264(HY3), 1265(HY3), 1266(HY3), 1267(PO3), 1268(PO3), 1269(SA3), 1270(SA3), 1271(SA3), 1272(SA3), 1273(SA3), 1274(SA3), 1275(SA3), 1276(SA3), 1277(HY3), 1278(HY3), 1279(HY3), 1280(PL2), 1281(PL2), 1282(SA3), 1283(HY3)^c, 1284(PO3), 1285(PO3), 1286(PO3)^c, 1287(SA3)^c.

JULY: 1289(SM3), 1290(HM3), 1291(HM3), 1292(HM3), 1293(EM3), 1294(HW3), 1295(HW3), 1296(HW3), 1297(HW3), 1298(SM3), 1299(SM3), 1300(SM3), 1301(SM3), 1302(ST4), 1303(ST4), 1304(SM4), 1305(SU1), 1306(SU1), 1307(ST4), 1308(ST4), 1309(ST4), 1310(SU1)^c, 1311(EM3)^c, 1312(ST4), 1313(ST4), 1314(ST4), 1315(ST4), 1316(ST4), 1317(ST4), 1318(ST4), 1319(SM3), 1320(ST4), 1321(ST4), 1322(HM3), 1323(AT1), 1324(AT1), 1325(AT1), 1326(AT1), 1327(AT1), 1328(AT1)^c, 1329(AT4)^c.

AUGUST: 1330(HY4), 1331(HY4), 1332(HY4), 1333(HY4), 1334(SA4), 1335(SA4), 1336(SA4), 1337(SA4), 1338(SA4), 1339(CO1), 1340(CO1), 1341(CO1), 1342(CO1), 1343(CO1), 1344(PO4), 1345(HY4), 1346(PO4)^c, 1347(BD1), 1348(HY4)^c, 1349(SA4), 1350(SA4), 1351(PO4).

c. Discussion of several papers, grouped by subject.

AMERICAN SOCIETY OF CIVIL ENGINEERS

OFFICERS FOR 1957

PRESIDENT

EDWARD GRAVES LOCKWOOD

VICE-PRESIDENT

Term expires October, 1957
FRANK MARSTON
CLIFFORD WOLCOMB

Term expires October, 1957
FRANCIS S. FISHER
NORMAN R. MOORE

DIRECTORS

Term expires October, 1957
GEORGE M. GARELTS
CHARLES R. PAULSON
W. S. RICHARDSON
W. G. SOUTT
GEORGE P. T. DAQUAM
LAWRENCE J. ELSENER

Term expires October, 1958
JOHN P. BILEY
GARRETT H. BROWN
NOLSON C. PRICHARD
ROBERT W. SHERLOCK
W. ROBINSON ROBINSON
CLARENCE L. ECKEL

Term expires October, 1959
CLINTON D. HOWARD
L. LELAND DURR
HOWARD R. WORRALL
FREDERIC C. LEE
JOHN C. LEVY
EDWARD ALEXANDER

PAST PRESIDENT

Members of the Board

JOHN L. O'BODEN

NEEDLES

EXECUTIVE SECRETARY
WILLIAM H. KELLY

TREASURER
CHARLES E. TROMBETTA

ASSISTANT SECRETARY
CHARLES E. TROMBETTA

ASSISTANT TREASURER
MILTON S. PROCHAZKA

PROCEEDINGS OF THE SOCIETY

CHARLES T. LARSEN
Manager of Technical Publications

PATRICK PARNELL

Editor of Technical Publications

COMMITTEE ON PUBLICATIONS

EDWARD GRAVES LOCKWOOD, Chairman
HOWARD R. WORRALL, Vice-Chairman
L. LELAND DURR
NOLSON C. PRICHARD